Performance Assessment and Modeling of Flexible Optical Networks

Djamel Amar

DOCTORAT EN CO-ACCREDITATION
TÉLÉCOM SUDPARIS- INSTITUT MINES–TÉLÉCOM
ET L'UNIVERSITÉ PIERRE ET MARIE CURIE

Spécialité : Réseaux et Télécommunications

École Doctorale : Informatique, Télécommunications et Électronique de Paris

Présentée par

Djamel AMAR

Pour obtenir le grade de

DOCTEUR DE TÉLÉCOM SUDPARIS

Modélisation et évaluation des performances des réseaux optiques flexibles

Soutenue le 12 Avril 2016
Devant le jury composé de :

Dominique Barth	Professeur, Université de Versailles	Rapporteur
Philippe Gravey	Directeur d'Etudes, Télécom Bretagne	Rapporteur
Jean-Claude Simon	Professeur Emérite, Université de Rennes I	Examinateur
Yvan Pointurier	Ingénieur de Recherche, Nokia	Examinateur
Cédric Ware	Maître de Conférences-HDR, Télécom ParisTech	Examinateur
Esther Le Rouzic	Ingénieur de Recherche, Orange Labs	Encadrante
Nicolas Brochier	Ingénieur de Recherche, Orange Labs	Encadrant
Catherine Lepers	Professeur, Télécom SudParis	Directeur de thèse

Thése n° NNT 2016TELE0007

PhD DISSERTATION
TÉLÉCOM SUDPARIS – UNIVERSITÉ PIERRE ET MARIE CURIE

Discipline: Networking and Telecommunications

Doctoral School: EDITE de Paris

Presented by

Djamel AMAR

Performance Assessment and Modeling of Flexible Optical Networks

Doctoral Committee:

Dominique Barth	Professor, Université de Versailles
Philippe Gravey	Director of Studies, Télécom Bretagne
Jean-Claude Simon	Emeritus Professor, Université de Rennes I
Yvan Pointurier	Research Engineer, Nokia, Nozay
Cédric Ware	Associate Professor, Télécom ParisTech
Esther Le Rouzic	Research Engineer, Orange Labs, Lannion
Nicolas Brochier	Research Engineer, Orange Labs, Lannion
Catherine Lepers	Professor, Télécom SudParis

Thesis n° NNT 2016TELE0007

Acknowledgements

Foremost, I would like to thank the committee members for the great honor that they have given me by accepting to evaluate this work.

I would like to thank also my academic supervisor Prof. Catherine Lepers for her precious time, and motivations during this thesis. Her guidance and insights were of great importance for both research work completion and thesis writing. I am indebted to her for teaching me both research and writing skills.

I sincerely express my deepest gratitude to my Orange Labs supervisors: Esther Le Rouzic and Nicolas Brochier for their precious help, numerous ideas, and great kindness. Their patient guidance and advices are the most important keywords of this success. Throughout these three years, their immense knowledge and constructive remarks have kept my PhD work in the right direction. Nicolas Brochier and Esther Le Rouzic, thank you very much! I will always remember your kindness and the nice atmosphere in which our work took place.

I would like to thank Maryse Guena and Ibrahim Houmid for kindly accepting me to join their team. I am thankful to my ex-manager Francoise Liégeois for her continued support and enthusiasm. Thank you Francoise Liégeois for your motivations and the excellent working conditions.

I would like to express my deep gratitude and sincere thanks to the people who motivated and helped me during the preparation and the completion of this thesis. I am most grateful to the people with whom I worked and collaborated: Jean-Luc Augé, Nancy Perrot, Edoardo Bonetto, Sina Fazel, Mohamed Kanj, and Pr. Bernard Cousin.

I owe thanks to the talented researchers who formed part of SOAN team: Bernard Arzur, Christophe Betoule, Erwan Pincemin, Gilles Thouénon, Nicolas Pelloquin, and Paulette Gavignet. Special thanks go to Jean-Luc Barbey, Julien Meuric, and Thierry Gouillossou for their endless kindness.

My sincere thanks go to my friends with whom I shared great and invaluable moments: William, Lida, Mengdi, and Ahmed (Triki). Many thanks to Bing and Danh for the valuable discussions.

I am very thankful to all my family members, especially my mother Fatimetou, my brother Mohamed Lemine and my wife Soumeya for the unconditional supports, and the continued push for tenacity.

To my dear daughter Samia.
To the loving memory of my wonderful father Mohamed Saghir.

Logic will get you from A to B. Imagination will take you everywhere.
Albert Einstein

Résumé

Avec la croissance exponentielle du trafic lié au développement de la vidéo et des services d'Internet, les systèmes WDM évoluent régulièrement pour augmenter la capacité de la fibre optique. Pour atteindre cet objectif, les concepts d'«élasticité» et de grille WDM flexible ont été introduits et ont conduit au développement de nouveaux équipements optiques. Dans le cadre des réseaux flexibles, le dimensionnement de réseaux se complexifie, et les outils de dimensionnement traditionnels doivent être repensés. De plus, des problèmes stratégiques et technologiques apparaissent avec l'arrivée de ce nouveau concept. Presque tous les équipements optiques doivent être remplacés par d'autres mieux adaptés, entraînant un coût de déploiement additionnel. Ce travail propose et implémente des nouveaux outils mathématiques et logiciels de dimensionnement multicouche des réseaux optiques flexibles. Des cas d'usage intéressants à étudier dans le cadre des réseaux flexibles sont aussi identifiés et proposés dans cette thèse. De même, ce travail traite les problèmes principaux émanant de la flexibilité optique. De façon plus spécifique, nous étudions le problème de la fragmentation du spectre WDM flexible dans les réseaux d'opérateurs et proposons des solutions. De plus, nous proposons et évaluons un cas d'usage qui combine l'élasticité et la restauration optique du trafic dans un contexte multicouche. Enfin, nous identifions et proposons une solution au problème lié à l'utilisation des amplificateurs optiques dans les réseaux flexibles.

Abstract

With the exponential growth of traffic driven by video and Internet services, WDM systems evolve regularly to increase optical fiber capacity. To meet the relentless need for capacity, advanced features have been integrated into optical layer leading to the notion of channel flexibility (datarate elasticity, flex-grid). In contrast, with the potential benefits that optical channel flexibility provides, network dimensioning gets even more complicated, and traditional dimensioning tools should be rethought. Moreover, some strategic and technological problems appear with optical layer flexibility. Almost, all legacy equipment in the optical layer needs to be replaced by greenfield and well-adapted equipment, which requires new investments. Furthermore, spectrum fragmentation has been identified as the main disadvantage of optical layer flexibility. This work proposes and implements different mathematical multilayer tools for network dimensioning with the aim of evaluating optical layer flexibility. It identifies profitable and advantageous use cases and networking scenarios that bring forward the interest of flex-grid and elasticity. This work also deals with the potential troubles of flexibility and provides solutions to them. Specifically, we thoroughly investigate spectrum fragmentation in operator network context, and propose some traffic engineering strategies. We propose and evaluate a new use case that combines datarate elasticity and optical restoration within a multilayer context. Finally, we state a new drawback of flex-grid technology regarding the use of legacy optical amplifiers with flex-grid networks and provide a solution to overcome this problem.

Contents

Acronyms

0-1 ILP 0-1 Integer Linear Programming

ABP Access Blocking Probability

AR Advance Reservation

ASE Amplified Spontaneous Emission

ATM Asynchronous Transfer Mode

BER Bit Error Rate

CA Channel Assignment

CAPEX Capital Expenditure

CDMA Code Division Multiple Access

CoS Class of Service

CTMC Continuous-Time Markov Chain

CWDM Coarse Wavelength Division Multiplexing

DCM Dispersion Compensation Module

DWDM Dense Wavelength Division Multiplexing

EDFA Erbium Doped Fiber Amplifier

EF External Fragmentation

EO Electrical to Optical

FEC Forward Error Correction

FF First-Fit

GFP Generic Framing Procedure

GMPLS Generalized Multi-Protocol Label Switching

IETF Internet Engineering Task Force

ILP Integer Linear Programming

IM Inverse Multiplexing

IP Internet Protocol

IR Immediate Reservation

IT Information Technology

ITU-T International Telecommunication Union - Telecommunication

MILP Mixed Integer Linear Programming

MLR Mixed Line Rates

MPLS Multi-Protocol Label Switching

NFV Network Functions Virtualization

NP Non-deterministic Polynomial time

N-WDM Nyquist-WDM

OE Optical to Electrical

OEO Optical-Electrical-Optical

OFDM Orthogonal Frequency Division Multiplexing

OPEX Operational Expenditure

OSI Open Systems Interconnection

OSPF Open Shortest Path First

OTN Optical Transport Network

OXC Optical Cross-Connect

PON Passive Optical Network

QoS Quality of Service

QoT Quality of Transmission

RMSA Routing Modulation level and Spectrum Assignment

ROADM Reconfigurable Optical Add Drop Multiplexer

RSA Routing and Spectrum Assignment

RSVP Resource ReSerVation Protocol

RWA Routing and Wavelength Assignment

SA Spectrum Assignment

SDFEC Soft Decision Forward Error Correction

SDH Synchronous Digital Hierarchy

SDM Space Division Multiplexing

SDN Software Defined Networking

SE Shannon Entropy

SLR Single Line Rates

SNR Signal to Noise Ratio

SONET Synchronous Optical Networks

TCP/IP Transport Control Protocol/Internet Protocol

TE Traffic Engineering

UDWDM Ultra Dense Wavelength Division Multiplexing

WDM Wavelength Division Multiplexing

WSS Wavelength Selective Switch

List of Figures

List of Tables

General Introduction

Optical transmission has revolutionized telecommunication world thanks to the high capacity and the long reach it provides. There are two main architectures for optical transport networks. The first one consists in grooming signals at each intermediate node in order to efficiently fill the optical channels, requiring however costly Optical-Electrical-Optical (OEO) conversions (opaque optical networks). The other one enforces an all-optical networking which avoids OEO conversions at intermediate nodes in order to save on regenerators, but may suffer from impairment accumulation (transparent optical networks). Nowadays, both architectures should coexist in the same translucent optical network, making larger the optimization space that is already suffering from the Non-deterministic Polynomial time (NP)-completeness of Routing and Wavelength Assignment (RWA), in optical mesh networks [1].

With the exponential growth of traffic, which is essentially driven by videos and Internet services, optical transmission systems and Wavelength Division Multiplexing (WDM) techniques evolve regularly to increase optical fiber capacity. For example, transponders operating at 100 Gbps are already in use and many ongoing studies are promising to go beyond [2–4]. However, the relentless need for capacity in terms of the number of channels and their maximum datarate, is still growing. It is the reason why fairly advanced features have been integrated into optical layer equipment thanks to hardware development leading to the notion of channel flexibility (datarate elasticity, flex-grid). Elasticity consists in adapting channel datarate to the actual traffic volume in order to increase the optical spectral efficiency as close as possible to the theoretical limit, or to better exploit optical link margins. Regarding flex-grid, it provides optical channels with the capability to exploit exactly the required spectrum using multiples of 12.5 GHz frequency slot. However, with the potential benefits that optical channel flexibility provides, network dimensioning gets more and more complicated, and traditional dimensioning tools should be rethought.

Beyond the impact on planning complexity, introducing channel flexibility makes network layers more dependent on one another, reducing rigidness and symmetry in dimensioning process. For example, the over-design of WDM channels that traffic grooming algorithms were dealing with, is no longer of the same importance [5, 6]. It means that network dimensioning should take into account both electrical and optical layers in such a way it can take maximum benefit from flexibility (multilayer optimization).

Apart from dimensioning complexity and multilayer aspect, some strategic and technological problems appear with optical layer flexibility. Almost, all legacy equipment

in the optical layer need to be replaced by greenfield and well-adapted equipment to flexibility. Reconfigurable Optical Add Drop Multiplexers (ROADMs) and Erbium Doped Fiber Amplifiers (EDFAs) are the most concerned entities by the new concept of flexibility [7, 8]. This could have considerable impact on network deployment, as the expected gain in terms of cost is somewhat controversial [9–11].

Furthermore, spectrum fragmentation like computer memory fragmentation, has been identified as the main disadvantage of optical layer flexibility [12–15]. It means that some blocks of frequency slots can be left scattered in the spectra, leading to traffic demand blocking in spite of the free existing resources. Consequently, theoretical spectrum gain can be hardly reached due to unusable blocks of saved spectrum.

In summary, in order to face the exponential growth of traffic, optical layer is getting even more smarter thanks to the relatively low cost of WDM equipment, and the recent advance in optical technologies. This evolution adds further complexity to the dimensioning of optical transport networks as they are already facing the issue of planning and resource provisioning. New dimensioning tools adapted to flex-grid and datarate elasticity are therefore needed, as the conventional ones can no longer be used.

The contribution of this thesis consists of two parts. The first contribution concerns the proposition and the development of different dimensioning tools that take into account the particularities of flexible optical networks. To that aim, we study the dimensioning problem in a hierarchical and then a multilayer dimensioning context. These tools are subsequently used for the purpose of evaluating and encircling the right gains of flex-grid technology and datarate elasticity.

The second contribution consists in identifying and proposing scenarios and use cases that highlight the interest of flexible optical networks. For example, a new multilayer architecture for traffic restoration is proposed. Furthermore, some traffic engineering strategies are proposed in order to minimize spectrum fragmentation impact on flex-grid expected benefits. Indeed, the present work deeply discusses spectrum fragmentation issue in operator network context, and proposes new metrics for fragmentation assessment. A new migration policy that allows keeping in use legacy power-limited EDFA amplifiers is also proposed and evaluated in this work.

The rest of this manuscript is organized as follows:
Chapter 1, gives a brief overview on transport optical network evolution, and highlights the key elements of the research context and the problematic of this dissertation.

Chapter 2 is dedicated to the state of the art of flexible optical networks. It thoroughly discusses the previous works, sheds some light on their weaknesses, and situates the present work.

Chapter 3 deals with the issue of spectrum fragmentation in the incremental context of operator network. In this Chapter, new fragmentation metrics are proposed and compared with existing ones. Subsequently, these metrics are used to evaluate spectrum fragmentation before proposing some well-adapted approaches stemming from traffic engineering, to the problem.

In Chapter 4, a multilayer dimensioning tool is proposed for elastic optical networks. This tool is used to evaluate a new class of service based multilayer architecture that

we propose for cost-effective traffic restoration taking benefits from the low priority of best-effort traffic in a multilayer context.

In Chapter 5, we propose a new link design method and evaluate the optical power limitation issue coming with flex-grid technology. Same chapter presents and evaluates a power adaptation approach that allows reducing flex-grid migration cost by maintaining in use legacy optical amplifiers.

Finally, this work is concluded, and the main results are summarized, as well as, the perspectives and the possible research lines.

CHAPTER 1

Research Context

1.1 Operator Network Hierarchy

In general, operator network hierarchy comprises three different parts, each of them having specific design depending on traffic requirements and dimensioning context.

Most of deployed optical access networks are Passive Optical Network (PON). They aim at providing end-users with connectivity to service providers, and constitute the lowest level of communication in the overall hierarchy. They are characterized by a relatively low traffic volume with respect to the other levels of the segmentation, and are less sensitive to service disruption as it impacts less customer count. For this reason, nodes in passive optical access networks are linked according to a tree physical topology, and downstream communications follow the point-to-multipoint principle as in PON technology [16].

Metropolitan networks (also called metro networks) constitute the second level of operator network hierarchy, and they are responsible for linking some specific areas or regions at nationwide scales. This part of operator network has the most important traffic growth rate [17], and are identified with their physical ring topology even if some of them are nowadays meshed. Therefore, traffic demand routing, resource provisioning, and recovery schemes are absolutely trivial in ring-based metro networks.

Core optical networks play an important role in telecommunications at worldwide scale, and have the purpose of interconnecting peering points and major cities to Internet, datacenters and other operators. Obviously, in core networks the most important traffic volume is concentrated, with an exponential traffic growth rate [17]. It is the reason why nodes are linked according to a meshed physical topology.

Core and metro optical networks constitute the so-called transport optical networks, which are mainly concerned by transmission and switching functionalities (Fig. 1.1). In this work, we focus on core optical network design and modeling where optical fibers are ubiquitous and channel flexibility might be first deployed.

1.1.1 Network Architecture Trends

Telecommunication networks have to fill some requirements in order to ensure the reliability of both data transmission and delivery. Hardware equipment hierarchically performs communication functions using specific binary language called protocols.

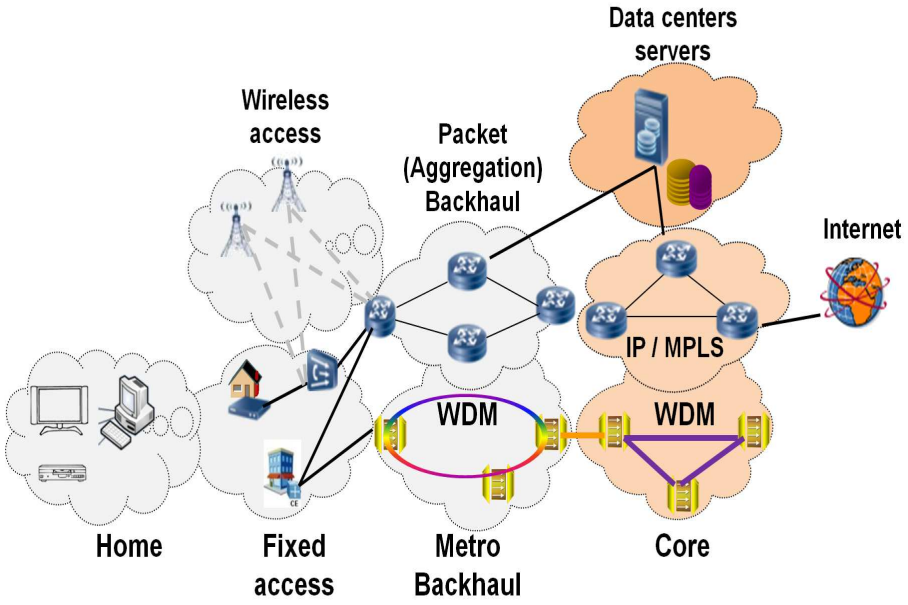

Figure 1.1 — Operator network hierarchy.

These functions are abstracted and classified into several groups or layers, with the purpose of ensuring effective coexistence and exchange between different vendor products. Open Systems Interconnection (OSI) [18], and Transport Control Protocol/Internet Protocol (TCP/IP) [19], are the most used models to describe modern day protocols, whereas TCP/IP is more in line with their implementations.

Over the last two decades, protocol stack has been evolving in operator network, and different protocols had to coexist in the same architecture leading to some inconsistency in core network level. For instance, transporting Asynchronous Transfer Mode (ATM) protocol by Synchronous Digital Hierarchy (SDH) has introduced a synchronization issue in the lower layers. Likewise, having Internet Protocol (IP) Over ATM leads to the fragmentation of IP packets due to their variable size and the fixed and small size of ATM cells. In order to overcome this inconsistency between different layers, and with the purpose of reducing the number of network equipment, the trend is being towards a unique and a simplified convergent solution: IP-Over-WDM. It consists in multiplexing IP packets into WDM optical channels (Fig. 1.2), via Generic Framing Procedure (GFP) or Ethernet protocol encapsulation and passing through Optical Transport Network (OTN) framing eliminating network components in intermediate layers as defined in International Telecommunication Union - Telecommunication (ITU-T) G.709 [20].
In this work, we consider the IP-Over-WDM architecture, and we do not take into account the possible grooming in OTN sub-layer.

Data plane is responsible for hardware functionalities like data segmentation, assembly, and forwarding, whereas control plane makes decision concerning where data have to be sent. Until recently, Generalized Multi-Protocol Label Switching (GMPLS) protocol was the main candidate standard [21] to realize the control plane of optical networks.

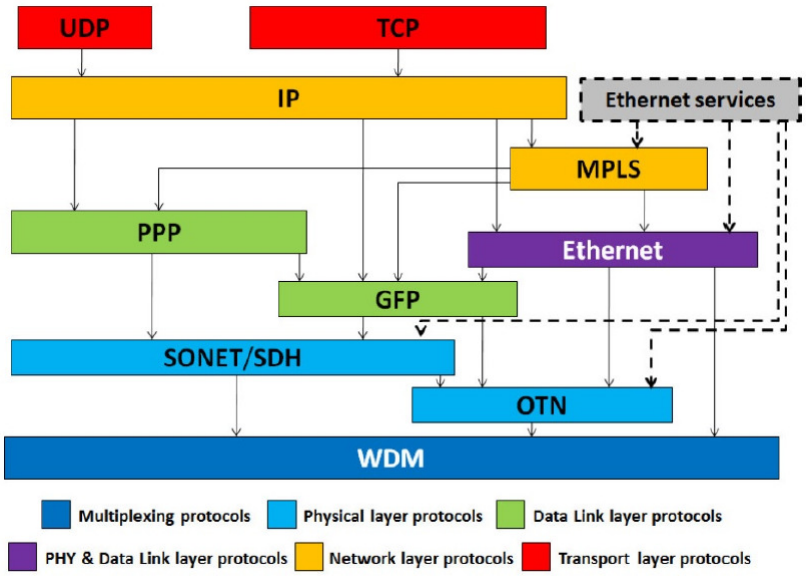

Figure 1.2 — Protocol stack in telecommunication network [23].

Some competitors have recently emerged coming from the intra-datacenter networking world like Software Defined Networking (SDN).

SDN is a promising architecture that decouples the data plane from the control plane, which are usually performed by the same distributed hardware equipment [22]. Control plane decisions are afterwards sent to forwarding nodes (switches and routers) using a communication protocol (e.g., OpenFlow, PCEP, NetConf etc.). This decoupling has been for long time usual in optical transport networks where SDN promises are expected to improve network flexibility in terms of automation. For example, moving control plane functionalities towards a centralized software entity (called SDN controller) is expected to make network management and administration dynamic, flexible, and independent from equipment manufacturers. SDN has also fully opened the door for Network Functions Virtualization (NFV) arrival, which enables an efficient sharing of hardware resources using some techniques inspired from Information Technology (IT) world.

Note that, specifying protocol stack architecture is necessary in this work, in order to define network equipment types that network dimensioning takes into account. Likewise, control plane automation aspect is a key element in the feasibility of some network operations, like spectrum defragmentation, datarate elasticity, and traffic restoration that will be later discussed in this dissertation.

1.1.2 Transport Mode Evolution

Two main architectures for optical nodes exist, depending on whether OEO conversions are enforced or not.

Accordingly, three transport modes for optical signals are possible, namely opaque,

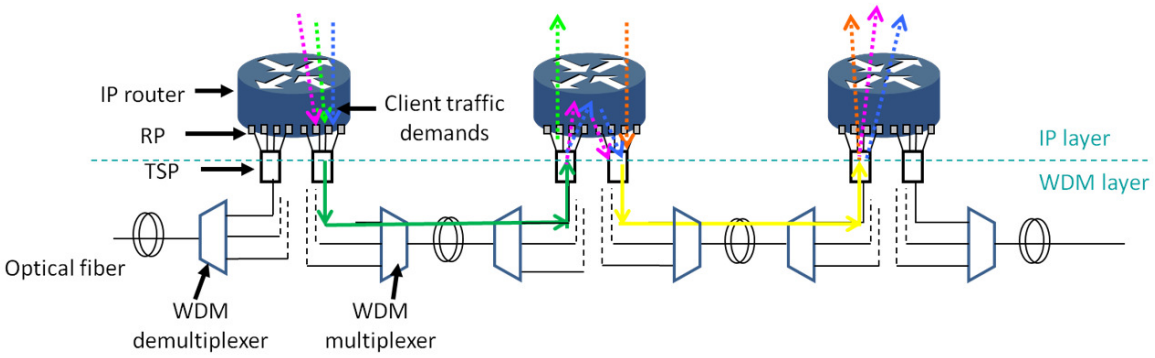

Figure 1.3 — Opaque node architecture. In this example, the electronic switching is performed in the IP layer via IP routers. RP and TSP stand for router port and transponder respectively.

transparent, and translucent.
In the following, characteristics of each transport mode are briefly described.

1.1.2.1 Opaque Mode

This is the historical mode that has been deployed in the optical layer for a while. It undergoes OEO conversions at all intermediates nodes along the path from source node to destination node, using WDM transponders (transmitter and receiver) and opaque switches (electronic switching) as shown in Fig. 1.3.

Opaque mode allows traffic demand grooming in the electrical domain in order to efficiently fill the optical channels. It has also the advantage of cascaded signal regenerations, preventing therefore physical impairments accumulation and avoiding wavelength continuity constraint. However, traffic grooming may bring little improvement in terms of filling if channels are already well occupied and in this case opaque mode can significantly impact network cost because of additional transponders, regenerators and potential router interfaces.

1.1.2.2 Transparent Mode

Unlike opaque mode, transparent mode keeps optical signals in the optical domain with no electrical conversion until they reach destination nodes. This mode is particularly efficient when the channels are highly filled. Transparent mode permits to reduce both Capital Expenditure (CAPEX) and Operational Expenditure (OPEX) because intermediate OEO conversions are avoided. However, it introduces the wavelength continuity constraint which can increase the number of required wavelengths per fiber link.

In addition, as a result of intermediate node bypass, the resulting path may accumulate a certain level of physical impairments, which makes the system not to operate: this adds complexity in determining path feasibility. This constraint also limits the size

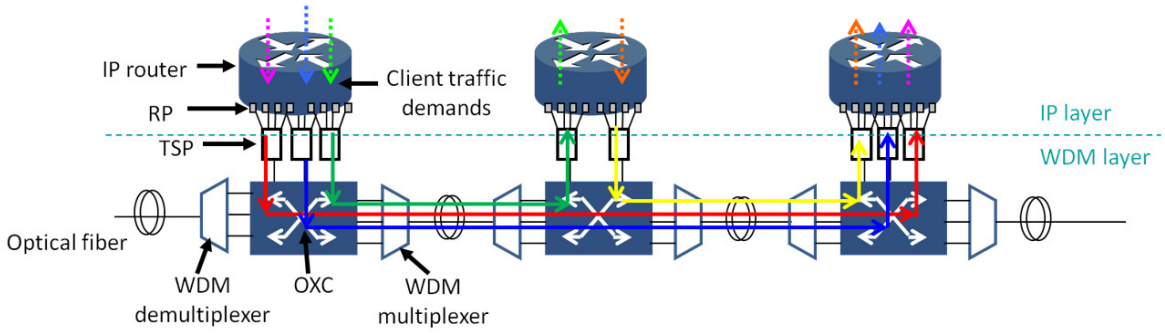

Figure 1.4 — Transparent node architecture. RP and TSP stand for router port and transponder respectively.

of the network (scalability). Figure 1.4 shows an example of a transparent node that uses a transparent Optical Cross-Connect (OXC). The OXC allows switching optical signals from input ports and/or add ports to output ports and/or drop ports. Here, add and drop operations are performed only to send or to receive optical signals.

1.1.2.3 Translucent Mode

Translucent mode (also called hybrid mode) takes benefit from both opaque and transparent networks in such a way that the best trade-off between traffic grooming, and signal regeneration is found, optimizing cost and removing network size limitation. In other words, every node in translucent networks can be opaque, transparent, or both according to traffic to satisfy, IP routing constraints, regenerator placement strategy, and optimization objective.

A translucent node is depicted in Fig. 1.5. Transparent switching is illustrated with the plain green arrow, and opaque is illustrated with the dashed pink and magenta arrows. Note that the electrical switching at the IP layer allows some client traffic grooming in this case (part of pink traffic is dropped while local traffic is added and regroomed with the transit traffic, before it is sent back to the optical layer via transponders).

In this work, we exclusively focus on this mode as it is representative of nowadays transport optical networks.

1.2 Optical Layer Flexibility

Over the last years, transport network traffic has been exponentially growing and will still increase, according to recent studies carried out by scientists from Cisco and Bell Labs [17, 24]. Consequently, the need for capacity is becoming more and more urgent, at the same time that existing services for end-users have to get cheaper and cheaper.

There are three main approaches to improve link capacity in transport optical networks. A straightforward solution consists in installing a new optical fiber on the link whenever

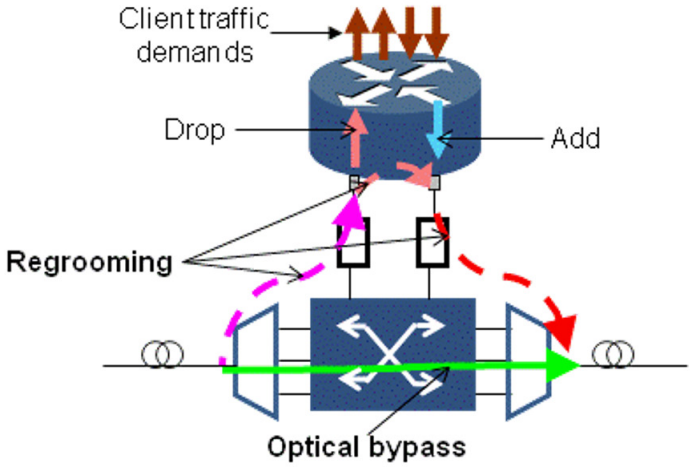

Figure 1.5 — Translucent node architecture.

bandwidth is needed. This approach can relax wavelength continuity constraint, but it leads to the deployment of new optical amplifiers, apart from the additional cost of WDM system deployment and its validation. Usually, this approach is used as a last resort.

The second approach focuses on increasing the per-channel datarate, using high level modulation formats within the same bandwidth (symbol rate) and/or higher symbol rates. The use of complex advanced modulation formats in phase, amplitude, and polarization together with coherent detection [25] allowed a breakthrough in fiber capacity evolution. Figure 1.6 depicts that fiber capacity evolution over the last four decades has been linearly increasing, offering enough capacity for the observed exponential growth of traffic. Nevertheless, the larger the number of constellation points is, the more sensitive to impairments the transmission is, which can involve significant impact on transmission reach. In addition, according to recent research in the field, fiber capacity of communication systems is getting close to the theoretical Shannon limit [26], which means that the observed evolution of fiber capacity will be broken in the coming years.

The third approach consists to increase the number of WDM channels within the C spectral band of optical fibers by reducing frequency spacing between WDM channels. Coarse Wavelength Division Multiplexing (CWDM) and Dense Wavelength Division Multiplexing (DWDM) technologies are good examples to illustrate such an approach. Using very cheap lasers, CWDM can transport up to 18 channels spaced by 20 nm from 1270 nm to 1610 nm, most of them however are outside the operating window of EDFA amplifiers, which results in short reaches for the WDM system (about 100 km) [29]. In contrast, DWDM technology uses a tighter channel spacing, typically 0.4 nm (50 GHz) yielding more than 80 channels per fiber in the EDFA amplifier C-Band, allowing longer reaches but requiring costly transceivers with respect to CWDM technology. Some studies have been performed on an Ultra Dense Wavelength Division Multiplexing (UDWDM) technology with even narrower spacing (<0.2 nm) and smaller per-channel signal bandwidth. However, UDWDM has not received as much attention

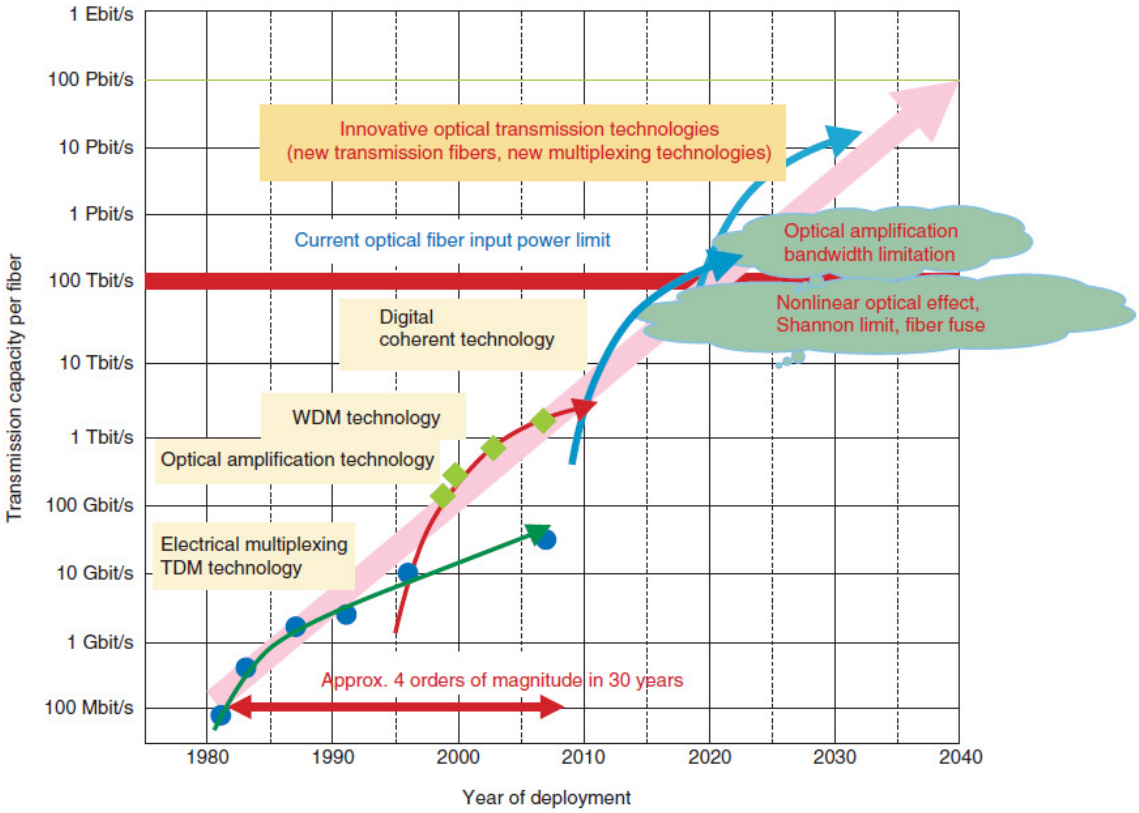

Figure 1.6 — Fiber capacity evolution over the last decades [27, 28].

as DWDM due to very limited reaches and ultra-costly lasers. In addition, UDWDM channel spacing does not match high single channel datarates requiring more than 25 GHz channel spacing (e.g., 100 Gbps).

On the other hand, optical networks can be classified into three categories according to the different datarates offered by optical transponders. In the first category, optical transponders are designed to support the same highest Single Line Rates (SLR) with the same longest optical reach, irrespectively of traffic demand volume and regardless of physical link lengths. In the second category, networks mix optical transponders with different fixed datarates, which can have different optical reaches. This Mixed Line Rates (MLR) allows overcoming the overdesign challenge of SLR transponders but with some rigidness in the network life cycle since datarates are fixed. The third category concerns elastic transponders with on-demand datarate adaptation [1,2]. Datarate adaptation can be performed on the fly thanks to coherent transmission and advanced digital signal processing, for instance changing symbol rate, modulation format or both [3].

Since capacity limit of optical fiber should be reached soon, there is a renewed interest on spectrum utilization. Indeed, conventional fixed grid optical networks are characterized by a non-optimized use of spectrum resources as a fixed channel spacing must be used, even if the required signal spectrum amount is smaller. Nevertheless, making the channel grid finer is not sufficient to overcome this inefficiency, because transponders

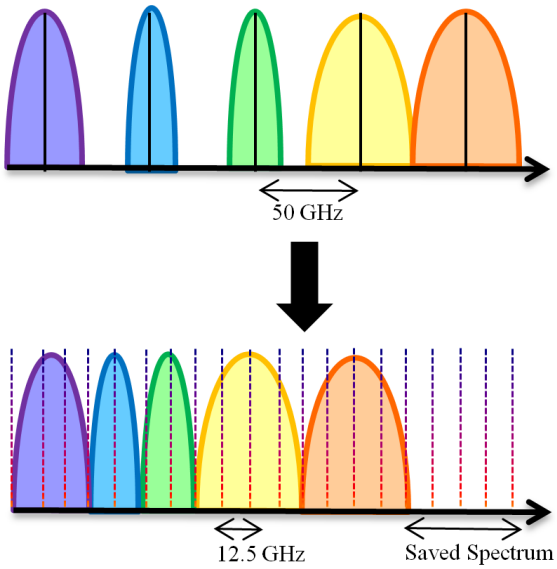

Figure 1.7 — Example of flex-grid benefits: at the top, some optical channels use symbol rates considerably lower than the traditional grid. At the bottom, these channels are assigned their real widths, and the remaining spectrum is saved.

with different datarates, operating on the same optical fiber, and requiring more or less spectrum amount, are already in use in today's optical networks (MLR networks). A promising alternative to improve the spectral efficiency and to reduce the overdimensioning of network resources, is to introduce a flexible channel spacing in the WDM grid (known as flexible grid or flex-grid), depending on the actual requirements of WDM transponders. Flex-grid technology consists in gathering several contiguous frequency slots in order to better match the required and the allocated spectrum [30]. A fully flexible grid is not possible, because of the filtering limitations of WDM equipment. Figure 1.7 shows an example of saved spectrum in flex-grid optical networks, thanks to both fine slot width and flexible grid.

In addition to flex-grid technology, elastic transponders offer an interesting adaptation capability as they can adapt dynamically their datarates to the actual traffic volume they are carrying. This capability has been proposed to deal with traffic fluctuations due to the daily traffic pattern for example, or to the variation of traffic distribution when some optimization processes are performed. Systematic datarate adaptation can be obtained by varying for example, modulation format, symbol rate, Forward Error Correction (FEC) overhead, or number of allocated sub-carriers in case of Orthogonal Frequency Division Multiplexing (OFDM) technology [2].

Datarate elasticity is expected to better optimize the spectrum usage, whereas flex-grid could expand optical fiber capacity by about 33% [31][1]. Therefore, combining both techniques would offer very promising perspectives for future optical networks [32].

In this work, we use "flexibility" term, and we refer to "flexible optical networks", when flex-grid technology is used with elastic transponders in the same optical network.

[1] or recover 25% of fiber spectrum

1.3 Network Dimensioning and Design

1.3.1 Problem Statement

Network dimensioning consists in determining, locating, and tuning all electrical and optical equipment which are used for a given traffic matrix on a known physical topology, while optimizing a specific objective (generally network cost). This implies a logical topology design in which traffic demands are routed on physical paths, assigned a part of spectrum (RWA), regenerated, protected, and groomed or split according to optimal solutions. [33, 34].

Network dimensioning is usually seen as a complex NP problem. Let us recall here the meaning of NP problems. A decision problem is said to be in the NP class, if a) it requires a non-deterministic Turing machine in order to be solved in polynomial time, and b) any given solution to it can be verified in polynomial time using deterministic Turing machine. It is NP-complete if a) it is NP and b) all NP problems can be reduced to it in polynomial time. It is NP-hard, if it satisfies at least the second condition. Therefore, all NP-complete problems are NP-hard, but not all NP-hard problems are NP-complete (Fig. 1.8). In other words, a NP-hard problem is at least as hard as any other NP problem and it is not necessarily in the NP class. This is because a NP-hard problem is not necessarily decisive, and can take much time to verify a given solution to it. The problem $P \stackrel{?}{=} NP$ is one of the most difficult problems in mathematics, and it was chosen among the seven millennium prize problems stated by the Clay mathematics institute in 2000 [35].

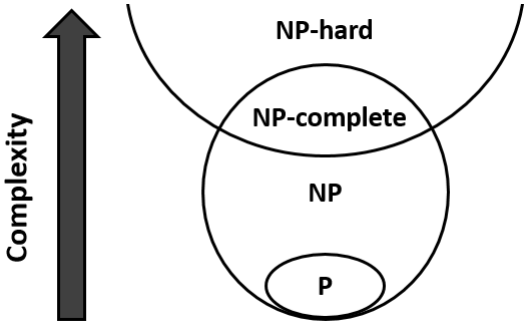

Figure 1.8 — Illustration of NP-problems and their complexity.

In the general form of RWA problem, authors in [1] have proven RWA NP-completeness, showing that it can be transformed to the NP-complete n-graph-colorability problem. In the particular form of chain topology, RWA can however be solved in polynomial time (class P) [36].

Taking into account the new constraints of flex-grid technology, traditional RWA algorithms can no longer be applied. Instead of RWA, dimensioning algorithms have henceforth to deal with Routing and Spectrum Assignment (RSA), which takes into account the following constraints:

- Traditional constraint of wavelength (now spectrum) **continuity** is conserved. It means that each transparent demand must be assigned the same wavelength along the physical path that is corresponding to its virtual link.
- New spectrum **contiguity** constraint is added, meaning that all the frequency slots being used by the same transponder must be spectrally contiguous. Spectrum fragmentation is a direct consequence of spectrum contiguity constraint as it happens when the free spectrum is not contiguous.
- One frequency slot can be attributed to at most one WDM transponder (**non-overlapping** constraint). This constraint is already considered in conventional optical networks, with however stronger impact in flex-grid technology due to spectrum contiguity constraint.

RSA NP-hardness has been proven in [37], meaning that it is more difficult than RWA problem, except in case where all WDM transponders require the same spectrum occupancy. In such a case, RSA transforms to RWA problem.

This complexity analysis concerns only the routing and spectrum allocation aspect of network dimensioning. Computational complexity is expected to grow, if sub-problems like regenerator placement, traffic grooming, and network resiliency are taken into account (e.g., multilayer dimensioning).

1.3.2 Multilayer Dimensioning

Given the complexity of multilayer dimensioning, network dimensioning is often performed for each layer separately. Multilayer dimensioning performs a joint optimization of all network layer resources, taking into account all network layer constraints, while optimizing a given objective (e.g., network overall cost). It should not be mixed up with a joint optimization of two or more sub problems (e.g., routing and regenerator placement), which can consider only optical layer cost, or neglects some relevant sub-problems like traffic grooming.

Multilayer dimensioning of flexible optical networks has to find the best trade-off between traffic grooming (e.g., IP layer), optical bypassing, regenerator placement, shortest path routing, and spectrum assignment, while being constrained by maximum transponder reach and capacity depending on elasticity parameters. Moreover, spectrum continuity and spectrum contiguity constraints may lead to solutions generating spectrum fragmentation, thus increasing the blocking probability and decreasing the spectrum efficiency in the network [13, 38–41]. Other solutions can be in favour of traffic grooming in order to better address the channel overdesign that the optical layer flexibility is expected to deal with [5, 6]. In other words, the new flexibility offered at the optical layer may compete with the one at the higher layer which adds complexity in the design decision: should grooming be performed in the IP layer to better fill optical layer resources? or should flexibility be applied to adapt optical layer resources to traffic needs? (this demonstrates the interest of multilayer dimensioning in flexible optical networks).

In a nutshell, multilayer dimensioning is much more complex than hierarchical dimensioning, and it concerns the most flexible optical networks. Therefore, the challenge is to properly model both WDM and IP layers in order to optimally explore the large optimization space, as conventional routing and spectrum allocation algorithms of traditional WDM networks can no longer be applied.

CHAPTER 2 State of the Art

2.1 Introduction

In Chapter 1, the research context of the thesis, and the main concepts/scientific terms have been defined. The concept of optical layer flexibility has also been introduced.

In this Chapter, we present an overview on optical layer flexibility, and thoroughly discuss the state of the art of the related works. Specifically, in Section 2.2, the new considerations and particularities of flexibility are detailed. Section 2.3 presents the activity research covering network dimensioning and related issues. Finally, the current work is positioned with respect to the literature in Section 2.4.

2.2 New Considerations

As mentioned earlier, optical fiber capacity is approaching its theoretical limit thanks to the recent advances in signal processing and transmission systems [25, 26]. Moreover, the rigid fixed grid in conventional optical networks cannot accommodate the future high symbol rates used to serve large traffic demands due to the constrained bandwidth. Inverse Multiplexing (IM) techniques, consisting in demultiplexing large traffic demands (e.g., 1 Tbps) into smaller ones (e.g., 10×100 Gbps) that can fit the conventional fixed grid, have appeared. Such techniques lead, however, to bandwidth wastage and are seen as a straightforward costly approach [38].

For these reasons, a new paradigm, known as flex-grid, dealing with the overall fiber capacity has emerged. It consists in tailoring the bandwidth to the actual requirement of traffic demands using a fine frequency slot as an elementary spectrum unit. The first-ever work introducing the concept of channel variable bandwidth was in 2001 [42]. However, it had no considerable success due to the non-mature technology. It was not until 2008 that the first completely flexible system, known as SLICE, has been experimentally demonstrated, using OFDM-based elastic transponders and well-adapted-to-flex-grid equipment [2].

It is very important to point out that flex-grid channels with large symbol rates are nowadays limited by the maximum sampling rate of digital-to-analogue and analogue-to-digital converters. In other words, it is not yet possible to design an optical transponder that can support symbol rates larger than 50 Gbaud even if flex-grid can easily

accommodate even larger bandwidths (in fact, it can support any bandwidth equals to multiples of 12.5 GHz).

This limitation leads to the concept of superchannels, which consists in splitting the traffic demand stream into multiple sub-band streams before they are grouped using either OFDM or Nyquist-WDM (N-WDM) based multiplexing techniques. Note that we consider N-WDM-based multiplexing techniques in this thesis work, although both N-WDM and OFDM present almost no difference in terms of spectral efficiency [43].

Superchannels are thus a good solution which provides large channel capacity and/or high spectrum efficiency. Indeed, superchannel sub-bands can be pushed closer than filtering limitation since they are not expected to be filtered along their path. For this reason, superchannels provide a good trade-off between capacity and reach.

The difference between IM and superchannel concepts is that guard bands are not required between superchannel sub-bands unlike IM channels. In addition, IM channels are independent from one another and they are less likely to be blocked by the lack of contiguous spectrum [38].

Optical channel flexibility concept relies on physical layer development, control plane, and network optimization. In this dissertation we focus more on network optimization, even though we take into account hardware limitation and control plane feasibility in our studies.

2.2.1 Hardware Aspect

Flex-grid technology requires some specific equipment in order to be implemented in conventional optical networks (Figure 2.1). The new accurately adjustable and flexible grid is the main purpose related to this requirement. That is why before building flex-grid-based optical equipment, the frequency slot width has been specified and standardized.

The concept of frequency slot has been first introduced in [44]. The appropriate frequency slot width has been intensively discussed in the literature. From the point of view of spectrum fragmentation, it has been found that frequency slot width should be equal to the bandwidth required for the lowest datarate [45].

From an economical point of view, it should be to some extent fine in such a way that the need for traffic grooming in the electrical domain gets alleviated. This could reduce multilayer energy consumption and gives rise to lower equipment count [46]. In [47], authors precise that a fully flexible grid (gridless) has a very small additional gain mainly due to upper layer traffic granularity, apart from related difficulties and technology limits. They found that a frequency slot width in the range of 2.5 GHz to 3.125 GHz, is quite enough in order to reap full benefits from optical layer flexibility. Similarly, a mini-grid of 3 GHz is compared to the full gridless scenario in [48]. Numerical results show that mini-grid scenario performs almost as well as the gridless scenario, with significant saving with respect to conventional fixed grid. However, the ultra-fine slot is particularly well-adapted for networks with lots of low datarates, and will not be in the long term as traffic volume evolves over time [49].

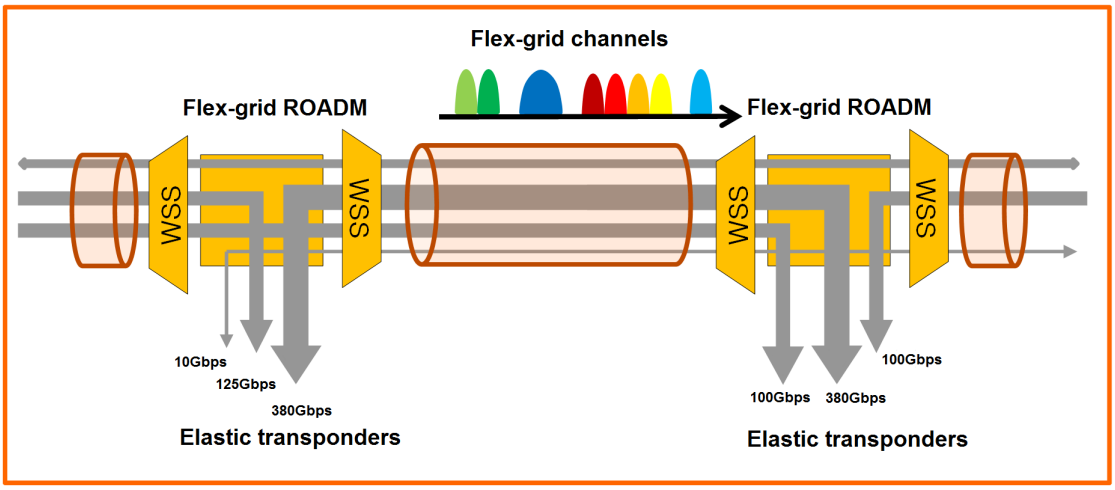

Figure 2.1 — Flex-grid technology concept - Required equipment.

Taking into account these considerations, and in order to be compliant with the existing 10 Gbps channels, a 12.5 GHz frequency slot has been defined [30]. This fine frequency slot needs a 6.25 GHz step to centralize the signal around its nominal frequency, as introduced in the G.694.1 recommendation of ITU-T [30].

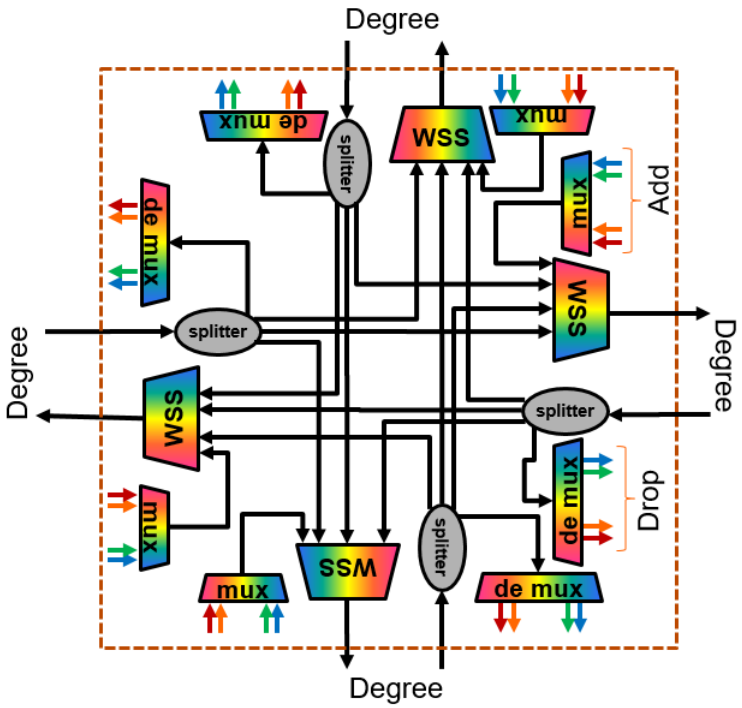

Figure 2.2 — Example of colored, directed four-degree ROADM, based on WSS and splitters. The structure uses a broadcast and select architecture. WDM mux and demux are used for Add and Drop ports.

A ROADM is a remotely reconfigurable device that can add, drop (terminate), or switch

an optical signal (wavelength) in/from/to an optical fiber. A Wavelength Selective Switch (WSS) is the main component in the ROADM block. It is a bidirectional $1 \times N$ switch that allows switching individual wavelength channels from the common input port to any output port (or from any input port to the common port if used in the $N \times 1$ direction).

Figure 2.2 shows an example of ROADM based on WSSs and splitters in a broadcast and select structure. In this structure, any incoming channel on a given direction (degree) can be switched to any other direction. Add-drop ports in this simple structure cannot however be switched freely to/from any direction and are bound to the fixed lambda multiplexers, demultiplexers, which makes this structure colored and directed. By opposition, there exist structures that provide colorless, directionless, and even contentionless add-drop capability [50].

Fixed grid WSSs can switch channels on a 50 GHz basis only. Flex-grid WSSs can switch any incoming optical channel whatever its width (multiple of 12.5 GHz).

Optical nodes (ROADMs) should be endowed with flex-grid WSSs [2, 42] in order to implement the flex-grid concept. In addition, almost all network equipment is somewhat affected i.e., optical amplifiers, optical transponders, and even routers.

An optical amplifier is used to compensate the loss of optical fiber spans. EDFA amplifiers are the most common type of amplifiers, which use doped optical fiber to amplify optical signals in C-band or L-band [51]. They are characterized by their maximum power, their maximum gain, and their noise figure stemming from the Amplified Spontaneous Emission (ASE).

A dual-stage amplifier is composed with two amplifiers packaged in the same module with a control unit in between (Fig. 2.3). Usually, a Dispersion Compensation Module (DCM) is placed between amplifier stages in order to manage and compensate for chromatic dispersion of the optical fiber. The control unit is responsible for the tuning of the preamplifier (first amplifier) and the booster (second amplifier). For example, it sets the gain of both preamplifier and booster in order to achieve the required gain for the overall system.

It has to be noticed that recent 100 Gbps transmission systems and beyond using coherent detection, are not compliant with DCM modules. These systems need to implement chromatic dispersion correction at the receiver side and not along the optical fiber. This work considers coherent transmissions, and therefore deals with variable gain dual-stage amplifiers with no in-line chromatic dispersion compensation.

Optical amplifiers are designed to support a given number of optical channels (namely 80 channels). Nevertheless, for a given spectral bandwidth (C band), flex-grid concept gives rise to the increase of the number of channels, requiring more optical power amplification in respect with the conventional fixed grid technology. This means that the optical power limit of legacy amplifiers may not be sufficient to support the expected channel number increase [8]. This issue is tackled in Chapter 5 of this dissertation.

Conventional optical transponders are responsible for emitting and receiving the optical signal at a typical datarate up to a given distance. In order to operate on the new flexible grid, conventional transponders need a basic change in the laser as it must

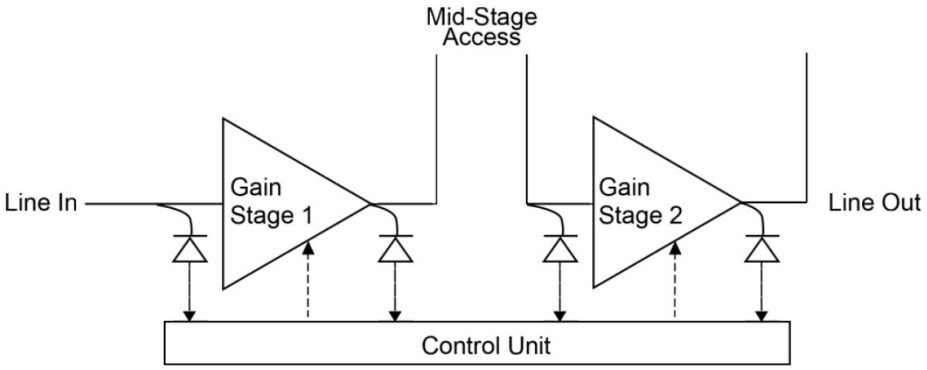

Figure 2.3 — Architecture of a dual-stage amplifier with mid-stage access.

be finely tunable to be centred in the allocated spectrum [7]. To be more efficient in spectrum use, optical transponders must be able to adapt their symbol rate to the real spectrum requirement of traffic demands (elasticity). This results from the fact that getting a different fixed rate transponder for each datarate is expensive, and does not meet the requirement for datarate adaptation in dynamic traffic contexts.

Indeed, transponder elasticity does not concern only symbol rate adaptation, but also modulation format type, FEC ratio over the payload, and channel spacing in case of single-band transmission. The number of sub-bands, sub-band spacing, and super-channel spacing can also offer additional degree of flexibility in case of multi-band multiplexing techniques. Effect of datarate elasticity should enhance channel capacity, optical reach, and/or spectral efficiency [52]. For instance, using higher modulation formats improves both channel capacity and spectral efficiency, but reduces optical reach. Similarly, increasing symbol rate allows improving channel capacity with a little enhancement of the spectral efficiency assuming that the channel spacing is somewhat correlated with the actual channel width (Table 2.1).

Parameters	**Metrics**		
	Capacity	Reach	Spectral efficiency
Symbol rate ↑	+	=/-	+
Format level ↑	+	-	+
FEC ratio ↑	-	+	-
Channel spacing ↑	-	+	-

Table 2.1 — Elasticity (datarate increase) effect on capacity, reach, and spectral efficiency depending on the tuned parameter.

In addition, elasticity simplifies network management and improves its autonomy, which can significantly reduce number of costly human interventions during network life time [53]. Datarate elasticity can also reduce total energy consumed by transponders, thanks to symbol rate adaptation when switching from higher to lower datarates [52].

Elasticity is mostly present through some use cases such as cloud computation [54], shared protection [55], multi-flow transponders [56], well-adapted spare for operator equipment, unified hardware platform for manufacturers [43], reach and latency optimization through FEC adaptation, and planning under uncertain traffic forecast [52] thanks to the high adaptability level it provides.In Chapter 4, we propose and evaluate a new use case that consists in triggering $1 + 1$ protection for high priority traffic and optical restoration for low priority traffic using elastic transponders in a multilayer context [57].

Note that, datarate elasticity can be advantageously used within the conventional fixed grid instead of the flexible grid [58], considering the additional investment in optical layer equipment required with flex-grid, and the traffic grooming which would allow to better fill the rigid fixed grid channels. Some studies do not agree with and claim that costly traffic grooming in upper layers can be even eliminated by the means of elastic transponders. Consequently, energy consumption in the network, and latency are well-optimized [33, 34, 43, 46, 56]. In dynamic traffic context, datarate elasticity is shown to be ineffective if elastic transponders do not allow the central frequency of the channel to be moved [59]. In this case, authors propose to implement the flex-grid technology with MLR transponders. Indeed, this statement cannot be generalized as it depends on the optimization objective. In Chapter 4 we compare both MLR and elastic optical networks within the fixed grid and show that the purpose of datarate elasticity is not only to improve the spectral efficiency.

However, in order to take full benefits from datarate elasticity in the optical layer, the IP layer has also to be elastic. In other words, router interfaces and intermediate equipment should have rate adaptation capability. In static networks, this adaptation can be simply achieved deploying only the required number of IP interfaces. In dynamic networks, the unused interfaces or routers can be switched off with the aim of reducing energy consumption. New standards are, however, needed if the IP layer should offer full-flexibility without being constrained by client interface discrete rate [7].

2.3 Network Optimization

Telecommunication network deployment requires a high number of devices which can be connected using different supports of transmission. CAPEX is the cost of the initial deployment, whereas OPEX concerns all expenses required for consumable resources, equipment repair and maintenance during network life time. Offline network dimensioning (known as network planning) is the dimensioning phase that generally minimizes CAPEX required for the initial deployment of the network. In the online dimensioning phase (known as network traffic engineering) some traffic demands are rerouted, aggregated, and reassigned different resources, in order to reduce, for instance, energy consumption by switching off some equipment in sleep mode (multi-hour problem). Online optimization can also be performed with the aim of balancing traffic between links, using different logical topologies each one adapted for a specific interval of time. A global optimization that considers both CAPEX and OPEX is possible. However,

it is quite difficult to perform a global optimization due to the added complexity in addition to the uncertain daily variation of traffic volume [60].

Offline resource provisioning is often accomplished using MILP formulations and meta-heuristics, unlike the online traffic engineering, which is usually performed with simple heuristics, due to the real-time constraints of ongoing connections. The advantage of mathematical formulations is that they can provide a measure of the optimality (optimality gap) of the solution they provide. Heuristics can also use these mathematical formulations for the same purpose. Approximation algorithms can provide a performance bound (e.g., $\rho \neq 1$) of their solutions with respect to the optimal solution (e.g., Γ). It means that the obtained solution is guaranteed to be in the interval $[\Gamma, \rho\Gamma]$ if $\rho > 1$, or in the interval $[\rho\Gamma, \Gamma]$ if $\rho < 1$. However, these bounds are often critical for large problems. The competitive ratio is also a validation criterion for inexact methods. It is the maximum ratio between the optimal solutions and inexact solutions for different instances. Analytical modeling is the most efficient tool to assess the performance of a given system. However, it is quite difficult to have a detailed analytical model for large problems.

In this work, our approach depends on dimensioning context. In general, it is a mix of Mixed Integer Linear Programming (MILP), heuristics and meta-heuristics.

2.3.1 Routing and Spectrum Assignment

As mentioned earlier, RWA problem is NP-complete and it is a particular case of RSA problem which is NP-hard [37]. RSA consists in routing every traffic demand, and allocating a part of spectrum to it for the optimization of a given objective. RSA problem reduces to Spectrum Assignment (SA) problem if traffic demand routing is given as input (e.g., shortest path routing). This approach allows reducing the problem size but does not strongly impact the problem complexity. SA NP-completeness has been proven for whatever physical topology using an analytical notation based on interval graphs [36]. It is even NP-hard in paths for four or more links [61].
In the following, we summarize the state of the art of RSA and SA problems in online and offline dimensioning contexts.

2.3.1.1 Offline RSA

Two approximation algorithms are proposed for RSA problem in chain and ring topologies in which traffic demand routing is trivial [36]. Performance bounds of these algorithms are equal to $2 + \epsilon$, and $4 + \epsilon$ for chain and ring topologies respectively. For arbitrary topology, authors propose and validate a new heuristic by extensive simulations.

In [62] a heuristic algorithm that minimizes the number of required frequency slots, number of hops or multiplication of both parameters, in addition to an ILP formulation is proposed. A new ILP formulation for RSA in OFDM-based flex-grid optical networks is proposed [37]. Such a formulation takes into account the sub-band guard band constraint in addition to RSA constraints (i.e., spectrum continuity, spectrum

contiguity, and non-overlapping constraints), and minimizes the total number of sub-bands used in the whole network. They also propose two heuristic algorithms for large problem sizes in terms of traffic demands and physical topologies.

Spectrum contiguity constraint could be skipped by the Channel Assignment (CA) approach which considers the slot assignment as input. This reduces the optimization space, as solutions that do not satisfy the spectrum contiguity constraint, are excluded from the beginning of the optimization problem. A link-path and a node-link-based formulation using CA approach have been proposed for RSA [63]. According to the authors, such an approach can effectively solve some optimization problems, involving the resolution of RSA, like multi-hour routing and multilayer dimensioning in flex-grid optical networks.

An exact RSA ILP is proposed for OFDM-based optical networks [64]. In the same work, RSA problem is divided into two sub-problems (i.e., routing and SA) each one being optimized separately. Similarly, in [65] both sub-problems are optimized separately using a genetic algorithm for traffic demand routing and a simulated annealing algorithm for spectrum assignment. A baseline algorithm (i.e., first-fit policy with shortest path routing) and a lower bound analytical method are used to validate such a hybrid meta-heuristic.

To summarize, most of heuristics proposed in the related works consider only RSA problem. Obviously, these heuristics cannot be used for the multilayer dimensioning as other sub-problems should be considered as well. In Chapter 3, we propose a k-path-based multi-period planning heuristic, that uses a 0-1 Integer Linear Programming (0-1 ILP) formulation for transponder selection and regenerator placement optimizing optical layer cost in flex-grid optical networks. In Chapter 4, we propose a multilayer genetic algorithm and a MILP formulation for the multilayer dimensioning of elastic optical networks. This MILP can also be used for flex-grid networks provided that the spectrum occupancy is optimized after cost (multi-objective hierarchical optimization).

2.3.1.2 Online RSA

Authors of [66] study the online RSA problem, and propose a new algorithm for ring topology with a competitive ratio of $min\{\theta(log(d_{max})), \theta(log(k))\}$ (where k is the total number of traffic demands, and d_{max} is the maximum number of sub-bands assigned to one traffic demand). They also propose an RSA online heuristic for arbitrary topology and measure its effectiveness by extensive simulations.

Multi-hour RSA in dynamic flex-grid optical networks is extensively studied in [59]. Authors propose an ILP formulation and biased random-key genetic algorithms (variant of genetic algorithms that encodes solution as a vector of random values) to address such a problem.

In dynamic traffic contexts, Routing Modulation level and Spectrum Assignment (RMSA) problem is a well-known problem. Authors of [44, 67] dissociate traffic demand routing from SA, and propose two different heuristic algorithms, with modulation format selection (i.e., datarate elasticity) for SLICE architecture [2]. Authors of [68] propose an extension of Dijkstra's algorithm for the same problem. This extension

aims at finding the shortest paths, taking into account both spectrum continuity constraint, and relationship between datarate and required spectrum (modulation format and channel width selection). Compared to conventional algorithms, this algorithm reduces the blocking of traffic demands.

Authors of [69] tackle RMSA problem with traffic grooming in optical metro ring networks. Because traffic demand routing is trivial in ring topologies, the problem reduces to modulation format selection with SA constraints. An ILP formulation and different algorithms are proposed and evaluated. Authors also show how to analytically compute feasible solutions that can be used as upper bounds for the addressed problem.

A complete non-linear mathematical formulation that takes into account datarate elasticity, and RSA in OFDM-based flex-grid transparent optical networks has been proposed [70]. This non-linear formulation supports both flex-grid and gridless networks. In addition, a decomposition method has been introduced in order to sequentially solve the RSA, and modulation format selection, using two different heuristic algorithms. Authors prove that their decomposition method can find the optimal solution for the complete RSA problem provided that RSA heuristic algorithms can find optimal solutions for the basic RSA problem.

In the literature, it is common to use a spectrum assignment policy when SA is involved in other complicated problems. The most used spectrum policies are:

a) First-Fit: it consists in choosing always the first free slots that satisfy spectrum assignment constraints. This policy is mostly used since it is not complicated in time. The Last-Fit policy is a variant of this provisioning policy as it starts by the last free slot. Generally both are considered as equivalent.

b) Smallest-Fit: it selects the smallest free block of slots. Here, the main idea is to reduce the blocking rate of large traffic demands.

c) Exact-Fit: this policy chooses the first block of slots that exactly fits the required number of slots. This is expected to reduce spectrum fragmentation.

d) Random-Fit: this policy randomly allocates spectrum resources. It is usually used for benchmarking purposes.

In dynamic traffic scenarios, these policies have been evaluated using a Markov chain model in terms of blocking probability [71]. Results show that Exact-Fit policy performed well compared to the other policies. An adaptation of this Markov model is proposed in Chapter 3, in order to evaluate some spectrum fragmentation metrics. A similar single-link Markov model, aiming at evaluating flex-grid performance, is proposed in [72]. This analytical model is subsequently validated by Monte-Carlo simulations in dynamic flex-grid optical networks.

In [61], authors show that SA is equivalent to a specific instance of the traditional multiprocessor scheduling tasks problem. If we consider that processors represent links, and tasks represent traffic demands, then the problem transformation is as follows: a given task must be treated at the same time by all processors (spectrum continuity constraint). A processor cannot interrupt a task after starting it (spectrum contiguity

constraint). The same processor can treat at most one task at the same time (non-overlapping constraint). Using this transformation, the conventional algorithms used for task scheduling on multiprocessor systems, can be used to solve SA problem in flex-grid optical networks.

In [73], authors propose a heuristic algorithm for SA problem together with regenerator placement in translucent optical networks. Heuristic efficiency is shown through the comparison with an ILP formulation that makes use of the CA approach proposed in [63]. They observe that installing additional regenerators in the network can be an effective manner to save on spectrum.

The current work does not thoroughly consider the online dimensioning, even if some proposed tools can be used as well for that purpose. For example, a spectrum fragmentation metric that we propose in Chapter 3 (Section 3.2.3), can be used for online resource provisioning if integrated in whatever RSA algorithm (explained later in Section 2.3.2.2). In addition, the multilayer tool proposed in Chapter 4 deals with the online aspect for a best-effort restoration of traffic in existing free resources (Section 4.3.2 of Chapter 4).

2.3.2 Spectrum Fragmentation

Fragmentation problem already exists in other domains than optical networks. It has been addressed, for time slot management in Synchronous Optical Networks (SONET) protocol [74], and Code Division Multiple Access (CDMA) systems in wireless networks [75]. Similarly, data fragmentation in computer memory, has been studied for a while [76]. However, the optical network context (routing, spectrum continuity, number of slots, network size...), makes spectrum fragmentation a different problem. Therefore, methods and algorithms that have been used to deal with fragmentation in these domains, cannot be used to address optical spectrum fragmentation.

Spectrum fragmentation in optical networks can be viewed according to two dimensions (Fig. 2.4). The first one occurs when some non-continuous free frequency slots are created along the path (horizontal fragmentation). Such fragmentation may be minimized by maximizing spectrum reuse (e.g., minimizing the number of used frequency sots), using for example a graph coloring method [77], a heuristic [41] or, in the worst case, installing costly wavelength converters. The second one occurs when the free spectrum is divided into a set of blocks smaller than the traffic demand width (vertical fragmentation). Therefore, in spite of resource availability, some traffic demands can be blocked due to the lack of enough contiguous free slots. In Chapter 3, we consider only this kind of fragmentation as it is specific to flex-grid technology and does not concern conventional fixed grid optical networks contrary to horizontal fragmentation (wavelength continuity constraint). In the rest of the manuscript, spectrum fragmentation refers to vertical fragmentation.

Several methods have been proposed to address spectrum fragmentation in flex-grid optical networks. These methods can be classified into two categories: proactive and reactive. Proactive methods try to avoid (minimize) spectrum fragmentation before

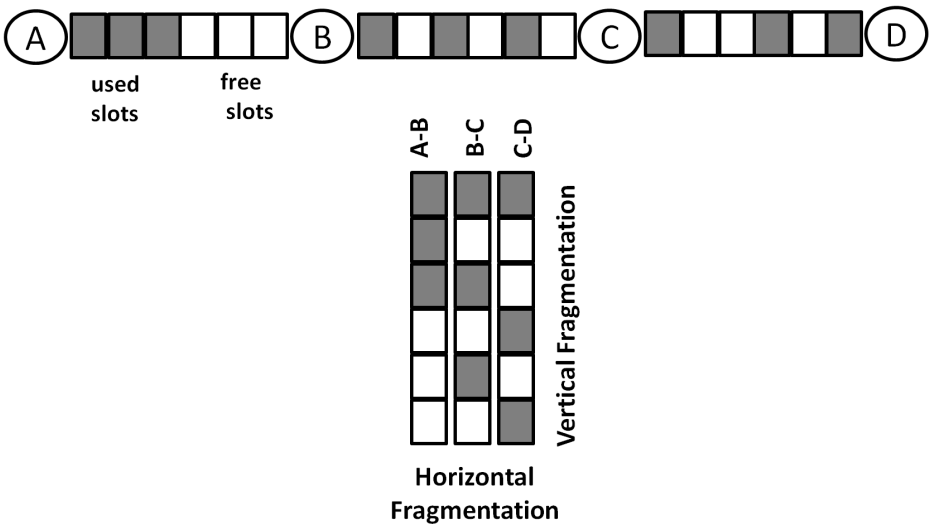

Figure 2.4 — Example of horizontal and vertical spectrum fragmentation for three 6-slot links. The Links B-C and C-D are vertically fragmented and all free slots are horizontally fragmented.

traffic demand blocking occurs, whereas reactive methods deal with spectrum fragmentation after it has taken place.

The most intuitive proactive method consists in considering a fragmentation aware RSA algorithm. It performs traffic demand routing in such a way that spectrum fragmentation is minimized [41]. This method adds complexity to the control plane and does not fully mitigate the issue. It can also have additional expenses if the optimization objective is not cost reduction (e.g., spectrum use).

Spectrum defragmentation can be performed in a proactive way, for example, in a periodical basis, or using a fragmentation threshold (fragmentation metric).

Spectrum defragmentation can also be reactively launched, upon traffic demand blocking. Spectrum defragmentation is however difficult to implement and it increases the complexity in the control plane as explained in Section 2.3.2.3.

Another reactive method consists in splitting the blocked traffic demand into several sub-demands (IM techniques) in such a way that they fit the scattered heterogeneous blocks of slots [38, 41]. However, this method suffers from losing capacity when it deviates from optimal solutions (e.g., superchannels). For instance, 10×100 *Gbps* transponders require more spectrum than 1 *Tbps* superchannel as, in a superchannel, guard bands are not needed between individual sub-bands.

Indeed, reactive approaches have a good knowledge of link fragmentation level as they are used after the blocking. However, they are either difficult to apply, like spectrum defragmentation or spectrally inefficient like IM techniques. In Chapter 3, we propose a new proactive method that allows alleviating spectrum fragmentation taking advantage of traffic forecast.

In the following, we review spectrum fragmentation metrics, used to identify to what extent the spectrum is scattered. We highlight the advantages and drawbacks of each metric and explain why more significant ones are necessary for an accurate assessment

of spectrum fragmentation. Subsequently, we present the most relevant works that have been focused on fragmentation aware RSA algorithms and spectrum defragmentation mechanisms.

2.3.2.1 Fragmentation Metrics

There is still no consensus on the way to quantify fragmentation, although it is considered as a severe problem in dynamic traffic scenarios, where demands arrive and leave randomly [12], and in incremental scenarios where they are continually growing [13]. Different metrics have been proposed to quantify the fragmentation for different purposes. These metrics are used to assess the level of fragmentation of a given network state [76]. They are also used to optimize the network dimensioning in order to improve the provisioning policy if integrated in a fragmentation aware RSA algorithm [3]. Similarly, these metrics are used to calculate the threshold from which defragmentation processes should be run [14, 78].

Spectrum fragmentation in optical network has been quantified using the internal fragmentation metric used in computer memory [71]. Total number of free blocks in the link (spectrum cut) is used as fragmentation indicator in [14, 39, 78]. The consecutiveness of the common free slots has been proposed and shown to be effective in [79]. The fragmentation index quantifies the degree of fragmentation as the maximum total traffic ratio that a link can serve in a given condition to that of the optimal case in which the spectrum is not fragmented [40]. In [13, 80], the entropy concept is used to state the relative fragmentation increase. Let us note that in [80], the horizontal fragmentation is also taken into account. Link and network spectrum compactness metrics are proposed to assess spectrum fragmentation at both link and network levels respectively [81]. The blocking ratio is still the most used indicator to evaluate Spectrum fragmentation. However, blocking ratio can reflect other blocking origins than fragmentation such as the lack of resources, or the blocking that is due to spectrum continuity constraint (horizontal fragmentation).

Nevertheless, none of these metrics consider neither the absolute spectrum loss, nor the transponder granularities. In chapter 3, we propose a new spectrum fragmentation metric called hereafter ABP. This metric identifies the absolutely lost frequency slots and takes into account the transponder model. ABP is evaluated and compared with other metrics using a Markov chain model in dynamic traffic context [82, 83].

2.3.2.2 Fragmentation aware RSA

A fragmentation aware RSA algorithm is an optimization method that consists in assigning paths and spectrum resources to traffic demands in order to minimize spectrum fragmentation. The fitness function of this objective can be, for example, one of the fragmentation metrics explained above.

In [40], four provisioning techniques are identified to allocate spectrum resources to traffic demands requiring heterogeneous datarates. In the "complete sharing" technique, all traffic demands are assigned resources regardless of their datarates using the

First-Fit policy. In "pseudo partition" technique, low datarates are allocated spectrum using the Firs-Fit policy, and high datarates are allocated spectrum using the Last-Fit policy. "Dedicated partition" technique divides the spectrum into different partitions each one being dedicated to a given datarate. Lastly, "shared partition" technique is a generalization of the previous technique, with the possibility for high datarates to access low datarates partitions. Authors conclude that "shared partition" technique allows alleviating spectrum fragmentation [40]. Similar concept of spectrum sharing and partitioning has been proposed in [84]. It has also been proposed taking into account datarate variation in dynamic scenarios [85].

Three fragmentation aware RMSA algorithms have been proposed and compared with both shortest path routing and balanced load routing [39]. These algorithms use as a fragmentation metric the cuts (vertical fragmentation) and the misalignment (horizontal fragmentation) that would be created if a given part of spectrum is allocated on a given lightpath. Their algorithms perform well on two different physical topologies.

The Shannon entropy metric is applied to an RSA algorithm in two different ways [13]. In the first way, Shannon entropy is applied to each block of slots in each link of the candidate path, before summing the quantified fragmentation on each link. The path and the continuous block with the lowest sum is selected. The other way consists in bitwise-OR'ing all links and then applying the Shannon metric to the resulting state of all bitwise-OR'ed links. The first method performs better and allows unblocking up to 10% of blocked traffic demands with respect to the classical shortest path routing scheme. In [81] the spectrum compactness metric is implemented in a distributed RSA algorithm, and used as a threshold from which the spectrum defragmentation is automatically triggered.

In [86], authors propose an idea similar to the "shared partition" technique proposed in [40]. It takes into account requests requiring Immediate Reservation (IR) and ones that can be known in advance requiring Advance Reservation (AR). The challenge is to guarantee a fair provisioning for both types of requests while reducing spectrum fragmentation. To this end, authors propose an RSA algorithm whose main idea can be summed up into three points:

- Classify spectrum into multiple prioritized area according to the required number of slots (i.e. transponder granularity)
- Divide each prioritized area into two sub-areas: the first is dedicated to IR requests, and the second is shared between IR and AR.
- IR requests can exploit any possible path, while AR requests are limited to the shortest one.

The efficiency of such a method is shown through simulation. However, results seem to strongly depend upon traffic matrix and traffic load.

In [87] authors propose to use a 3D RSA algorithm that takes into account spectral, temporal and spatial dimensions. With this algorithm, the blocking probability is remarkably reduced compared to a shortest path routing algorithm with a First-Fit provisioning policy.

2.3.2.3 Spectrum Defragmentation

Spectrum defragmentation consists in changing the central frequencies of existing connections with the aim of reducing spectrum fragmentation. Four spectrum defragmentation techniques have been proposed, each one having its advantages and drawbacks.

a) Conventional defragmentation (CD): in this type of spectrum defragmentation all the existing connections are interrupted and allocated their new optimized central frequencies [14]. This technique can be seen as a simple rerouting of traffic demands with however the interruption of each connection to be moved. The advantage of this approach is that the physical path can be changed too, which allows better minimizing spectrum fragmentation.

b) Make-Before-Break (MBB): this technique is a particular case of conventional defragmentation. It relies on the reservation of the spectrum required for the connection to move, before transmitting on the new central frequency [88]. It is a hitless (no traffic interruption) technique since the old connection is kept working until the new one is established. This can be seen as a drawback as this technique necessitates twice the spectrum used by each connection, and additional transponders.

c) Push-And-Pull (PAP): it consists in shifting the spectrum towards its new central frequency. This is possible by simply tuning the transmitter over the spectrum, while maintaining traffic emission. However, all intermediate frequencies must be free at the moment of switching, and all ROADMs (on the transparent lightpath) must be tuned accordingly. The first constraint can be quite restrictive due to the spectrum continuity constraint. Push-And-Pull advantage compared to Make-Before-Break is in the spectrum use, as the former does not require twice the channel spectrum, nor additional transponders [78].

d) Hop Tuning (HT): in this technique the transmission is interrupted during a very short interval of time, in which the connection can be moved to any desired location with no impact on the existing connections. This interruption allows avoiding the limitation of intermediate frequencies, and it is estimated to be below $400ns$, exploiting fast tunable lasers [89]. The advantage of this technique is that it allows moving several connections simultaneously, and it permits to make a full defragmentation. The main inconvenient lies in the complexity in the receiver side as the receiver should be able to track automatically the transmitter, when moving to the spectrum target, within a short period of time [90].

Table 2.2 shows a qualitative comparison between the spectrum defragmentation techniques. It is worth noting that each one of these techniques can be implemented in a fragmentation aware RSA in either reactive or proactive way.

These techniques can be combined with the aim of reducing the total number of interrupted connections. In [91], authors propose two adaptive algorithms for an efficient spectrum defragmentation in dynamic flex-grid optical networks. The first algorithm is based on both conventional defragmentation and Make-Before-Break technique, whereas the second algorithm makes use of both conventional defragmentation

Defragmentation technique	CD	MBB	PAP	HT
Defragmentation time	Very slow	Slow	Slow	Fast
Traffic interruption	Yes	No	No	Yes
Additional transponder/spectrum	No	Yes	No	No
Spectrum limitation	No	No	Yes	No
Full defragmentation	Yes	No	No	Yes

Table 2.2 — Comparison of spectrum defragmentation techniques.

and Push-And-Pull techniques. Results show that combining both algorithms allows reaching good blocking performance while reducing the number of interrupted connections. Hop Tuning and Push-And-Pull techniques are compared in terms of bandwidth blocking probability, and average number of operations in [90]. Results indicate that Hop Tuning defragmentation allows achieving better performances. Conventional defragmentation and Push-And-Pull techniques are triggered together, using a reactive RSA algorithm. This algorithm uses as threshold the number of recursion resulting from the Push-And-Pull technique. Results show that a trade-off between performance and running time can be found with variation of recursion threshold [92].

In a nutshell, spectrum fragmentation is somewhat controversial in the state of the art. It is sometime considered as a serious problem that necessitates a quite effective defragmentation technique [12–15]. Another point of view assumes that its impact is negligible for some physical topologies that mostly use the same small channel width (i.e., 3 slots) [67]. According to the authors of [93, 94], triggering spectrum defragmentation dynamically is difficult to implement from a control plane point of view, and it is avoidable in networks with moderate dynamicity [95]. In Chapter 3 we provide an in-depth study on this matter, and propose some well-adapted strategies to the specific incremental traffic context of operator core network.

2.3.3 Survivability in Flexible Optical Networks

Network operators have been looking for a robust and a cost effective way of designing optical networks in order to minimize service disruptions. Many restoration architectures, with different cost and performance, have been proposed. For example, upon failure detection, IP restoration sends a failure notification to the control plane and concerned entities and establishes physically disjoint and IP ended lightpaths within tens of milliseconds [96]. Optical restoration (also called photonic restoration) consists in switching traffic in the photonic layer onto a dedicated redundant lightpath using a photonic switch instead of an electrical switch, while maintaining the use of the same end-point equipment previously used by the failed connection [97]. It can significantly reduce the number of deployed pieces of equipment as long as backup paths do not require much signal regenerations, with the drawback that edge nodes remain unprotected, unlike in IP restoration. Optical restoration time is also another drawback of this architecture, as it can last several minutes leading to an ill-adapted process regarding Quality of Service (QoS) requirements of some requests.

Multilayer restoration is a recovery process in which both IP restoration and optical restoration are involved. In the literature, many works have thoroughly discussed the required interactions between both layers in a differentiated class of service context [98, 99]. Elastic transponders have been proposed for IP restoration for high priority traffic (or gold traffic) in order to support longer backup paths, adapting datarate to the gold traffic. In this use case, best effort traffic is either restored in the free existing resources or dropped [100].

In [101], authors shed light on the fact that in current transport optical networks, traffic requests are groomed in the IP layer irrespectively of their QoS requirements, leading therefore to a blind QoS-unaware treatment in the optical layer. Consequently, they propose a novel application-centric architecture that grooms traffic demands with same/similar requirements, which simplifies leveraging differentiated services with respect to traffic requirement. This architecture allows performing an optical restoration for low priority traffic, and an IP protection for service disruption/latency-sensitive requests. Authors believe that flex-grid technology is an efficient mean to overcome spectrum overprovisioning that would occur within the fixed grid due to the new constraint of traffic grooming (i.e., grooming of demands with similar requirements).

Under single failure assumption, authors of [55] propose a novel shared protection architecture based on datarate elasticity and flex-grid technology. This architecture allows different backup traffic demands to share spectrum if a) their working demands are disjoint, and b) if these backup traffic demands share the same physical link. Datarate elasticity herein allows managing the overlapping of the contiguous channels that are grooming backup traffic with working traffic.

In Chapter 4, we propose a new optical restoration use case that benefits from datarate elasticity and lowest priority traffic in a multilayer context. Compared to previous studies, our proposed use case performs the optical restoration with elastic transponders in a differentiated Class of Service (CoS) context, taking advantage from the slow optical restoration time.

2.3.4 Flex-grid and Link Margins

Conventional networks were designed to maximize link capacity and transponder reach, regardless of the actual traffic volume. This has resulted in the overdimensioning of some optical resources increasing link margins. For example, we can cite the amplifier power reserve (e.g., amplifier maximum power is significantly more than the optimum required power in the design), the channel width (e.g., real spectrum width is significantly less than the channel spacing), and the Signal to Noise Ratio (SNR) (e.g., real distance is significantly less than the transponder reach).

Flex-grid technology combined with datarate elasticity, allows a good provisioning of some of these wasted resources, and can translate their use in favour of the optimization of some objectives like cost [102], capacity [103, 104], and energy [52].

In the literature, link margins are mostly used to increase network capacity, by using for example, high order modulation formats or freeing spectral resources for future use. Different strategies have been discussed with the aim of reducing link margins,

taking benefit from datarate elasticity [105]. Power management in MLR fixed grid optical networks has been discussed in [106]. The optimal combination of launch powers depending on required channel datarates, is shown to lead to considerable savings in network overall cost. Considering a load-dependent reach, the number of signal regenerations in the network can be significantly reduced for lower-order modulation formats thanks to power optimization [102]. Adapting the SNR to the signals and adapting the signals to the available SNR are shown to be equivalent in terms of network throughput with further complexity in the former approach [104]. Link margins can also be used to significantly increase network capacity using high order modulation formats at SNR limit [103].

In summary, researchers are already aware of the wastage of these margins, and they have been looking for relevant use cases in order to overcome this issue. Optical layer flexibility simplifies this task, but it does not deal with all the underlying reasons for that wastage (e.g., optical power). In Chapter 5, we propose to use power margins to minimize the cost of flex-grid network deployment by keeping in use power-limited EDFA amplifiers.

2.4 Contribution Positioning and Concluding Remarks

In the literature, flexible optical networks are seen as the main candidate for the next generation of transport optical networks. Their significant theoretical increase of fiber capacity (i.e., 33%) and their capability to accommodate future high datarates requiring more than 50 GHz, in addition to the relevant use cases they provide, are the main reasons for this potential evolution. However, with the advent of optical layer flexibility (i.e., flex-grid and datarate elasticity) several issues arise, and some questions are still open with no credible and/or convincing responses.

Flex-grid gain in capacity being, say, the first argument that pushes network operators to migrate their networks is not really agreed. It depends on how it is calculated: in bps (throughput) or in Hz (freed spectrum). This is related to the fact that fiber capacity is different from network capacity, due to RSA constraints. In the literature, different values can be found, and they can even exceed 100% being widely far from the theoretical gain.

We explain this exceeding by the impact of two parameters. The first one is the transponder model, from which the theoretical gain in capacity is defined at the link level. The second parameter is the maximum number of paths that can be used to serve a given traffic matrix (i.e., K-path routing). This last parameter operates at the network level, and it prevents from having a quantifiable theoretical limit for flex-grid capacity gain as it depends on many factors: the physical topology, the way path lengths are calculated (distance or hops), the single/multi-fiber planning, and the optimization objective (cost or capacity).

In the current work, we aim at surrounding flex-grid gain in capacity, considering different topologies, and opting for the next generation of WDM transponders which

we consider to be the most probable in the coming years. We also consider a hierarchical optimization that first minimizes cost and then spectrum occupancy, while constraining the k-shortest path routing by realistic limits (up to five paths).

Potential savings in cost are also covered in this work, even if researchers seem to confirm that they are rather produced in the long term. Indeed, this is due to the in-first-day deployment of flex-grid specific equipment like ROADM and EDFA amplifiers. Datarate elasticity also has an additional cost with respect to conventional fixed rate transponders. Both Chapter 4 and Chapter 5 are dedicated to the potential impact of flex-grid equipment on flexibility gains in terms of cost and capacity. Specifically, a new class of service based architecture for traffic restoration is proposed and evaluated. In addition, a novel migration policy that takes benefit from link margins is evaluated, in order to keep in use legacy EDFA amplifiers, and therefore minimize flex-grid additional cost. In Chapter 5, we show the extent of this impact and propose to set per-channel optical powers to their minimum requirements depending on the traffic volume.

Spectrum fragmentation as the main drawback of flex-grid technology is somewhat controversial leading rise to different studies and results in the field. In Chapter 3, we propose new relevant metrics to quantify spectrum fragmentation in an operator network context. Indeed, the absolute spectrum loss induced by spectrum fragmentation has never been quantified in the literature. Subsequently, we focus on the fragmentation resulting from the non-contiguity of frequency slots as it is specific to flex-grid technology. We propose some traffic engineering strategies to deal with spectrum fragmentation instead of hardly implementing some spectrum defragmentation techniques.

Regarding the methodology aspect and tools, it has to be noted that related works are more focused on RSA problem independently from sub-problems together with their related use cases. Therefore, the challenge is to propose comprehensive tools that take into account, in addition to RSA, all sub-dimensioning problems (i.e., traffic demand grooming, WDM regenerator placement, wavelength conversion capability, transponder/IP interface selection) for flex-grid and/or datarate elasticity.

To that end, we study the dimensioning problem in two different manners. First, we consider a hierarchical dimensioning that considers all the sub-problems above using cascaded heuristics and MILP/Integer Linear Programming (ILP) formulations. Indeed, this approach is commonly used thanks to its lower complexity and because of some operational constraints (explained later on in Chapter 3).

Afterwards, we move to the multilayer dimensioning that considers a joint optimization of all sub-problems above in a joint manner. A genetic algorithm for large instances and a MILP formulation for its validation are proposed and detailed in Chapter 4. In the same Chapter, a mix of both approaches is used for the evaluation of much more complicated scenarios combining both online and offline dimensioning.

To complete the dimensioning tools above, we propose a new link design method that estimates the performance of the established connections and allows launched power adaptation while guaranteeing acceptable performances for optical signals (Chapter 5).

CHAPTER 3

On the Evaluation of Spectrum Fragmentation

3.1 Introduction

In Flex-grid technology, the fine frequency slot together with the flexible grid allows an adjusted tailoring of the channel width which permits to save a significant part of spectrum resources. Nevertheless, due to filtering limits, optical channel narrower spacing may reduce transmission performance (optical reach). Guard bands solve this filtering issue but reduce flex-grid saved spectrum.

Superchannels [107] are an interesting solution to this problem. Actually, they offer an ideal trade-off between spectrum saving and transmission performance. It is due to the fact that guard bands are only required between superchannels themselves and no longer between individual sub-channels.

However, considering both superchannels and flex-grid technology, spectrum resources are more sensitive to spectrum fragmentation due to heterogeneous channel widths (i.e., transponder granularity). Thus, large traffic demands are more likely to be blocked even with free frequency slots. Moreover, this fragmentation can create unusable isolated slots or blocks of slots that can affect flex-grid technology benefits.

Related works often consider dynamic traffic scenarios to evaluate spectrum fragmentation and different approaches have been proposed [12, 38, 39, 41, 79]. These approaches consist in either avoiding as much as possible spectrum fragmentation in planning processes, splitting traffic demands or reallocating some central frequencies (spectrum defragmentation). The blocking ratio is frequently used to demonstrate the robustness of a given approach even if there are other origins of traffic demand blocking than fragmentation.

We believe that spectrum fragmentation definition can be refined. To this end, we propose a clearer definition, and we use it to identify the best suited approaches in operator network context. We consider the fragmentation resulting from the spectrum continuity constraint and the fragmentation resulting from the spectrum contiguity constraint. Indeed, the latter appears with flex-grid technology and is related to optical channel flexibility (optical channels can have different widths), while the former

already exists in conventional networks and it can be completely solved using wavelength converters. For this reason, we do not evaluate the fragmentation that is due to spectrum continuity constraint. We then classify spectrum losses due to spectrum fragmentation into two categories explained hereafter: absolute and relative spectrum losses, and propose a fragmentation metric for each category. Subsequently, we compare the relative fragmentation metric with others in dynamic traffic context.

We next focus on a specific operator network context in which traffic behavior is incremental. In order to identify the possible relationship between superchannels and spectrum fragmentation, a new traffic strategy that promotes superchannels is defined and evaluated.

Conventional fixed grid networks do not face the spectrum contiguity constraint. However, the optical channel flexibility is introduced when superchannels are used with respect to this conventional fixed grid (this is equivalent to flex-grid with a fixed 50 GHz frequency slot width). In this way, we can identify the impact of using a fine grid on spectrum fragmentation, and dissociate it from the one due to heterogeneous granularities (channel flexibility).

In a nutshell, we aim at evaluating to what extent spectrum fragmentation is a problem in operator network context, by identifying parameters that influence spectrum fragmentation and deriving good practices in this specific context.

3.2 Fragmentation Metrics

Spectrum fragmentation leads to two types of spectrum loss in optical networks. The absolute spectrum loss occurs when some free slots cannot be used whatever the required granularity is. This kind of loss can be modeled as a knapsack problem whose objective is to optimally fill the fiber (knapsack) with used granularities (objects): G= $\{G_1, G_2...G_m\}$. Free slots (places) are then completely lost and cannot be used unless a spectrum defragmentation process is performed.
Model (3.1) allows quantifying these lost slots ($LS = SB - Z$) where SB denotes the size of the block to be evaluated, Z is the maximum number of slots that can be used in the most favorable case, and Y_i is the number of times the granularity $G_i \in G$ must be used in optimal solution.

$$Max\ Z = \sum_i Y_i G_i \tag{3.1a}$$

$$Subject\ to\ Z \leq\ SB \tag{3.1b}$$

$$Y_i \in \mathbb{Z}_0^+ \tag{3.1c}$$

The second kind of spectrum loss is relative as large granularities are more likely to be blocked than minor ones. Thus, for a given state of the fiber a relative value is needed in order to assess the level of fragmentation. This is what some existing metrics aimed at.

The most used criterion to demonstrate that a given metric minimizes the fragmentation is the traffic blocking ratio between blocked demands and served demands. However, the information given by this criterion is insufficient, as traffic blocking ratio can result from lack of resources or spectrum continuity constraint in transparent networks. For this reason, it is relevant to identify another criterion to quantify the blocking caused only by spectrum fragmentation.

To compare different metrics, mathematical modeling methods are more efficient and more accurate compared with simulation ones. A Markov chain model is proposed in [71] to compare usual spectrum allocation policies in flex-grid network. To evaluate metric performance, we adapt this model to identify the metric that allows the best spectrum use and minimizes spectrum fragmentation. To this aim, we use the blocking probability due to fragmentation as an efficient criterion for the comparison (referred as fragmentation blocking probability).

It is difficult to build an exhaustive fragmentation metric taking into account all fragmentation sources while keeping a low implementation complexity compliant with a possible implementation in a control plane. However such a metric could be used to quantify the spectrum fragmentation level in order to eventually reduce its impact. Nevertheless, only few metrics exist and the existing ones suffer from some limits that we are detailing hereafter.

To compare the relevance of the different metrics applied to optical networks, we compute their complexity defined by the number of operations, and determine a relative value meaning mark with a number of stars from 1 to 7. This secondary criterion shows to what extent a metric returned value is meaningful (Table 3.1). Mark attribution is done according to whether the metric can identify the following seven link cases or not:

(a) all slots are free (spectrum is not fragmented)

(b) all slots are used (spectrum is not fragmented: blocking caused by lack of resources)

(c) all free slots are contiguous (spectrum is not fragmented)

(d) fragmented cases that do not reduce fiber capacity (spectrum is not fragmented)

(e) all free slots are lost (spectrum is completely fragmented: absolute loss)

(f) the more the spectrum is fragmented the greater is the returned value (relative fragmentation)

(g) non-complexity

3.2.1 External Fragmentation Metric (EF)

Fragmentation in computer memory has been intensively studied in the literature. Although it is different from spectrum fragmentation problem, External Fragmentation

(EF) metric can be used in the optical network context. The most common metric consists in calculating the ratio of the largest free contiguous fragment of memory to the free memory [76] as in Equation 3.2.

$$EF = 1 - \frac{Largest\_Free\_Fragment}{All\_Free\_Memory} \tag{3.2}$$

The main limit of EF metric is that it does not take into account small fragments if the size of the largest block does not change. Thus, it does not prevent from creating small fragments. Furthermore, EF returned value is not always meaningful because this metric is not able to determine if memory resources (i.e. spectrum by analogy with optical networks) are completely fragmented or to identify the potential fragmentation impact on fiber capacity.

Regarding the complexity, EF considers only the largest block and has a simple formula (g). It can identify the case (c) in which all free resources are contiguous, since in this particular case the largest block size is equal to the total free memory. EF also gives a relative value correlated with fragmentation level that can identify the relative fragmentation increase: case (f). However, this metric is not able to distinguish the fully fragmented cases since it never reaches the value one. Based on these considerations we attribute three stars to EF (Table 3.1).

Table 3.1 — Characteristics of metrics

metric	Characteristics		
	Complexity (n[1], m[2])	Output interval	Value meaning
EF	$n+1$	$[0,1[$	***
Shannon Entropy (SE)	$4n$	$[0,+\infty[$	***
ABP	$4n(m-\frac{1}{4})$	$[0,1]$	****

3.2.2 Shannon Entropy Fragmentation Metric (SE)

In information theory, the entropy estimates the information amount contained in a message. Based on this concept, Shannon entropy has been used in [13] as a quantitative metric for spectrum fragmentation measurements.

For every free fragment f if S_f denotes the number of slots in f and S denotes the total number of slots in a fiber, SE estimates the fragmentation value as in Equation (3.3a).

Since the number of free slots is constant in all provisioning possibilities and as S is a constant term, equation (3.3a) can be simplified to Equation (3.3b) which returns the same logical value when different cases are compared, and it allows reducing SE complexity by half factor.

[1] number of fragments
[2] number of granularities

Like EF metric, SE cannot conclude whether the spectrum is completely fragmented or not as it does not consider the absolute loss. The only case in which SE value makes sense is when all resources are free: in this case it returns zero (a). For instance when all used frequency slots are contiguous (spectrum with no fragmentation), SE value depends on the number of these frequency slots. Plus, this metric does not differentiate the case in which spectrum fragments match the available granularities (fiber capacity is not impacted) from the unsuitable fragmented cases. However, SE can efficiently identify relative fragmentation and can be used for the comparison between two fragmented cases (f). Regarding the complexity criterion, SE linearly depends on the number of fragments like EF (g). Therefore, we mark SE value meaning with three stars (Table 3.1).

$$SE = \sum_{f} \frac{S_f}{S} ln\left(\frac{S}{S_f}\right) \tag{3.3a}$$

$$SE' = \sum_{f} S_f ln\left(\frac{1}{S_f}\right) \tag{3.3b}$$

3.2.3 Access Blocking Probability Metric (ABP)

We propose ABP to quantify the fragmentation. The concept of ABP is as follows: based on the fact that blocking is strongly dependent on transponder granularities being used, ABP calculates the ratio between the sum of the cardinalities of the granularity set that can be used in every fragment fi and the cardinality of the granularity set that can be used if all free slots are contiguous as in Equation (3.4).

$$ABP = 1 - \frac{\sum_{i=1}^{n}\sum_{k=1}^{m}(f_i \ DIV \ G_k)}{\sum_{j=1}^{m}(\sum_{l=1}^{n} f_l) \ DIV \ G_j} \tag{3.4}$$

where DIV denotes the integer division and G is the available granularity set.

ABP metric can meaningfully determine the fragmentation level. For instance, when all fragments are smaller than the smallest granularity (spectrum is completely fragmented) ABP is equal to one: case (e). It is equal to zero when the spectrum is not fragmented: cases (a) and (c) or when the fragments match the available granularities: case (d). ABP can also be used for the comparison (relative fragmentation) as it returns a relative value between zero and one: case (f). However, like EF metric, ABP cannot differentiate the link case (a) from the link case (c). Based on these considerations, this metric appears to be more relevant than the other metrics and we attribute four stars to its value meaning (Table 3.1).

Figure 3.1 shows different values measured by each metric for four ten-frequency slot links. Due to the fact that EF and SE do not take into account the possible granularities, they may favor situations where some granularities cannot be used. For instance, according to these metrics in Fig. 3.1 c) spectrum is less fragmented than in Fig. 3.1 b) whereas it is just the opposite, because in the former the two-slot block can no longer

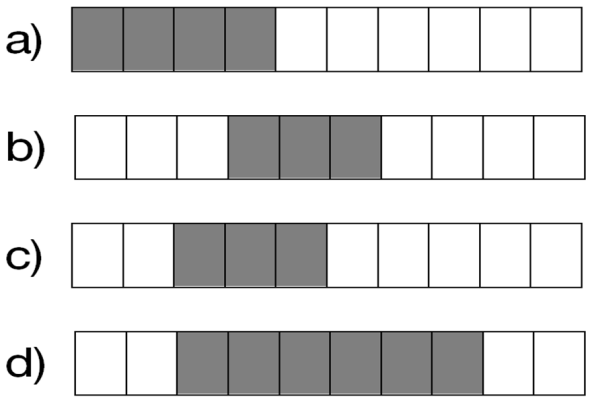

Figure 3.1 — Example of fragmentation measured value by each metric for four different links (used slots in gray and free slots in white) with 3 slots, 4 slots as possible granularities.
a) EF=0.00, SE=0.30, ABP=0.00 b) EF=0.42, SE=0.72, ABP=0.00
c) EF=0.28, SE=0.66, ABP=0.33 d) EF=0.50, SE=0.64, ABP=1.00

be used, since it is smaller than the smallest granularity (three in this example). ABP metric has thus the advantage to deal with available granularities. As we can see in Fig. 3.1 b) the fragmentation value is zero because this kind of fragmentation does not affect the fiber capacity. In Fig. 3.1 d) all free resources are absolutely lost, this information can simply be read from ABP returned value.

However, ABP formula is complex compared to other metrics since it depends on both the number of free fragments and the number of possible granularities as shown in Table 3.1.

In the previous sections, we have introduced fragmentation metrics and have made a global comparison. General results indicate that ABP is more meaningful than the others but more complex. We expect that the impact of the added complexity will be acceptable, seeing that it depends on the number of transponder type in the stock. However, our metric assumes that the use of all transponders is equiprobable. If not, weighting the granularities would improve the significance of relative fragmentation values.

In the following, we perform an accurate comparison of the metrics above, in terms of fragmentation blocking probability and spectrum use in dynamic traffic scenario.

3.2.4 Single Link Modeling

In order to properly model the system, the analytical model is chosen to be independent from all metrics. It has also to consider the blocking caused by spectrum fragmentation only, when it calculates the blocking probability as mentioned above.

We adapt the model proposed in [71] using a Continuous-Time Markov Chain (CTMC) to compare the different metrics. CTMC is a stochastic memoryless approach (the transition from one state to another depends only on the current state and not on the previous states) with a limited state sequence, in which the holding time follows an exponential distribution.

Table 3.2 — Demand types

Granularity (slots[4])	Datarate (Gbps)
1	10
2	40
3	100
4	200

As mentioned earlier, we are only interested in the vertical spectrum fragmentation caused by flex-grid technology. Thus, the system can be well and truly represented by one fiber and its frequency slots [72][3]. All possible instantaneous fiber states (instantaneous spectrum occupancy) represent the CTMC state space S_t.

Considering a dynamic provisioning scenario, different demand types in Table 3.2, are following a Poisson distribution with a homogeneous arrival rate λ and an exponential holding time $1/\mu$. The load of the system is therefore λ/μ.

Every metric has its own CTMC depending on whether the transition between states is possible or not, and therefore, there is a different steady-state vector (π) for every metric.

In order to illustrate the model, we show the state diagram for a three-slot fiber (number of slots per fiber SL=3) and we consider only one possible granularity assumed equal 1 slot (Fig. 3.2). In this particular case, the state diagram is the same for all metrics.

Since demand departure is independent from the metrics, the network dynamic behaviour can be considered as the most important parameter leading to spectrum fragmentation in the investigated system. If the dynamic feature was not allowed, most of the transitions to fragmented states would have been canceled.

From the state diagram, the so-called transition rate matrix (Q) can be easily found (Table 3.3). The maximum number of states in the diagram is 2^{SL-1}. The diagonal of the matrix Q must be filled in such a way that the sum in each row is equal to zero.

Once the Q matrix is constructed, the linear system (3.5) has to be solved. Equation (3.5a) is obtained based on the stationary distribution property when time tends to infinity ($t \to \infty$). Equation (3.5b) constrains the set of possible solutions for Equation (3.5a), because the sum of all steady-state probabilities must be equal to one.

$$\pi Q = 0 \tag{3.5a}$$

$$\sum_{i \in S_t} \pi_i = 1 \tag{3.5b}$$

[3]In the case of a real network, the metrics can be applied on all the paths by calculating the sum of fragmentation values corresponding to different links

[4]These demands types are only used with the dynamic provisioning scenario and not in incremental scenario.

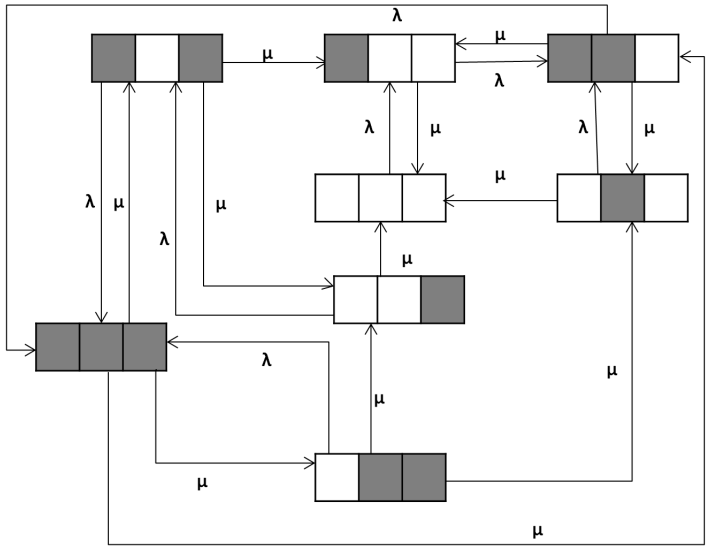

Figure 3.2 — Example of diagram state for a three-slot fiber and 1-slot granularity. A used (free) slot is in gray (respectively white). Transition from one state to another is represented by a directed arrow with an arrival or a service rate depending on the event: arrival or departure. In this particular case, all metrics have this diagram state in common.

where $\pi(\pi_0, \pi_1 ... \pi_{2^{SL}-1})$ is the steady-state vector for the matrix Q (π_i is the probability that the system is in state $i \in S_t$).

To distinguish the blocking states that are due to resource lack from the ones due to fragmentation, the blocking probability P_g^i for different demand types $G_g \in G$ in the state $i \in S_t$ can be calculated as in Equation (3.6). This equation only considers the blocking if there are free resources. For instance, in Fig. 3.2 there is no blocking caused by spectrum fragmentation for the granularity ($G_g = 1$). The only blocking is caused by resource lack when all slots are used.

$$P_g^i = \begin{cases} 1 \; If \; ((G_g \leq \sum_l f_l) \; and \; (G_g > largest(f_l)) \\ \\ 0 \qquad\qquad\qquad\qquad\qquad\qquad Otherwise \end{cases} \tag{3.6}$$

The total blocking probability in the system for a demand type $G_g \in G$ equals the sum of the probabilities corresponding to states in which this demand type is blocked because of spectrum fragmentation: Equation (3.7). In other words, P_g is the time fraction during which the system is in states where the granularity G_g cannot be used because of spectrum fragmentation. Note that P_g cannot be equal to one, even if the granularity G_g is greater than the maximum number of possible slots in the fiber, simply because P_g concerns only the blocking due to fragmentation.

The sum of blocking probabilities for every demand type ($G_g \in G$) is denoted P. This sum is used in the following as an efficient criterion correlated with the blocking in the

[5]For simplicity the state identifier in Fig. 3.2 is converted from binary to decimal, for example, the state in which all slots are used (111) is called here 7.

Table 3.3 — Transition rate matrix

States[5]	0	1	2	3	4	5	6	7
0	$-\lambda$	0	0	0	λ	0	0	0
1	μ	$-\lambda-\mu$	0	0	0	λ	0	0
2	μ	0	$-\lambda-\mu$	0	0	0	λ	0
3	0	μ	μ	$-\lambda-2\mu$	0	0	0	λ
4	μ	0	0	0	$-\lambda-\mu$	0	λ	0
5	0	μ	0	0	μ	$-\lambda-2\mu$	0	λ
6	0	0	μ	0	μ	0	$-\lambda-2\mu$	λ
7	0	0	0	μ	0	μ	μ	-3μ

whole system as in Equation (3.8): the fragmentation blocking probability.

$$P_g = \sum_{i \in S_t} P_g^i \pi_i \tag{3.7}$$

$$P = \sum_{G_g \in G} P_g \tag{3.8}$$

Based on the same steady-state vector, Equation (3.9) calculates the average throughput (Th) in the whole system for a given metric, where n_{ig}, b_g, μ_g denote respectively the number of current demands in state $i \in S_t$, the datarate and the service rate corresponding to the demand granularity $G_g \in G$. n_{ig} is calculated based on the maximum capacity, the current state can sustain.

$$Th = \sum_{G_g \in G} \sum_{i \in S_t} n_{ig} b_g \mu_g \pi_i \tag{3.9}$$

3.2.5 Comparison Results

Since the size of the state space S_t is exponentially proportional to the number of slots by fiber (SL), numerical results have been obtained for a ten-slot fiber only. However, these results can be generalized for larger instances.

In order to demonstrate the interest of using metrics instead of an allocation policy for spectrum provisioning, we compare the widely used First-Fit (FF) conventional allocation policy with the three metrics (EF, SE, and ABP). This policy always allocates the first free slots to demands upon their arrival.

In Fig. 3.3, we compute the blocking probability in the whole system for FF, EF, SE and ABP versus the system load. ABP metric is the best one in terms of blocking probability whatever the traffic load value. This is mainly due to the fact that ABP metric deals with available granularities and tries to avoid situations where these granularities

are blocked. As expected, in comparison with FF policy, the three metrics significantly reduce the blocking probability. This confirms the necessity to apply a more efficient provisioning strategy in order to reduce the spectrum fragmentation, instead of the ones commonly used in conventional optical transport networks. This is typically true when the network is highly loaded (the blocking probability of FF exceeds 30%), and thus when fragmentation is the most probable.

Figure 3.4 shows the theoretical average throughput, the system can reach. The throughput is a relevant performance criterion because it is strongly affected by spectrum fragmentation: when the number of free and contiguous frequency slots increases in the system, its theoretical capacity increases too. In Fig. 3.4 the average throughput is decreasing with the load increase. In other words, when the load increases, the system remains longer in states where the free spectrum is either fragmented or null. Reversely, when there is no demand in the system, the theoretical average throughput is maximum: all resources can be used.

ABP metric is again the most efficient metric in terms of average throughput, but the curves in Fig. 3.3 and Fig. 3.4 have rather different behaviors. As described above, the average throughput is directly derived from the steady-state vector (Equation (3.8)). It is then influenced at the same time by the spectrum fragmentation and the lack of resources. It explains the observed difference between the curves in Fig. 3.3 and Fig. 3.4. Indeed, in Fig. 3.4, the gap between FF and the other curves is smaller than the gap in Fig. 3.3 and it is wider between EF and SE.

Since FF policy creates more fragments in the spectrum (Fig. 3.3), it rejects more demands than the metrics do, and consequently it is less blocked due to resource lack. It allows FF to improve its behavior in comparison with the results observed in Fig. 3.3. For the same reason, the difference between results from SE and EF metrics is more noticeable.

In conclusion, the gaps between the different curves from Fig. 3.4 are explained by the ability of the different schemes (FF policy or ABP, SE and EF metrics) to remain more or less time in states where the free spectrum is fragmented.

In Fig. 3.5, different metrics are compared in terms of probability to be in the state where there is no free slot (all resources are used). It is an interesting parameter because it reflects the blocking ratio: the more a metric rejects demands (because of fragmentation), the less it is in this state. Fig. 3.5 shows that all curves (case in which all slots are used) are growing with the load increase, as expected, with an advantage of ABP metric to be more efficient in terms of spectrum use.

Please note that fragmentation impact will be more important for real instances, because the number of cases where blocking is related to fragmentation (not to resource lack) is proportional to the number of slots in the fiber. Note also that comparison results (Fig. 3.3, Fig. 3.4, Fig. 3.5) are valid in low traffic load scenarios but they cannot be represented on the same scale as the high load results. In low link load scenarios, spectrum fragmentation has no significant impact. This point will be discussed later on when the relationship between link load and spectrum fragmentation is tackled.

So far, fragmentation metrics are compared with a FF provisioning policy in dynamic traffic scenario. Results show the interest of using a fragmentation metric instead of a

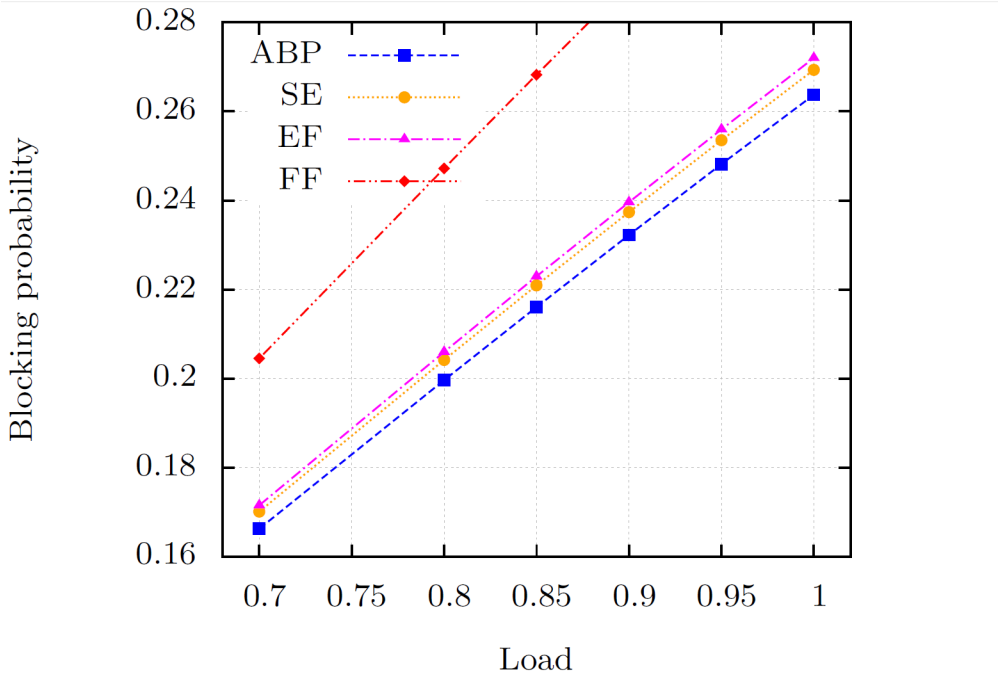

Figure 3.3 — System blocking probability versus system load for ABP (Access Blocking Probability), SE (Shannon Entropy Fragmentation), EF (External Fragmentation) metrics and FF (First-Fit) provisioning strategy.

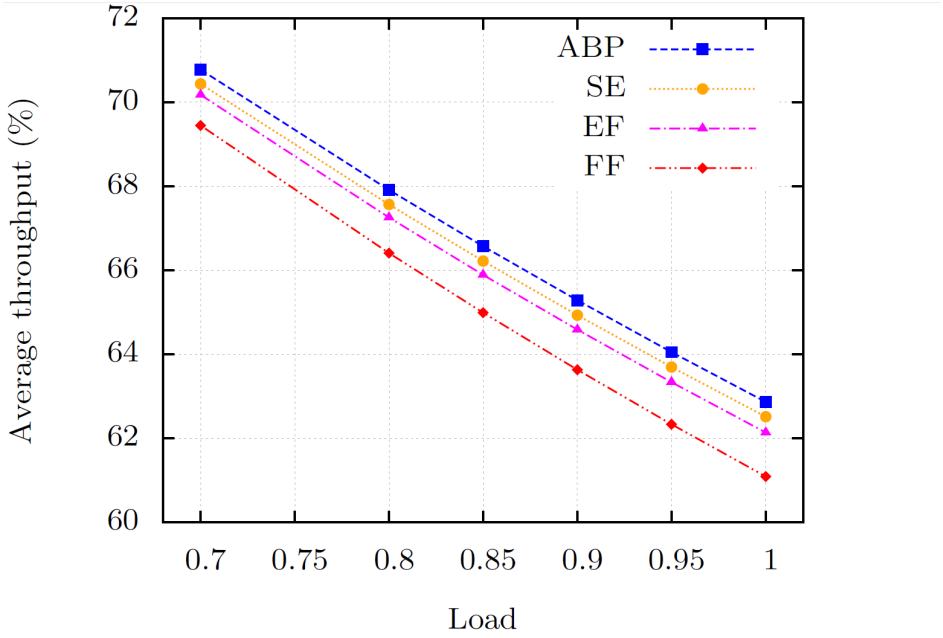

Figure 3.4 — Average throughput percentage in the maximum achievable throughput for different metrics: ABP (Access Blocking Probability), SE (Shannon Entropy Fragmentation), EF (External Fragmentation) and FF (First-Fit) provisioning policy versus the load.

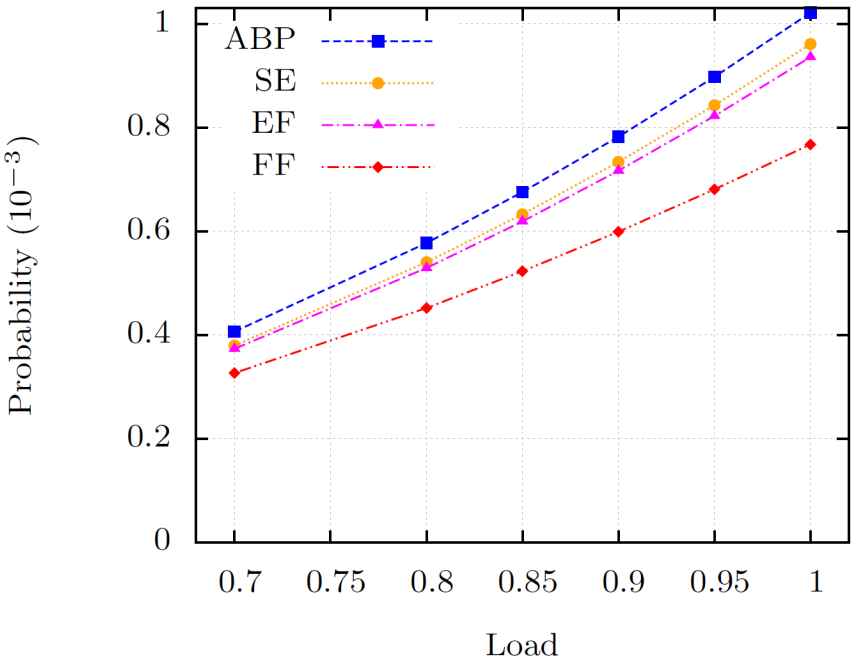

Figure 3.5 — Probability of being in the state where all slots are used for different metrics: ABP (Access Blocking Probability), SE (Shannon Entropy Fragmentation), EF (External Fragmentation) and FF (First-Fit) provisioning policy versus the load.

simple provisioning. Compared to other metrics, ABP reduces the total blocking probability in the system, improves the average throughput and leads to a good spectrum use.

In the following, ABP is used to evaluate spectrum fragmentation and not to avoid it. In this way, spectrum fragmentation is evaluated in real circumstances corresponding to today's way of operating optical networks.

3.3 Operator Network Context

In operator core networks, the traffic behavior is less fluctuating and, usually, demands do not disappear like in dynamic traffic scenarios. Besides that, the spectrum resource assignment follows a FF provisioning policy and there are some operational constraints that might make spectrum fragmentation behavior different. The following study aims at quantifying this behavior. Unlike the previous section that provided a generic mathematical evaluation of the fragmentation metrics, in this section, we use simulation tools and finely model the operator optical network. Notably, we consider requirements and characteristics of today's commercial products for the optical layer to model transponders, ROADMs and to estimate transmission reach.

The traffic follows an incremental growth to reproduce successive discrete intervals of time (period) set to 12 months. The maximum number of periods, the network can sustain before the first blocking occurs, is considered using the different grid scenarios and traffic strategies detailed below. Traffic growth is assumed to be exponential with

an annual growth rate $\alpha = 35\%$. Equation (3.10) calculates the traffic demand DP_i at the period $i+1$ as a function of the same initial traffic demand (DP_0) in the first period.

$$DP_i = \alpha \times (1+\alpha)^{i-1} \times DP_0 \tag{3.10}$$

The network dimensioning is performed respecting the following operational constraints:

- Demand blocking is not allowed. When demands can no longer be served, the current period is not taken into account.
- When a traffic demand grows, the additional part can be split and served by other transponders if the already installed resources are completely used.
- When several transponders are selected to serve the same traffic demand, the corresponding physical path must be the same.
- The same logical topology is used for each period.
- Assigned demands of previous periods are kept unchanged.

3.3.1 Transponder Model

An uncompensated Orange core network scenario deployed with 100 Gbps and beyond is considered. More specifically, several possible transponders and superchannel types to allow different datarate generation: 100, 200, 400 and 1Tbps are used as shown in table 3.4. We filled this table based on the references [108] and [109] as detailed below.

The granularity represents the 12.5 GHz frequency slot number that the transponders occupy. The maximum transmission reach is determined for each channel or superchannel using the Gaussian noise model proposed in [109]. The optical transmission link is composed of 100 km span lengths of single mode fiber (span loss = 22dB) with EDFA amplifiers having a Noise Figure of 6 dB. All transponders and superchannels use a Soft Decision Forward Error Correction (SDFEC).

The filtering penalty from transit through ROADMs is modeled by an additional SNR penalty, considering the presence of a ROADM after every 3 spans. This penalty is calculated using the following assumptions: a ROADM penalty of 0.05 dB is allocated for 32 Gbaud transponders, occupying 4 frequency slots, 0.64 dB [108] for 32 Gbaud transponders occupying 3 slots and 0.05 dB for the 16 Gbaud transponder. The individual channels of superchannels do not suffer from filtering penalties since the demultiplexing of superchannels into individual sub-channels is not possible in intermediate nodes.

Filtering penalties are only considered at the edges of superchannels. By considering the spectrum guard band on each superchannel side equivalent to the one we have on the 32 Gbaud transponders occupying 4 frequency slots, we have considered 0.05 dB SNR penalty per ROADM for the superchannels too.

Table 3.4 — Characteristics of transponders

	Datarate(Gbps)	Modulation format	Baudrate (Gbaud)	Granularity (slot)	Reach (km)	Cost (a. u.)
Single channel	100	16QAM SDFEC	16	3	400	0.7
	100	16QAM SDFEC	16	4	400	0.7
	100	QPSK SDFEC	32	3	1400	1
	100	QPSK SDFEC	32	4	2100	1
	200	16QAM SDFEC	32	3	300	1
	200	16QAM SDFEC	32	4	400	1
Superchannel	200	2×QPSK SDFEC	2×32	7	1900	2
	400	2×16QAM SDFEC	2×32	7	400	2
	400	4×QPSK SDFEC	4×32	13	1900	4
	1000	5×16QAM SDFEC	5×32	16	400	5
	1000	10×QPSK SDFEC	10×32	31	1900	10
	1000	10×QPSK SDFEC	10×32	32	1900	10

The cost model is based on the reference cost fixed at 1 for the 100 Gbps QPSK regardless of the allocated slot number. The cost of a superchannel is calculated summing its individual sub-channel costs. Consequently, the cost of a partially equipped superchannel is calculated based on the cost of sub-channels that are really used (even if the total number of slots of the entire superchannel is reserved to a single source-destination). Superchannels based on photonic integration components, which are supposed to reduce superchannel overall cost, are not considered in this study.

3.3.2 Traffic Strategies

To highlight traffic growth anticipation impact on both flex-grid technology benefits and spectrum fragmentation issue, the following traffic strategies are compared:

- Best Fit strategy (BF): this strategy chooses the set of transponders that exactly fit the required datarate. For instance, this strategy selects either three 100 Gbps transponders or one 100 Gbps and one 200 Gbps to serve a 300 Gbps traffic demand. The choice is depending on the objective function and available paths.

- Over-Dimensioning strategy (OD): this strategy oversizes the required capacity when it does not fit 100 Gbps, 200 Gbps, 400 Gbps, nor 1 Tbps solution. For instance this strategy selects a 400 Gbps solution for a 300 Gbps traffic demand. In this way, superchannels interest and potential traffic anticipation benefits are combined. Future traffic demands can then be assigned the additional unused capacity respecting the rules detailed above.
  Note that unused transponders are not considered in the cost calculation even if the spectrum is reserved for them.

3.3.3 Grid Scenarios

Combined with previous traffic strategies (BF and OD), we compare the following grid scenarios to identify the impact of channel spacing and grid flexibility on both spectrum fragmentation level and flex-grid technology gained capacity:

- Fixed Grid without superchannels (FG): this scenario allows only the four-slot based transponders and will be used as a reference for other scenarios. When the FF provisioning policy is used, FG scenario does not create unsable blocks.
- Fixed Grid with SuperChannels (FGSC): to be compliant with the traditional fixed grid and to take advantage of superchannel solutions, scenario all superchannels that occupy a multiple of four slots are allowed in FGSC.
- FleX-grid (FX): this scenario allows using all type of transponders granularities without any restriction. In this way, the spectrum efficiency is improved compared to previous scenarios (FG and FGSC). However, FX scenario is more subjected to spectrum fragmentation.

3.3.4 RSA Algorithm

The RSA problem np-hardness has been proven whatever the network topology is [37]. To solve RSA problem, we use a k-shortest path routing algorithm that uses a FF provisioning policy and calls the model (3.11) to optimally select transponders and place regenerators (Algorithm 1). Each traffic demand D is then served on the first possible shortest path selecting the set of transponders that optimizes in a hierarchical way both cost and spectrum usage. Wavelength regeneration process must respect the constraint that all regenerators can only be placed in an existing node and not anywhere else on the link.

$$Min \sum_{i}\sum_{p}\sum_{k} X_{ipk}C_i + \epsilon \sum_{i}\sum_{k} X_{ik}S_i \tag{3.11a}$$

$$Subject\ to \sum_{i}\sum_{p}\sum_{k} X_{ipk}U_{pe}D_i = D\ \forall e \in E \tag{3.11b}$$

$$\sum_{p} X_{ipk}U_{pe} = X_{ik}\ \forall i \in I, \forall k \in K_i, \forall e \in E \tag{3.11c}$$

$$L_p X_{ipk} \leq R_i\ \forall i \in I, \forall p \in P, \forall k \in K_i \tag{3.11d}$$

$$X_{ik}, X_{ipk} \in \{0,1\} \tag{3.11e}$$

Model (3.11): Equation (3.11a) is the objective function minimizing the cost. When several solutions have the same cost, it minimizes the spectrum occupancy (ϵ is a small coefficient that weights this second objective). Equations (3.11b) ensure the total traffic of every link of the path PA is equal to D. Equations (3.11c) ensure that all sub-paths which are used by a transponder of type i have no shared link. Inequalities (3.11d)

Table 3.5 — Data and variables

DATA	
PA(E, P)	A path *PA* where E is the set of links e and P is the set of all possible sub-paths p
I	Set of transponder types (Table 3.4)
D	Demand size (Gbps)
D_i	Datarate of transponder type i (Gbps)
S_i	Number of slots that a transponder of type i occupies
K_i	$K_i = \left\lfloor \frac{D}{D_i} \right\rfloor$ indicates the maximum number of transponders of type i that can be used to serve D, $\{1, 2, ...K_i\}$ is the set of what is called here lines
L_p	Length of sub-path p (km)
R_i	Reach of transponder of type i (km)
C_i	Cost of transponder of type i (a.u.)
U_{pe}	Equal to 1 if the sub-path p passes through the link e ; 0 otherwise
VARIABLES	
X_{ik}	Equal to 1 if the transponder of type i is used on the line k, 0 otherwise
X_{ipk}	Equal to 1 if the sub-path p is used by the transponder of type i on the line k, 0 otherwise

Table 3.6 — Network topology

Number of links		42
Number of nodes		32
Link length (km)	Min	10
	Mean	280
	Max	930

mean that the length of a sub-path p must be less than the reach of corresponding used transponders. Finally, equations (3.11e) specify variable types (variables and data are explained in Table 3.5).

3.3.5 Numerical Results

Simulations are performed on a 32-node and 42-link typical transcontinental European backbone topology (Table 3.6). At most three 360-slots-fiber pairs by link can be deployed. The logical topology is chosen according to the following assumptions.

Independently of the physical topology, Fig. 3.6 shows the granularities of selected transponders for each couple (demand, distance) when FGSC scenario is enabled. Most importantly, it shows that when the traffic volume is less than 1 Tbps FGSC scenario is equivalent to FG scenario (no saved spectrum) whatever the logical topology is and therefore the spectrum will not be fragmented.

For FX scenario, the three-slot granularity widely dominates the optimal choice when

Algorithm 1 RSA algorithm

Require: $number\_path > 0, number\_slots > 0$
  $sort\_demands\_decreasing\_way$
  $dimensioning \leftarrow true$
  $period \leftarrow 0$
  while $(dimensioning = true)$ **do**
    $demands \leftarrow new\_demands$
    for d *in* $demands$ **do**
      $served \leftarrow false$
      $k \leftarrow 0$
      while $((served = false)\, and\, (k < number\_path))$ **do**
        $k \leftarrow k + 1$
        $sl \leftarrow 0$
        while $((served = false)\, and\, (sl < number\_slots))$ **do**
          $sl \leftarrow sl + 1$
          $Model\ 3.11\ (PA(k), d)$
          if $((served = false)\, and\, (sl = number\_slots)\, and\, (k = number\_path))$ **then**
            $stop\_dimensoning$
          end if
        end while
      end while
      $period \leftarrow period + 1$
    end for
  end while

the path length is less than[6] 1400 km (see Fig. 3.7). This means that the spectrum gained capacity in this interval is closer to flex-grid technology theoretical gain. Similarly, the fragmented spectrum should be small because of the three-slot granularity dominance. Thus, we conclude that the diversity of spectrum slot occupancy that leads to spectrum fragmentation strongly depends on the logical topology.

Since it is more likely to have high spectrum fragmentation when different granularities are used, we can estimate that favoring a logical topology in this way should lead to the worst case of spectrum fragmentation. We, thus, choose a logical topology in such a way that path lengths are mostly outside that interval.

Simulation results are averaged over thirty initial traffic matrices (set of DP_0) normalized to 6 Tbps and randomly drawn according to the logical topology. For each combination [strategy scenario], simulation tool computes network cost, gained spectrum, relative spectrum loss (using ABP), and absolute spectrum loss (using the model (3.1)).

Thanks to the used strategy to calculate superchannel cost with OD, there is no significant difference between both strategies for a given scenario. After the first period, the additional cost percentage oscillates around 0% because of the interplay between overdimensioning cost and traffic anticipation benefits. Therefore, OD can be consid-

[6] Maximum reach of three-slot transponders

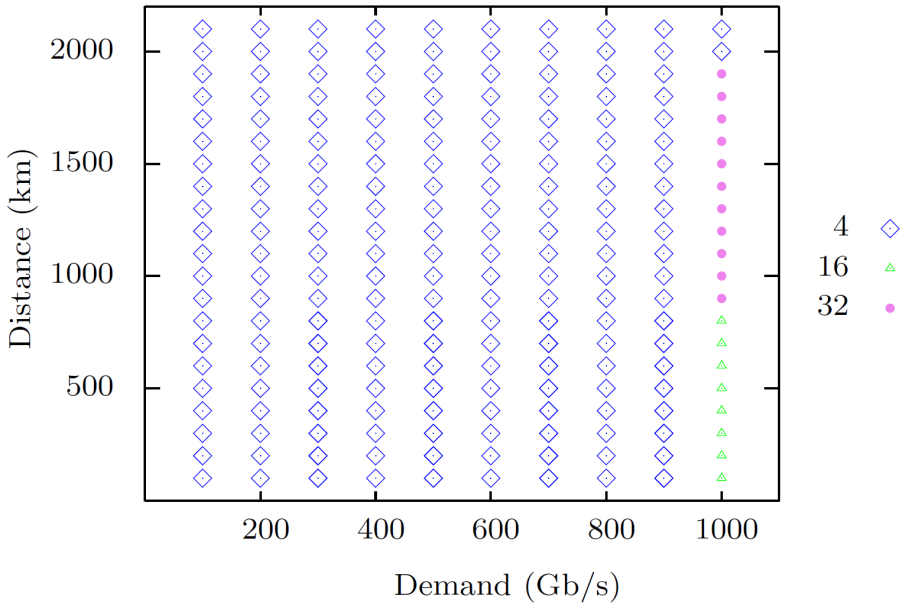

Figure 3.6 — Variation of used granularities in terms of traffic volume and required reach for FGSC scenario.

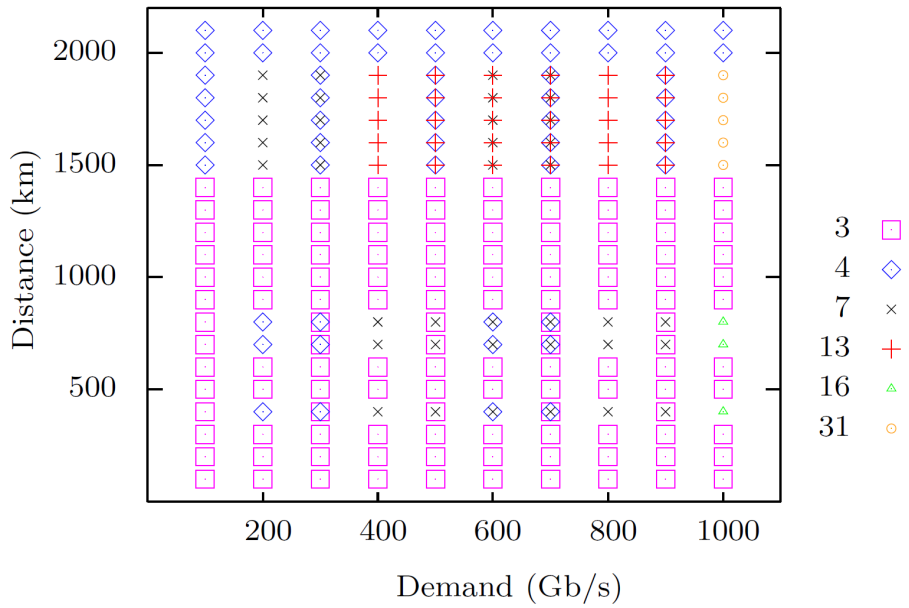

Figure 3.7 — Variation of used granularities in terms of traffic volume and required reach for FX scenario.

ered as expensive as BF (not illustrated in a figure).

Figure 3.8 shows the percentage of saved spectrum for different combinations between scenarios and strategies with respect to the reference best fitted conventional fixed grid scenario (BF FG). As expected, both FX and FGSC scenarios allow saving the spectrum with more advantage for the former. This gain is due to the fact that four-slot based transponders are replaced either by superchannels (for both scenarios) or by three-slot based transponders (for FX scenario). Besides, the traffic growth anticipation strategy OD is more efficient with FGSC scenario[7]. This is because there are more possibilities (in terms of transponder diversity) when FX scenario is used with BF strategy. In this particular case, OD moves from a near optimal choice to an optimal choice which limits its gain.
Remarkably, BF FGSC had to wait until the sixth period before saving the spectrum as the reference FG is equivalent to FGSC when traffic volume is less than 1 Tbps (shown in Fig. 3.6). In other words, in FGSC scenario, superchannels are only used when traffic volume attains 1 Tbps which impacts the saved spectrum.

Actually, the k-shortest path routing penalizes the most the FG scenario, since this scenario occupies more spectrum resources, and therefore it earlier starts using longer paths. In spite of that, the gained capacity is still about 13% (flex-grid theoretical gain is equal to 25%) for FX scenario when traffic growth is not anticipated. We explain this by observing that four-slot based transponders are often selected according to the chosen logical topology (earlier discussed in Fig. 3.7). Indeed, three-slot based transponders that allow to attain the theoretical gain, do not necessary correspond to optimal solutions (combining cost and spectrum as in Equation (3.11a)) due to their limited reaches.

Figure 3.9 shows the relative fragmentation measured by ABP metric in the best fitted FX scenario versus FGSC scenario when superchannels are favored through overdimensioning[8]. Due to the flexibility introduced by superchannels and due to the significant differences between possible granularities (e.g., 4, 16, 32), the relative fragmentation exists in FGSC scenario and it is comparable to the one in FX. Another reason is the correlation between network load and spectrum fragmentation (shown later). In fact, in spite of having the same amount of traffic in both cases, the network link load is not the same due to the different scenarios.

However, a part of the saved spectrum (Fig. 3.8) may not be usable because of heterogeneous blocks of slots that have been created. In order to evaluate this loss, we compute the number of unusable slots as defined in Section 3.2.
Fig. 3.10 illustrates the percentage of unusable slots in the saved spectrum for different combinations between scenarios and strategies. As expected, FGSC scenario does not lose the spectrum since in the worst case (i.e., four-slot based transponders) can unblock the situation. In the FX scenario, traffic growth anticipation through overdimensioning reduces this loss by half in the last period.

Note that the only way to recover this loss is by spectrum defragmentation. However,

[7]The gap between OD FGSC and BF FGSC is greater than the one between BF FX and OD FX
[8]OD FGSC and BF FX are compared in terms of spectrum fragmentation since they are comparable in terms of saved spectrum.

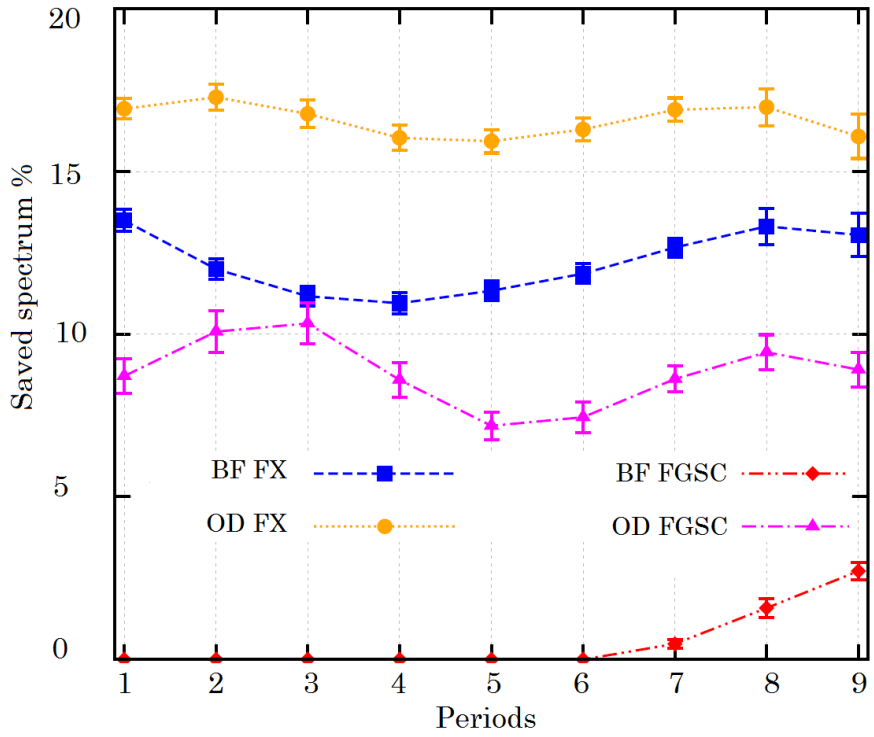

Figure 3.8 — Saved spectrum slots for different scenarios/strategies with respect to conventional FG scenario using a 95% confidence interval.

this may not appear relevant, because the loss is very small: in BF FX case this loss is still less than 6% out of 13% (i.e. $< 1\%$ of saved spectrum). Furthermore, this small loss means that when some demands are blocked, switching to less large granularities would often unblock the blocked bandwidth.

Another advantage of traffic growth anticipation represented by OD strategy is its impact on relative fragmentation (Fig. 3.11). Relative fragmentation level is reduced on every fiber in the network. This is due to superchannels that are more likely to be chosen when traffic is anticipated. Indeed, superchannels impose the contiguity of its sub-channels that leads to the free spectrum contiguity and then reduces spectrum fragmentation. This should not be confused with the case in which superchannels are an origin of fragmentation. More clearly, large granularities are more subjected to the blocking due to spectrum fragmentation. However, once considered, favoring them (as OD strategy does) leads to less fragmented spectrum.

For best fitted FX scenario, Fig. 3.12 shows the strong relationship between relative fragmentation and link occupancy in the last period represented by a high correlation coefficient equal to 0.93. Since OD strategy reduces link occupancy (because it saves the spectrum), this strong relationship is then another reason for which traffic growth anticipation reduces spectrum fragmentation. In addition, this strong relationship means that load balancing between links will make spectrum fragmentation lower.

Traffic growth anticipation is then a successful strategy to save the spectrum and to reduce both absolute and relative losses caused by spectrum fragmentation. However, when significant errors are considered in the growth anticipation approach, these ben-

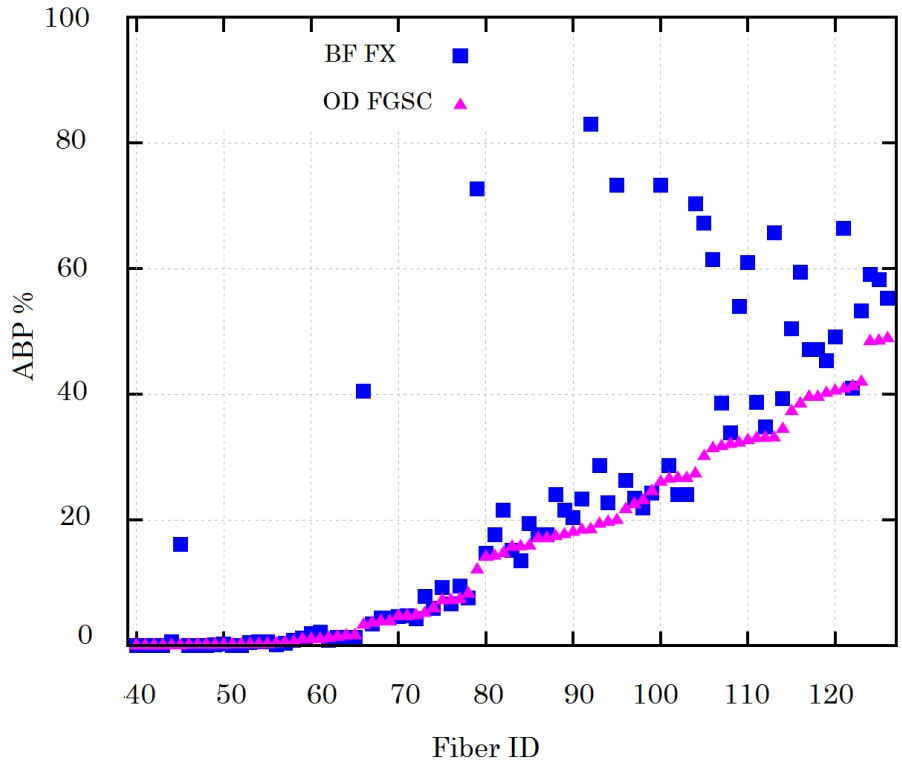

Figure 3.9 — Relative fragmentation in FGSC when traffic growth is anticipated versus BF FX (last period). Fibers are ordered according to FGSC values.

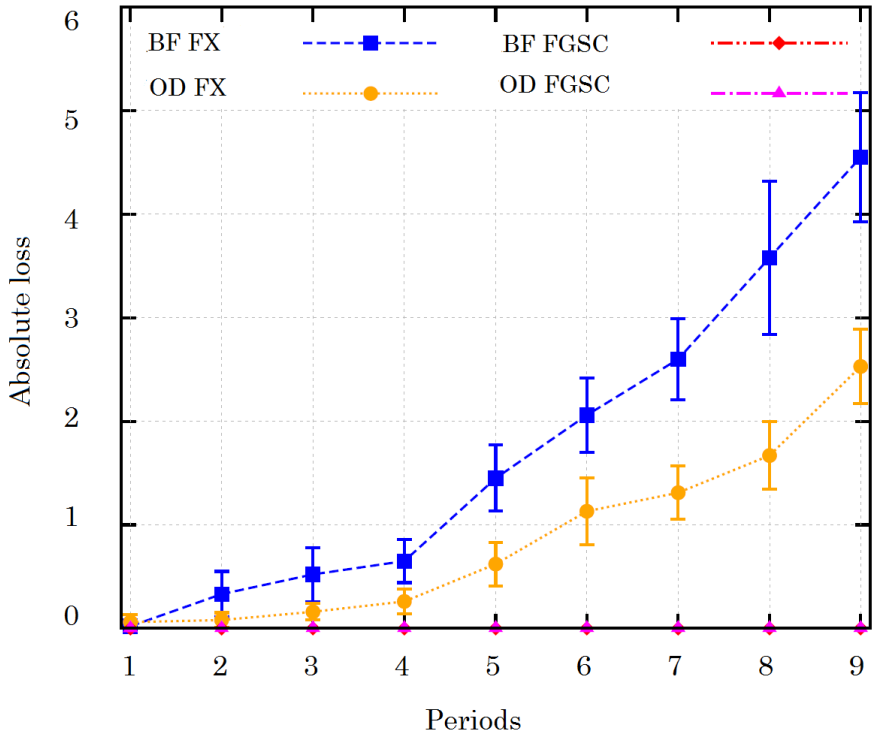

Figure 3.10 — Percentage of unusable saved spectrum in the saved spectrum shown in Fig. 3.8 for different scenarios/strategies using a 95% confidence interval.

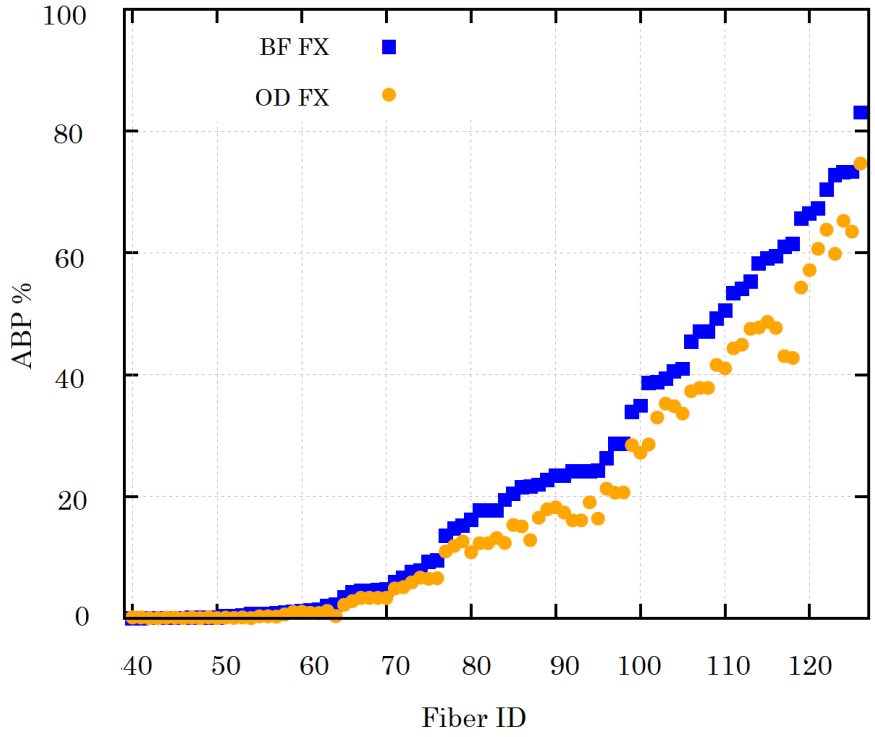

Figure 3.11 — Traffic anticipation impact on relative fragmentation in FX scenario (last period). Fibers are ordered according to BF values.

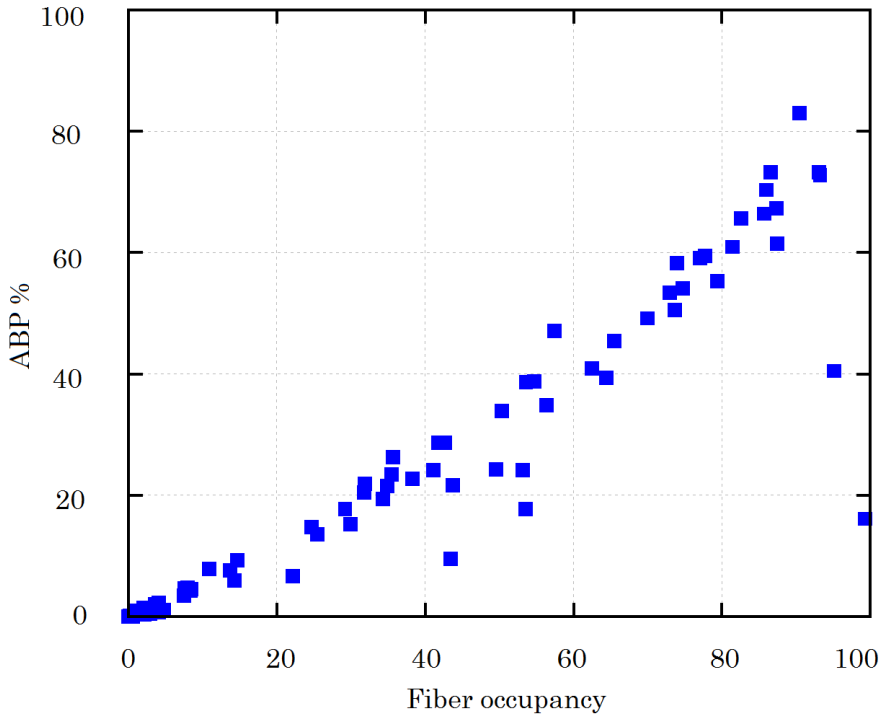

Figure 3.12 — Correlation between relative fragmentation and link occupancy in FX scenario (last period).

efits could be reduced. Similarly, some simple approaches like load balancing and the use of minor granularities are expected to reduce the residual fragmentation.

3.4 Traffic Forecast Impact on Fragmentation

While the traffic engineering is defined as "to put the traffic where the bandwidth is", network planning through traffic forecasts consists to "put the bandwidth where the traffic is forecasted to be" [110]. In this way, some optimization processes can be performed in advance and traffic dynamicity causing spectrum fragmentation can be kept down. However, since a perfect knowledge of future traffic is not possible, the uncertainty in traffic forecast represents a major issue [110]. Indeed, when the uncertainty in traffic forecast is introduced in the network planning, a trade-off between the robustness and the overdimensioning cost is required.

In conventional core optical networks, traffic behavior is less fluctuating and it continually grows in an incremental way. Therefore, an incremental model, in which only discrete intervals (periods of time) are considered, is more appropriate. In incremental traffic scenarios, a new traffic matrix is computed at the beginning of each period and possible errors in the traffic forecast are taken into account. For short periods (6-12 months) the impact of these errors can be mitigated using, for example, traffic rerouting strategies.

We model the uncertainty in the traffic forecast as a random additional variable (randomly drawn for every new demand) not exceeding a tunable uncertainty level β added to the predefined annual growth rate α. Furthermore, considering the fact that spectrum fragmentation is strongly dependent on link occupancy [82, 83], we evaluate the worst case where the optical network is under-dimensioned ($\beta \geq 0$).

In addition to FG and FX scenarios defined in Section 3.3.3, we evaluate the following scenario:

- Forecast FleX-grid (F-FX): it is an all-period forecasting flex-grid strategy that anticipates traffic growth and serves all traffic demands in one period. When uncertainty is considered ($\beta \neq 0$), an additional volume of traffic must be considered at the end of the dimensioning.

  Note that traffic forecast is equivalent to an active defragmentation process with adaptive rerouting and it does not have the operational constraint above since traffic forecast is an all-period strategy.

3.4.1 Numerical Results

Figure 3.13 gives statistics about used transponders (superchannels) for both FX (in the last period) and F-FX scenarios. Transponders are represented in the form of datarate_granularity_reach. The first two sets are respectively three-slot and four-slot based transponders; the latter set items are all superchannels. By forecasting, the number of four-slot-based transponders is remarkably reduced and new superchannels

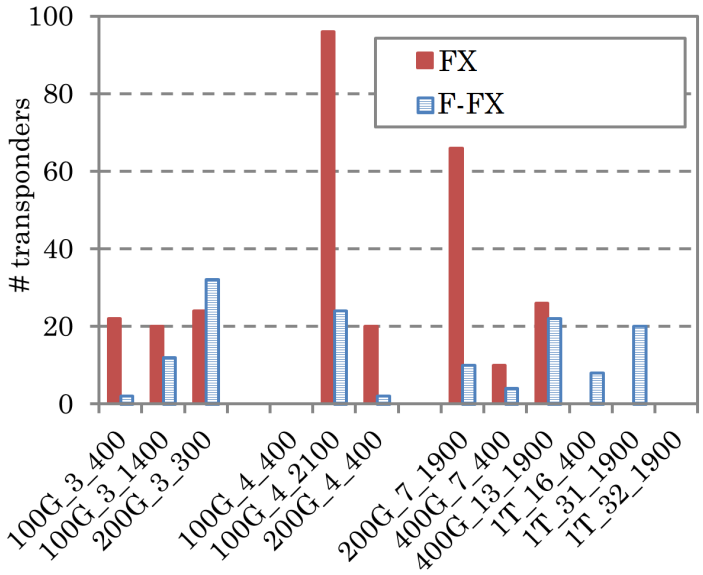

Figure 3.13 — Number of used transponders for both FX (in the last period) and F-FX scenarios.

appear which impacts both the cost and the spectrum use. This is due to the fact that when current and future demands are jointly served, a part of spectrum is saved thanks to superchannel solutions.

For different forecast period durations and different traffic volumes, Fig. 3.14 shows the evolution of saved spectrum percentage compared to conventional FG provisioning. Using a 95% confidence interval, the spectrum gain does not exceed 15% for FX scenario as significant parts of optimally selected transponders are four-slot based solutions (shown in Fig. 3.13). Accordingly, traffic forecast permits to improve this gain using additional superchannels solutions, which are a trade-off between reach and spectrum occupancy, without any impact on the overall cost. That is why F-FX scenario is considered at most as expensive as FX scenario.

Figure 3.15 presents the spectrum fragmentation level after six years for different scenarios using ABP metric. Considering an exact forecast, spectrum fragmentation issue is almost solved (ABP is around 5%). The residual fragmentation is unavoidable because of spectrum continuity constraint and then it can be solved with only wavelength converters (not considered here).

Moreover, if we consider 10% of uncertainty on the yearly traffic growth rate, results in Fig. 3.15 and Fig. 3.16 show that spectrum fragmentation remains limited and does not reach the values of flex-grid incremental scenario. This allows to go on getting benefit from superchannel solutions that are more subjected to bandwidth blocking.

Note that 10% of uncertainty is considered significant in core networks compared to the growth rate α and it gives rise to large absolute uncertainty due to exponential growth.

Indeed, serving jointly an important traffic volume is always better in terms of the contiguity of used spectrum and then its fragmentation.

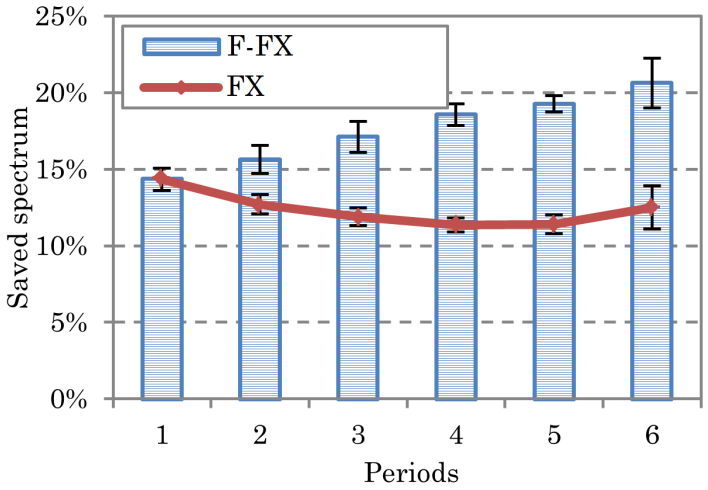

Figure 3.14 — Percentage of saved spectrum for both F-FX and FX scenarios compared to conventional FG provisioning.

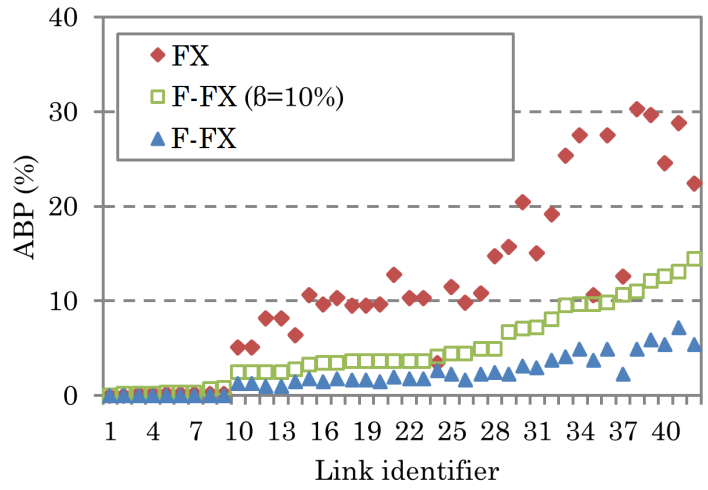

Figure 3.15 — Link fragmentation level at the last period for the different scenarios. Links are ordered using ABP values of F-FX scenario with uncertainty.

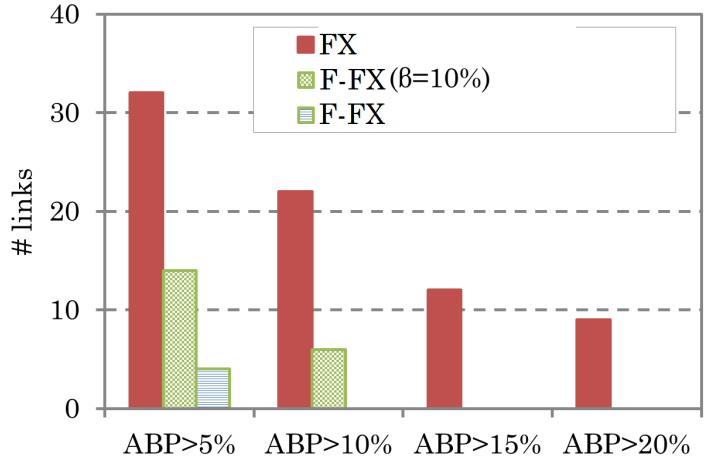

Figure 3.16 — Number of links whose fragmentation exceeds certain value of ABP for the different scenarios in the last period.

3.5 Conclusions

In this Chapter, we evaluated spectrum fragmentation issue in both dynamic and incremental traffic scenarios and proposed some simple approaches to face this problem in the context of operator network.

In dynamic traffic scenario, several fragmentation metrics are compared using a Markov modeling approach. Numerical results show the efficiency of using a fragmentation metric instead of a traditional allocation policy like the First-Fit (FF) provisioning.

Shannon Entropy based metric (SE) and External Fragmentation metric (EF) already offer good performances. However none of them consider transponder granularity and both of them are more interested in leaving large free blocks even if inconvenient blocks of slots are simultaneously created. We have proposed Access Blocking Probability (ABP) and demonstrated that it performs well compared to other metrics. This is because it takes into account possible transponders and avoids creating spectrum blocks that do not match their granularities.

Despite the advantages of these metrics to evaluate and/or reduce fragmentation, they add more complexity to the control plane and may be difficult to apply in highly dynamic large networks due to large computation time.

In incremental traffic scenario, we evaluated spectrum fragmentation in the context of operator network. We have shown that fragmentation is not only due to the traffic behavior, but also strongly dependent on the granularity diversity, on the logical topology, and on the network load.

Numerical results indicate that spectrum fragmentation is a real effect but does not compromise flex-grid technology benefits in incremental traffic scenarios.

Specifically, as the absolute loss is negligible and seeing that the higher values of relative fragmentation correspond to links close to full capacity, we conclude that periodical defragmentation processes are not needed in the context of operator network.

Instead, spectrum fragmentation can be better addressed during network planning phase. For example, using a specific fragmentation metric for resource provisioning, balancing traffic between links, switching to minor granularities when the blocking occurs, and/or forecasting traffic would be good strategies to address such a problem.

Indeed, traffic forecast is a successful active, hitless and costless strategy that allows to spare spectrum and avoid spectrum fragmentation. Simulations reveal that even with 10% of forecast uncertainty on traffic growth rate, spectrum fragmentation remains lower compared to the FX scenario.

However, these results did not consider the eventual change in the logical topology (some traffic demands may appear or vanish), during the network life. This case is expected to be seldom in core optical networks.

CHAPTER 4

On the Interest of Multilayer Restoration in Elastic Optical Networks

4.1 Introduction

DISPONIBILITY and resilience of operator networks are a challenging issue over time. Operators must provide an acceptable level of resource availability with the minimum expenses. Based on this constraint, different network architectures have been proposed with their different drawbacks and advantages as explained in Chapter 2.

In this chapter, we study another aspect of optical layer flexibility which is datarate elasticity. Unlike in Chapter 3, we do not consider the flexible grid herein, and assume datarate elasticity within the conventional fixed grid.

We propose and investigate a new multilayer network architecture for traffic restoration in IP over WDM optical networks. Our solution takes benefit from both datarate elasticity and low QoS requirements of best effort traffic.

We propose to use 1+1 IP protection scheme for only gold traffic by doubling its resources on two disjoint physical paths. Then, best effort traffic is restored as much as possible in the existing free resources (free capacity).

The remaining non-recovered best effort traffic is later restored, performing optical restoration with elastic transponders on lower datarates (e.g., longer reaches assuming modulation format adaptation). In other words, since gold traffic corresponding to the failed connection is already protected assuming single failure resiliency[1], its resources can be freed and used to improve the reach of transponders by switching to lower datarates. This improvement should allow the established connections to support the longer lengths of backup paths with no need for costly WDM regenerators.

Our architecture is expected to reduce network overall cost taking advantage from optical restoration which allows using the same equipment (e.g., transponders and IP interfaces) for both initial and backup traffic. It takes advantage as well from datarate elasticity to reduce WDM regenerator count as explained above.

[1] It means that two failures or more cannot occur at the same time.

The remainder of the chapter is organized as follows. In MLR and elastic optical networks, our architecture is explained and briefly compared with conventional IP protection scheme in Section 4.2. In Section 4.3, we present the mathematical aspect of the multilayer dimensioning tool that we propose for resource provisioning. This multilayer dimensioning tool considers three dimensioning phases, each having specific algorithmic and optimization tools. In Section 4.4, we then discuss simulation results considering two different topologies and two different transponder models in multilayer and single layer contexts. Finally, we conclude the chapter in Section 4.5.

4.2 Restoration Scenarios

As mentioned earlier, we evaluate a new use case that consists in triggering 1+1 protection for gold traffic and optical restoration for best effort traffic using elastic transponders in a multilayer context. This use case is expected to be interesting for the following reasons.

The first reason is that the slow process of optical restoration has no impact here as it can be supported by best effort class of service (it has no QoS requirements). The second reason is that, assuming single failure cases, only a part of traffic (i.e., best effort) should be restored with optical restoration process, since gold traffic would be already sent via backup resources ($1 + 1$ protection).

Therefore, transponders can reduce their datarates using less complex modulation formats in order to increase the optical reach and to support the longer length of backup paths. In addition, transponders are not necessarily used at their maximum capacity (full elasticity is not possible). A part of backup best effort traffic can therefore be split and served at no additional cost in the existing resources using IP restoration. This additional grooming and re-routing step can help in creating more opportunities to benefit from datarate elasticity when optical restoration is later performed.

Furthermore, available transponders operating on failed links must wait for several minutes before the failed connection is released back into service (slow process of optical restoration). Datarate can then be adapted right upon failure within the optical restoration duration. Consequently, a traffic recovery scheme using elastic transponders is more suitable to optical restoration rather than to IP restoration. Indeed, in the case of IP restoration, datarate of backup elastic transponders is adapted during transponder operation which affects current traffic. In the case of optical restoration, datarate is adapted during optical switching time, while transponders are not in operation.

We consider a transponder model with fixed symbol rate (32 Gbaud) and modulation format adaptation within the traditional fixed grid as in Table 4.1. The cost of fixed rate transponders is assumed identical whatever the modulation format, and used as a normalized cost reference in this study. An elastic transponder is able to provide all the datarates of fixed rate transponders, with the same features except for an extra cost α added to the reference to take into account elasticity cost. The cost of one 100 Gbps IP interface is assumed twice equal to the normalized reference cost [111]. Transponders with datarates less or equal to 100 Gbps require one 100 Gbps IP interface. If the

datarate exceeds 100 Gbps, additional IP interfaces are added (for example two IP interfaces are required in the case of 200 Gbps transponder). The cost of one WDM regenerator is assumed equal to the cost of two optical transponders (See Table 4.1).

Table 4.1 — Transponder and IP interface model

Datarate	Format	Reach	Transponder cost	Regenerator cost	Elastic transp. cost	Required IP int.	IP int. cost
25 Gbps	SP-BPSK[2]	6000 km	1	2×1	$1 + \alpha$	1×100 Gbps	1×2
50 Gbps	DP-BPSK[3]	4800 km	1	2×1	$1 + \alpha$	1×100 Gbps	1×2
75 Gbps	PS-QPSK[4]	3200 km	1	2×1	$1 + \alpha$	1×100 Gbps	1×2
100 Gbps	DP-QPSK[5]	2100 km	1	2×1	$1 + \alpha$	1×100 Gbps	1×2
200 Gbps	DP-16QAM[6]	400 km	1	2×1	$1 + \alpha$	2×100 Gbps	2×2

Figure 4.1(a) shows an example of multilayer architecture of IP over WDM optical networks. All nodes in the IP layer are equipped with routers, and all optical layer nodes with ROADMs.

For example, consider the following traffic demands: $D_1 : A \rightarrow B$ (70 Gbps); $D_2 : B \rightarrow C$ (50 Gbps); $D_3 : A \rightarrow C$ (100 Gbps) each one being routed on its shortest path using a 100 Gbps transponder as depicted in Fig. 4.1(a). For the sake of simplicity, we focus on the way the backup of D_3 is done considering the transponder model of Table 4.1. In the next paragraph, we describe different restoration scenarios (Fig. 4.1(b), Fig. 4.1(c), and Fig. 4.1(d)) and show how optical restoration combined with datarate elasticity can be a cost effective approach if considered in a differentiated class of service based dimensioning context.

4.2.1 IP Protection (IP-P)

This scenario does not differentiate between the classes of services of traffic demands. All demands are assumed to be of high priority, and their resources are assigned according to 1+1 protection scheme using fixed rate transponders. The main advantage of this scenario is its availability level of network resources. Indeed, the recovery scheme can be very fast assuming, for example, Multi-Protocol Label Switching (MPLS) local protection [112]. In addition, IP-P scenario can also extend its protection from physical links to network nodes. The main drawback of this scenario is that the network is dimensioned to support twice the traffic volume, which can be a rather expensive solution. In contrast, the additional cost can be mitigated taking advantage of multilayer dimensioning through demand splitting and traffic grooming.

Figure 4.1(b) shows how the traffic demand D_3 (100 Gbps) of the previous example is protected in this scenario. A part of it (i.e., 30 Gbps) can be split and carried in the free resources on the paths of traffic demands D_1, and D_2 (A-B-C). The remaining 70

[2]Single-Polarization Binary Phase-Shift Keying (SP-BPSK)
[3]Dual Polarisation Binary Phase-Shift Keying (DP-BPSK)
[4]Polarisation Switched Quaternary Phase-Shift Keying (PS-QPSK)
[5]Dual Polarisation Quaternary Phase-Shift Keying (DP-QPSK)
[6]Dual Polarisation 16 - Quadrature Amplitude Modulation (16-QAM)

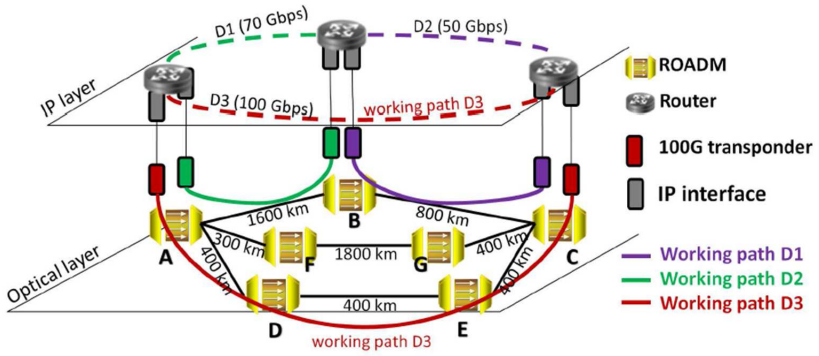

(a) Network architecture, topology, and offline provisioning

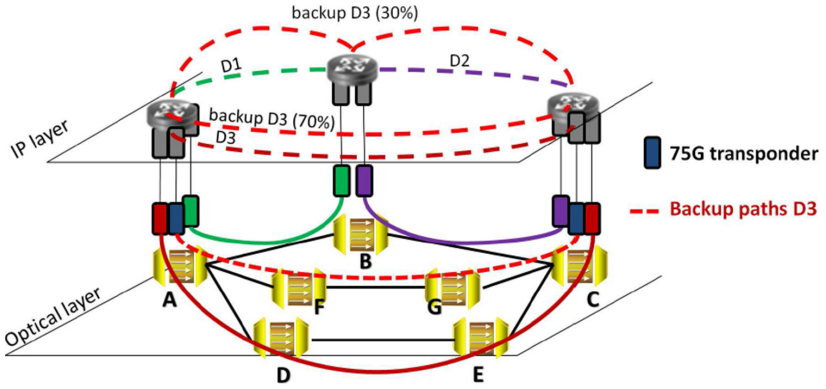

(b) IP-P

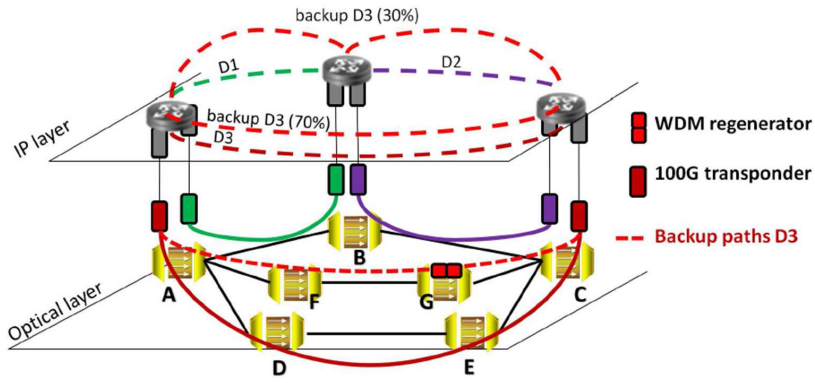

(c) M-MLR

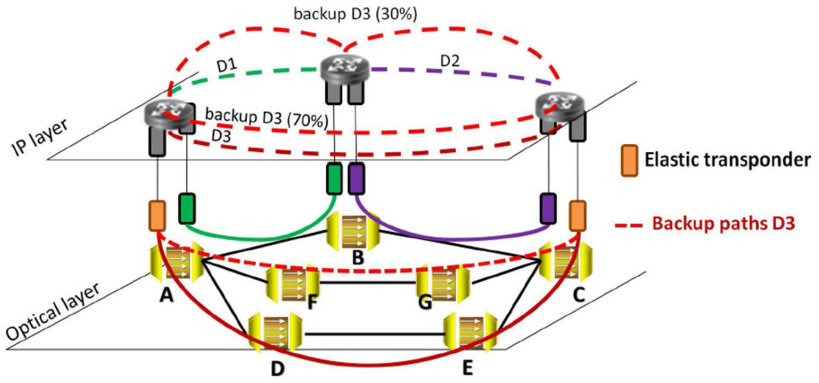

(d) M-ELS

Figure 4.1 — Illustration of the different scenarios in IP over WDM networks.

Gbps is routed on another disjoint path (*A-F-G-C*) deploying two additional 75 Gbps transponders and their related IP interfaces with no need for signal regeneration.

4.2.2 Multilayer Restoration in MLR Optical Networks (M-MLR)

Unlike IP-P, this scenario performs 1+1 protection for gold traffic only, which represents about 30% of initial traffic according to [99]. Afterwards, all best effort traffic is offloaded to the optical layer in order to be restored later on with the available fixed rate transponders and IP interfaces corresponding to the failed links. This step can be absolutely costless in the case where backup paths do not require signal regeneration. Otherwise, the additional cost induced by WDM regenerators may call into question the interest of such an approach especially when backup paths are much longer compared to the ones used for working traffic. In Fig. 4.1(c), backup gold traffic of demand D_3 (i.e., 30 Gbps) is provisioned using the free existing resources on the path (*A-B-C*). The remaining 70 Gbps best effort part is restored using the same 100 Gbps transponder and the same IP interface that are previously used with the initial traffic demand D_3 (optical restoration) on a disjoint path (*A-F-G-C*). However, a new WDM regenerator is required due to the longer length of backup path.

Note that, both network layers have to coordinate upon a failure, in order to achieve an optimal traffic restoration.

4.2.3 Multilayer Restoration in Elastic Optical Networks (M-ELS)

In this scenario, best effort backup traffic is not considered in network dimensioning phase. It is later offloaded to optical layer restoration as in M-MLR scenario. The main difference between both scenarios is that elastic transponders used here can adapt their datarates to fit the best effort traffic amount and consequently operate on longer reaches. It is the reason why the required WDM regenerator considered in the previous scenario (Fig. 4.1(c)) can now be avoided (Fig. 4.1(d)).

In a nutshell, elastic transponders may potentially reduce the additional cost of optical restoration, induced by WDM regenerators, provided that they allow reach adaptation. Nevertheless, it is necessary to take into account the additional cost of elastic transponders and to perform a robust optimization in order to be sure that all important parameters are taken into account.

4.3 Dimensioning Phases and Tools

As explained in Section 1.3.2 of Chapter 1, multilayer dimensioning is a complex problem that cannot be easily solved for large network instances. In Section 4.2, it can be noticed that both online and offline aspects of network dimensioning are involved in

the restoration scenarios. Therefore, the problem gets more complicated seeing that both multilayer restoration and multilayer dimensioning are concerned.

In current work, the problem is dealt with as follows. We first perform a multilayer dimensioning for working traffic (gold + best effort), and gold backup traffic in the offline dimensioning phase (Phase I). A MILP formulation is proposed for small and medium networks with sparse traffic matrix instances. For large networks and dense traffic matrices, a genetic algorithm is proposed and validated with the MILP formulation.

Moreover, in order to find near-optimal solutions within a reasonable time, path disjunction property is guaranteed giving disjoint paths as input to the dimensioning process. However, This prevents from the grooming of demands whose precomputed paths are disjoint: they might have one or more links in common if precomputed paths are not given as input.

Afterwards, best effort restoration is accomplished combining heuristics and exact ILP formulations in a hierarchical way. Specifically, grooming and re-routing of best effort backup traffic in the existing resources (Phase I) is performed separately (Phase II) using a heuristic method. WDM regenerator placement required for optical restoration is accomplished with an exact ILP model (Phase I).

Note that optimizing jointly the three phases is quite difficult to carry out, and not necessary for this study. Indeed, the decomposition is done according to the dimensioning context and the relevant parameters for the comparison.
In the following, mathematical tools used in each phase, are explained within their corresponding phase descriptions.

4.3.1 Network Planning and IP Protection (Phase I)

In this first and offline phase, gold backup traffic resources are provisioned in the same way as the working traffic, assuming a 1+1 protection scheme. Two different strategies are possible, when different types of transponders can serve a given logical link at the same minimal cost:

- Lowest Datarate First (LDF): this strategy chooses the transponder with the lowest datarate among all possible solutions having the same cost. This can be useful later on for optical restoration thanks to enhanced transponder reach. Note that, additional cost induced by signal regenerators and IP interfaces, is considered in the selection process.

- Highest Datarate First (HDF): contrary to LDF, high datarate transponders are more likely to be chosen with this strategy. As the network is somewhat over-dimensioned, new traffic demands can then be served over time with no need for new resources. Such an interest is not studied here as no traffic demand growth is considered in this study.

For this dimensioning phase, we propose a MILP formulation for multilayer dimensioning of MLR WDM networks. Subsequently, we propose a genetic algorithm to deal with

real traffic instances and large network topologies. The efficiency of such an algorithm is verified on small and medium topologies with sparse traffic matrices.

Table 4.2 — Data and variables used in mathematical formulations

Data	
$G(N, E)$	Graph G with set of nodes N and Links E
C_I	Cost of one 100 Gbps IP interface
C_T	Cost of one transponder
S_{xy}	Shortest path between nodes x and y
P	Set of virtual links P_l
P_{sd}	Path between nodes s and d
R_k	Datarate of a transponder of type k
β_{opk}	Equals 1 if a transponder of type k can be used on the shortest path between nodes o,$p \in N$ without regenerator; 0 otherwise
β_{lk}	Equals 1 if a transponder of type k can be used on the physical link corresponding to the virtual link $P_l \in P$ without regenerator ; 0 otherwise
Δ_{sd}	Traffic demand between nodes s,$d \in N$
B_I	IP interface capacity (100 Gbps)
D_B	Best effort traffic to be restored in Phase III
Decision Variables	
$Z_{ij}^{sd\lambda}$	Traffic between nodes s,$d \in N$ routed on the lightpath (i,j) with wavelength λ
$Y_{po}^{ij\lambda}$	Traffic on lightpath (i,j) and sub-lightpath (o,p) with wavelength λ
I_{ij}^{λ}	Number of IP interfaces corresponding to the lightpath(i,j) and used with the wavelength λ. For example, two 100 Gbps interfaces are required with a 200 Gbps transponder
$X_{opk}^{ij\lambda}$	Equals 1 if a transponder of type k is used on a sub-lightpath (o,p) corresponding to a lightpath (i,j) with a wavelength λ; 0 otherwise
$X_{k\lambda l}$	Equals 1 if a transponder of type k is used on the virtual link $P_l \in P$ with wavelength λ; 0 otherwise

4.3.1.1 MILP Formulation

The objective of the MILP (4.1) is to find the best trade-off between traffic grooming, optical transparency, and regenerator placement, taking into account the transponder model and IP interfaces from Table 4.1, while satisfying wavelength uniqueness constraint in MLR networks. This formulation is also used to set the initial datarates of elastic transponders.

Let us note that IP interfaces are required only during grooming process and not for signal regeneration. To model this, we consider that each traffic demand (s, d) can be routed on a lightpath (i, j), provided that the precomputed path between the nodes i and j belongs to the one linking s and d. This constraint is always satisfied in case of shortest path routing. However, shortest path routing cannot be used when protection is considered due to the disjunction property. To overcome this, our MILP model

enforces routing through intermediate lightpaths whose shortest paths are belonging to the precomputed backup path. This can generate an additional cost in some cases, but as backup paths are often longer, this constraint can be satisfied with no further cost in most of the cases. Each lightpath is then identified by two nodes and one wavelength. It can be divided into several sub-lightpaths (o, p), depending on whether one or more regenerators are required. In this case, wavelength conversion can occur only on grooming nodes and not on regeneration nodes. This restriction has no effect if there are enough wavelengths on each link.

IP interfaces are counted according to the set of logical links of type (i, j) and not (o, p), contrary to transponders that should be counted on both grooming and regeneration nodes. This last assumption lies in the fact that one WDM regenerator is equivalent to two optical transponders.

$$Min\ C_I \sum_{i,j} \sum_{\lambda} \left(I_{ij}^{\lambda} + I_{ji}^{\lambda}\right) + C_T \sum_{i,j} \sum_{op} \sum_{k} \sum_{\lambda} \left(X_{opk}^{ij\lambda} + X_{pok}^{ij\lambda}\right) \tag{4.1a}$$

$$Subject\ to \sum_{k} R_k X_{opk}^{ij\lambda} \beta_{opk} \geq Y_{op}^{ij\lambda} \quad \forall (i,j) \in N^2, \forall (o,p)/S_{op} \subset S_{ij}, \forall \lambda \tag{4.1b}$$

$$\sum_{i,j} \sum_{o,p/(m,n)\subset S_{op}} \sum_{k} X_{opk}^{ij\lambda} \beta_{opk} \leq 1 \quad \forall (m,n) \in E, \forall \lambda \tag{4.1c}$$

$$\sum_{i} \sum_{\lambda} Z_{ij}^{sd\lambda} - \sum_{i} \sum_{\lambda} Z_{ji}^{sd\lambda} = \begin{cases} -\ \Delta_{sd/S_{ij}\subset P_{sd}} & if (s = j) \\ \Delta_{sd/S_{ij}\subset P_{sd}} & if (d = j) \\ 0 & otherwise \end{cases} \quad \forall (j,s,d) \in N^3 \tag{4.1d}$$

$$\sum_{o} Y_{op}^{ij\lambda} - \sum_{o} Y_{po}^{ij\lambda} = \begin{cases} -\ \sum_{s,d/S_{ij}\subset P_{sd}} Z_{ij}^{sd\lambda} & if (i = p) \\ \sum_{s,d/S_{ij}\subset P_{sd}} Z_{ij}^{sd\lambda} & if (j = p) \\ 0 & otherwise \end{cases} \quad \forall (p,i,j) \in N^3, \forall \lambda \tag{4.1e}$$

$$I_{ij}^{\lambda} B_I \geq \sum_{s,d} Z_{ij}^{sd\lambda} \qquad \forall (i,j) \in N^2, \forall \lambda \tag{4.1f}$$

$$I_{ij}^{\lambda} \qquad Integer \tag{4.1g}$$

$$X_{opk}^{ij\lambda} \qquad Binary \tag{4.1h}$$

$$Y_{op}^{ij\lambda}, Z_{ij}^{sd\lambda} \qquad Real \tag{4.1i}$$

Table 4.2 explains data and variables used in the MILP (4.1) and the ILP (4.5) formulations presented later on. Concerning the MILP (4.1), Formula (4.1a) minimizes network overall cost accounting for transponders and IP interfaces. Inequality (4.1b) is responsible for logical topology design as it specifies for each traffic demand, the intermediate lightpaths, and their sub-lightpaths, and it ensures that sufficient resources exist on each sub-lightpath. Inequality (4.1c) guarantees wavelength uniqueness and continuity constraints, meaning that every wavelength may be used at most once on each physical link. Equation (4.1d) ensures the flow conservation constraints on each lightpath. Equation (4.1e) ensures the flow conservation constraints on each sub-lightpath.

Inequality (4.1f) counts the number of IP interfaces required on the lightpath (i, j). Constraints (4.1g), (4.1h), and (4.1i) specify the types of decision variables.

Note that, the MILP (4.1) can also be used for flex-grid network dimensioning. In such a case, Formula (4.1a) should minimize the number of used frequency slots as well. This can be easily added optimizing both cost and spectrum occupancy in a hierarchical way as in the ILP (3.11) (proposed in Chapter 3).

4.3.1.2 Genetic Algorithm

The MILP formulation has been implemented and tested on the IBM ILOG CPLEX solver using a professional license. Solutions cannot be found for large topologies and real traffic instances with an acceptable optimality gap. It is the reason why we propose a well-adapted genetic algorithm for multilayer dimensioning, and we use the MILP formulation to validate it on medium sized network topologies and sparse traffic matrices.

Genetic algorithms inspired by biological evolutions are one of the most used meta-heuristics in combinatory optimization. They are efficient for different types of problems and in different contexts, depending strongly on the way the problem is encoded [113]. The structure of a given solution (individual) should have access to the decisive details of the problem while keeping as little as possible the genetic representation size (number of genomes). In other words, a good genetic representation must be expressive, evolvable, and should keep as far as possible individual diversity over time.

The main idea of the genetic algorithm we propose, is as follows. Since physical paths are calculated and given as input to the dimensioning tool for each working and backup traffic demand, it is just enough to determine which wavelength is used with which traffic demand in order to get a global solution. Traffic demands that use the same wavelength and that share at least one physical link are then groomed on the links they have in common. Once the grooming points are determined, transponder type (according to the working strategy: LDF or HDF) is selected, and regeneration nodes are determined based on the reach of selected transponder. Some solutions could be, however, not feasible due to transponder limits. It happens when the total amount of groomed traffic demands is larger than the maximum datarate. In this case, it is impossible to choose several transponders to satisfy all the groomed traffic as they would have to operate on the same wavelength. It also happens when an intermediate node does not exist on the physical path and regeneration is required. These impossible solutions are neglected, and the cost of a feasible solution is easily calculated as transponder types, regeneration and grooming points are known.

When traffic demands are allowed to be split, each traffic demand is split with respect to a randomly drawn value that does not exceed a pre-defined constant number (splitting constant) that the algorithm takes as an input parameter. Each part of every traffic demand is then randomly assigned a wavelength and it becomes independent from the other demand slices.

Apart from the optimality level, we can now see why in this context a random assignment of wavelengths to traffic demands is sufficient to get a solution that stems from multilayer dimensioning (i.e., signal regeneration, traffic grooming, wavelength assignment, and transponder/IP interface selection).

Figure 4.2 shows what a randomly drawn individual (equivalent to chromosome here) might look like. Each traffic demand has two components: working and backup. The number of columns in each component is equal to the splitting constant (herein two). The first row represents the slices of its corresponding traffic demand, and the second row represents their assigned wavelengths. The sum of slices in each component must be equal to the traffic demand volume if it is a working component, and equal to the traffic to be protected if it is a backup component.

To take a simple example, assume that traffic protection, and traffic demand split are not considered. Consider also the following traffic matrix: D_1: $1 \rightarrow 2$ (50 Gbps); D_2: $1 \rightarrow 4$ (40 Gbps); D_3: $2 \rightarrow 5$ (50 Gbps); D_4: $1 \rightarrow 6$ (130 Gbps) being routed on the six node network topology of Fig. 4.3, using a shortest path routing. Suppose that the first random draw of the initial population gave the following chromosome: (D_1, λ_2), (D_2, λ_1), (D_3, λ_1), (D_4, λ_2) (Fig. 4.3). It can be noticed that demands D_2 and D_3 are groomed from node 2 to node 4 since they use the same wavelength λ_1 on the same physical link (2, 4). Therefore, some IP interfaces (their number depends on which transponder is selected) have to be installed for grooming on nodes 2 and 4, in addition to the other interfaces that are required at the edge nodes of demands. Likewise, D_1 and D_4 are groomed on the link (1, 2), with an additional regenerator for demand D_4 - assuming that a 200 Gbps transponder is selected - on node 4. The fitness function calculates exactly the cost of this chromosome using Algorithm 2. The final result is shown in Table 4.3, using the transponder model of Table 4.1. This is how the initial population is created before completing the traditional operations (selection, crossover, and mutation) of evolutionary algorithms. Afterwards, the best chromosomes survive and the evolutionary process is repeated until the maximum number of generations is reached. Note that, we choose single point crossover, and perform mutation at the component level.

Contrary to the MILP formulation that allows wavelength conversion wherever the

	Working		Backup	
D_1	S_{11}	S_{12}	S'_{11}	S'_{12}
	λ_{11}	λ_{12}	λ'_{11}	λ'_{12}
D_2	S_{21}	S_{22}	S'_{21}	S'_{22}
	λ_{21}	λ_{22}	λ'_{21}	λ'_{22}
⋮			⋮	
D_n	S_{n1}	S_{n2}	S'_{n1}	S'_{n2}
	λ_{n1}	λ_{n2}	λ'_{n1}	λ'_{n2}

Figure 4.2 — General model for the chromosome structure. A chromosome is compound of n demands, each one having two components in which traffic demands are, if need be, split and assigned wavelengths.

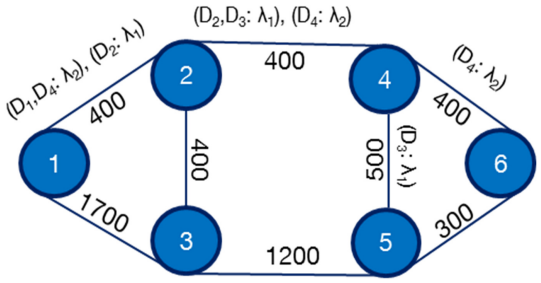

Figure 4.3 — Six node topology with link lengths in km. The figure shows how grooming points can be found out, once wavelengths are assigned, provided that physical paths are known (e.g., shortest path routing).

Table 4.3 — Cost of the chromosome shown in Fig. 4.3

Lightpaths		Traffic Demands	Candidate Transponders	# IP Interfaces	Regeneration?	Cost
λ_1	$(1,2)$	D_2	50, 75, 100	2	no	6
	$(2,4)$	D_2, D_3	100	2	no	6
	$(4,5)$	D_3	50, 75, 100	2	no	6
λ_2	$(1,2)$	D_1, D_4	200	4	no	10
	$(2,6)$	D_4	200	4	yes	12
					Total cost	40

traffic grooming is performed, this genetic algorithm does not permit such a process to

Algorithm 2 Chromosome Cost Calculation

Require: *Links*, *Wavelengths*, *Demands*, *Chromosome*, *SplittingConstant*

1: **for** λ in *Wavelengths* **do**
2: enumerate all physical links $\in$ *Links* on which λ is used
3: **for** *link* in *Links* **do**
4: enumerate all traffic demands $\in$ *Demands* that are routed through *link*, using λ.
5: **end for**
6: **end for**
7: infer all the logical links: physical links that are adjacent and that use the same wavelength with the same set of traffic demands, each one having the same traffic amount (in case of demand split, i.e., *SplittingConstant* > 1) must be concatenated to constitute one logical link.
8: infer the transponder type that is used on each logical link, according to the selected strategy (*LDF* or *HDF*). Determine the regeneration nodes. Deduce solution feasibility.
9: **if** solution is feasible **then**
10: calculate network overall cost (*ChromosmeCost*)
11: **end if**
12: **return** *ChromosmeCost*

happen. As previously stated, such a limitation should not have a significant impact on results provided that the number of wavelengths per link is quite enough with respect to the traffic matrix. In contrast, all solutions of the genetic algorithm are still a particular case of the ones of the MILP formulation, meaning that they can be provided to the MILP model as warm start point.

4.3.2 IP Restoration for Best Effort Traffic (Phase II)

In Phase I, only gold backup traffic is provisioned. In Phase II, best effort traffic corresponding to failed connections is restored using the free capacity of the non-failed connections operating on disjoint paths. It can be completely or partially restored depending on the available resources which strongly depend on the selected strategy. For example, with HDF strategy, it is most likely to get free resources for whatever logical link as high datarate transponders are often selected contrary to LDF strategy. We use Equations (4.2)-(4.4) to identify all the possible logical links on a given backup path, and then infer the one with the maximum free capacity, which is subsequently used for best effort traffic restoration.

$$P(k,l) = \sum_{i=k-1}^{l-1} P(k-1,i) \tag{4.2}$$

$$P(1,l) = 1 \tag{4.3}$$

$$P(l) = \sum_{k=1}^{l} P(k,l) \tag{4.4}$$

Equation (4.2) recursively counts the number $P(k,l)$ of valid sub-path combinations, compound of k sub-lightpaths, and that can be routed on a given path of l physical links (namely the backup path). For example, for a three node physical path A-B-C ($l = 3$), there can be one logical link A-C compound of one ($k = 1$) sub-lightpath A-C, and one logical link A-C compound of two ($k = 2$) sub-lightpaths A-B and B-C. Equation (4.3) is the trivial solution of the recursion in Equation (4.2). It means that there can be only one lightpath per wavelength compound of one sub-lightpath whatever the physical link number is. The total number of logical links for a given path of l physical links is therefore found summing up all possible logical links irrespectively of the number of sub-lightpaths k as in Equation (4.2).

All regenerator placement possibilities can subsequently be found tracking the recursion in Equations (4.2)-(4.4). The existing connection with the largest free capacity is used to partially or completely restore best effort traffic at no additional cost.

4.3.3 Optical Restoration for Best Effort Traffic (Phase III)

As earlier mentioned, some works propose to drop best effort traffic after a failure if there are not enough free resources for costless restoration. Here, we propose to restore the remaining best effort traffic amount with optical restoration. As the same equipment for both working and backup best effort traffic is used, a 1+1 recovery scheme is not possible. Instead, it is a matter of 1:1 restoration schemes that offload a part of best effort traffic to optical layer with eventual regeneration cost induced by backup path lengths. At this stage, all regenerator placement possibilities and free wavelengths are given as input to ILP (4.5) with suitable datarates set, according to restoration scenario. For instance, M-MLR scenario considers only datarates corresponding to the failed link, as the others cannot be used for regeneration. In contrast, in M-ELS restoration scenario, no restriction on regenerator datarate occurs thanks to transponder elasticity.

$$Min \sum_{k}\sum_{\lambda}\sum_{l} X_{k\lambda l}\, C_T \tag{4.5a}$$

$$Subject\ to \sum_{k}\sum_{\lambda} R_k\, X_{k\lambda l}\, \beta_{lk} \geq D_B \quad \forall p_l \in P \tag{4.5b}$$

$$\sum_{k} X_{k\lambda l}\, \beta_{lk} \leq 1 \quad \forall \lambda,\ \forall p_l \in P \tag{4.5c}$$

$$X_{k\lambda l} \qquad\qquad Binary \tag{4.5d}$$

$$\tag{4.5e}$$

Table 4.2 explains data and variables that are used in ILP formulation (4.5) whose objective is to minimize optical layer restoration cost as in formula (4.5a). Equation (4.5b) ensures there are sufficient resources to restore the remaining best effort traffic amount D_B. Inequality (4.5c) satisfies wavelength uniqueness and continuity constraints along the path. Formula (4.5d) defines the variable type in the ILP formulation.

Note that, ILP formulation (4.5) returns all the required transponders to optimally serve the backup of best effort traffic whether it concerns edge nodes or intermediate ones. Therefore, only transponders operating at intermediate nodes have to be taken into account as the others are already existing (optical restoration concept). For the same reason, this formulation does not take into account IP interfaces which are required at the edge nodes. In a nutshell, the additional cost in optical restoration can only be due to signal regenerators deployed at intermediate nodes.

4.4 Results and Discussions

Simulations are performed for NSFNET (14 nodes, 21 links shown in Fig. 4.4) network with a randomly drawn 6 Tbps bidirectional traffic matrix and 80 wavelengths per link. Gold percentage is set to 30% according to reference [99], and it is assumed the same for every traffic demand.

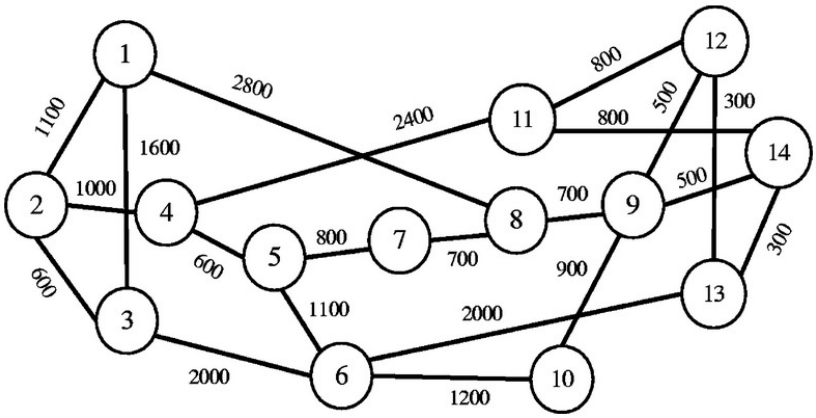

Figure 4.4 — NSFNET topology.

In the offline dimensioning phase (Phase I), scenarios and strategies are evaluated using the already detailed genetic algorithm with the following parameters. Mutation probability is set equal to 5% with 100 chromosomes in each population. The maximum number of generations, used as a stopping criterion, equals $10,000$ for each instance. This means that the near optimal solution is picked out of one million solutions. We also assume that each traffic demand can at most be split twice (splitting constant equals two). This choice depends on the traffic matrix, and can severely improve simulation run time if well adapted to the problem, since splitting constant and optimization space size are strongly correlated.

We compared the results obtained with the MILP formulation (4.1) to the ones stemming from the genetic algorithm in Phase I. We found that the optimality gap, calculated by relaxing the integer variables, is in the interval of $10\% - 20\%$, but expect that it would be significantly reduced if the MILP formulation could be run for enough time (limit of memory). Using medium sized topologies (up to ten nodes); our genetic algorithm gives the optimal solution within few minutes, whereas the MILP (4.1) can take up to several hours. The MILP (4.1) is therefore used for validation purposes and the results hereafter are obtained using the genetic algorithm.

Figure 4.5 shows the fitness function evolution of genetic algorithm as a function of the number of generations for traffic protection in Phase I. It depicts a sharp drop in the first thousand generations for all scenarios before continuing to fall steadily until it can be practically considered to be convergent. The gap between the curves is due to the fact that M-MLR and M-ELS scenarios have less traffic volume to deal with because backup best effort traffic is left for later restorations. As expected, M-MLR and M-ELS present no difference in terms of cost in this offline dimensioning phase, since elastic transponders are restricted to offer the same discrete rates as fixed rate transponders.

Figure 4.6 shows network overall cost from both IP and optical layers including optical restoration additional cost for different scenarios. It can be noticed that M-MLR scenario under HDF strategy assumptions, has the highest optical cost mainly due to WDM regenerators. However, IP-P is the costliest in terms of network multilayer cost, due to some IP interfaces that are avoided in both M-MLR and M-ELS scenarios

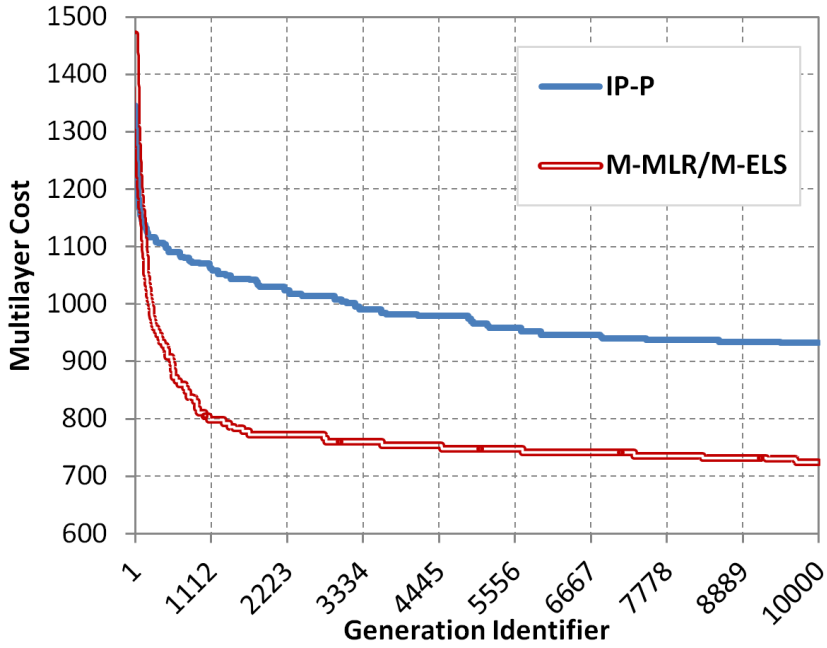

Figure 4.5 — Evolution of fitness function in the offline dimensioning phase (Phase I) as a function of the number of generations.

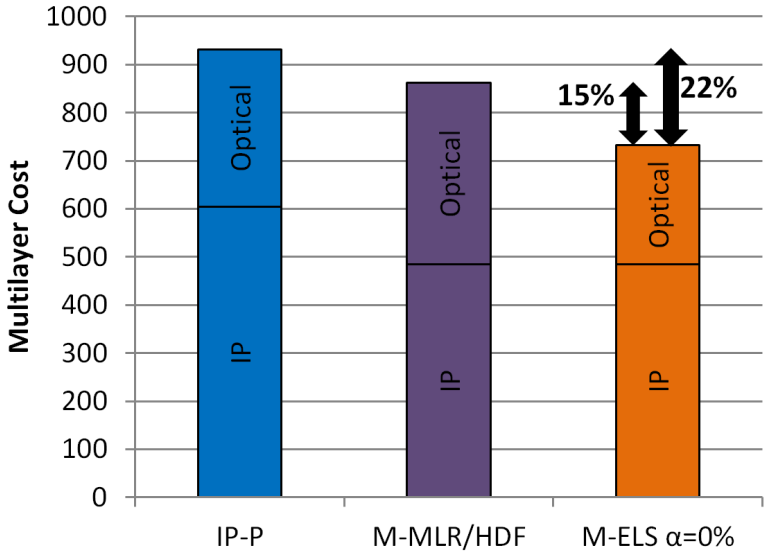

Figure 4.6 — The overall cost of the network after the three provisioning phases for three different scenarios.

gained from optical restoration. This means that optical restoration in MLR networks is instead of interest in a multilayer context. Importantly, M-ELS scenario allows reducing the multilayer cost of the network by more than 20%, taking advantage of both optical restoration and transponder elasticity assuming its extra cost is negligible ($\alpha \approx 0$).

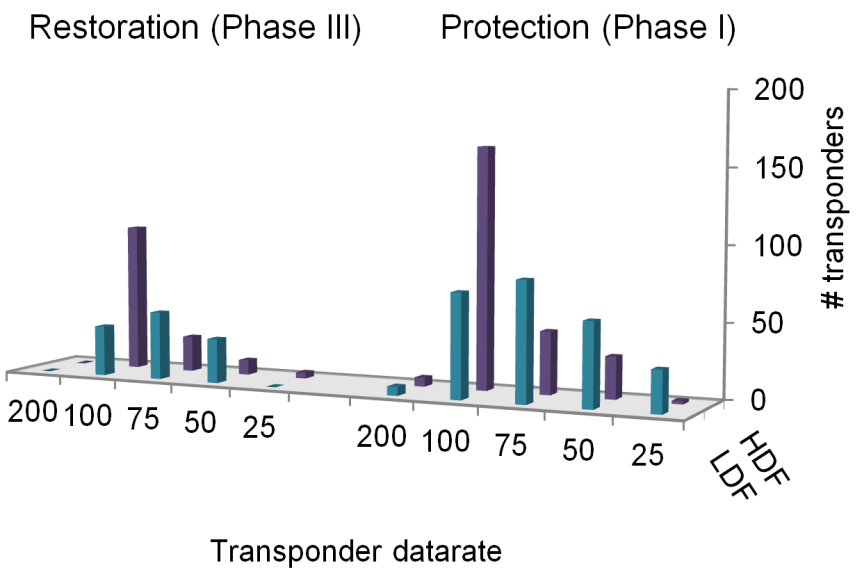

Figure 4.7 — Number of optical transponders (including regenerators) used in M-MLR scenario with both strategies LDF and HDF. In Phase II there is no resource provisioning.

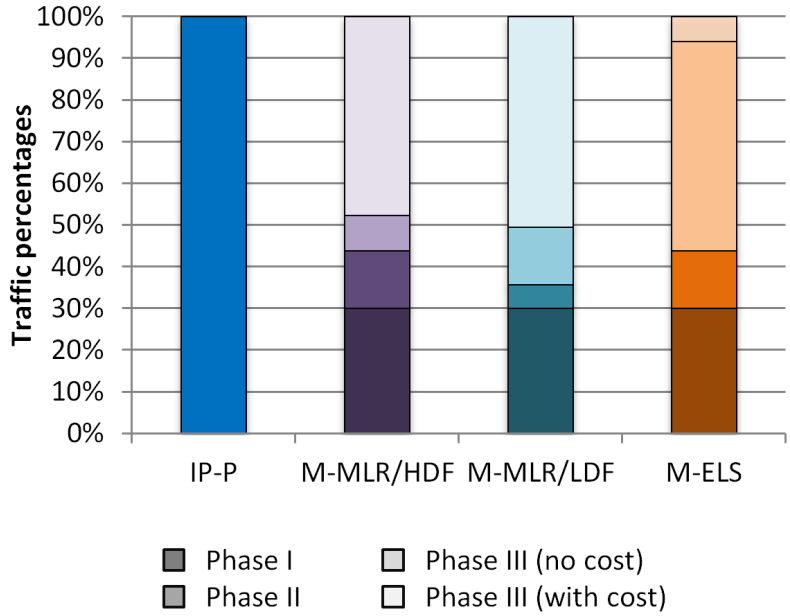

Figure 4.8 — Best effort percentage restored or protected in each phase for different scenarios. Phases can be distinguished based on the color intensity: from darkest (Phase I) to lightest (Phase III). There is no need to precise α value in M-ELS scenario as this percentage is independent from it.

In the following, we focus only on the optical layer cost given that both M-MLR and M-ELS scenarios have the same IP cost as already shown in Fig. 4.6. Note that, transponder selection strategy and elasticity additional cost, have no impact on IP

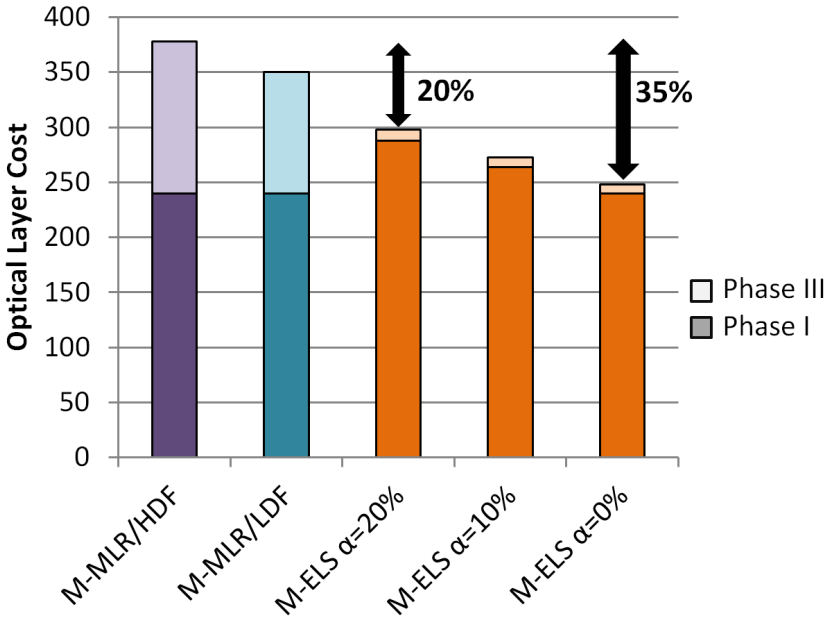

Figure 4.9 — Optical layer cost for M-MLR (LDF, HDF) and M-ELS with elasticity extra cost variation (i.e., α). Phase II has no cost.

layer cost. The later might have some impact for non-realistic values ($\alpha > 1$).

Figure 4.7 shows how transponder distribution in MLR networks is dependent on the transponder selection strategies (HDF and LDF). Remarkably, 200 Gbps transponders were little used with both strategies, which can be explained by the following reasons. First, 200 Gbps transponders cannot support most of the links of NSFNET network due to their limited reach. Second, these transponders require an additional IP interface, and are more likely to be regenerated.

Unexpectedly, Fig. 4.7 shows that favoring high datarate transponders (HDF) does not necessarily imply a strong impact on optical restoration cost. In fact, it would be the case if the remaining free capacity in the network is not used for best effort restoration (Phase II). In other words, favoring high datarate transponders increases the free capacity in the network, and permits to restore completely more traffic demands at no additional cost, with no need for optical restoration. If however traffic demands are partially served in the free capacity, the cost of optical restoration in MLR networks will be the same as if there is no free capacity. This is due to fixed rate transponders which cannot adapt their datarates and therefore take advantage of this reduction. It is obvious in Fig. 4.8 where the percentage of backup best effort traffic served in each provisioning phase with different scenarios is shown. It can be noticed that HDF strategy serves much more traffic at no additional cost in free capacity (Phase II) than LDF does.

In contrast, LDF strategy serves much more traffic in Phase III with no additional cost (no need for WDM regenerators) with optical restoration, doubtless because of extended reaches of low datarate transponders. That is why M-ELS scenario thanks to datarate elasticity can take benefit from both the free capacity using higher datarates,

and the enhanced reach of low datarate transponders at the same time, leading therefore to recovering more than 90% of best effort traffic at no further cost. In other words, if best effort traffic drop is allowed, only 10% of best effort traffic will be dropped in M-ELS versus 70% in M-MLR scenario.

Figure 4.9 distinguishes the optical layer cost coming from traffic protection (Phase I) from that coming from optical restoration (Phase III), considering three different values for elasticity extra cost α (i.e., 0%, 10%, 20%). We notice that optical restoration using elastic transponders reduces optical layer cost by up to 35% with respect to M-MLR scenario, with almost no additional cost from optical restoration thanks to elasticity concept. This gain is still significant for elasticity extra cost up to 20%, and can be further improved if only fixed rate transponders that are concerned by optical restoration are equipped with elasticity. This migration scenario is conceivable, given that elasticity feature can be integrated as an optional license in transponders.

So far, results are obtained for a single topology (i.e., NSFNET), a single percentage of gold traffic, and a single transponder model in a multilayer layer context. Some results have been shown on optical layer equipment only, but they have been found carrying out a multilayer optimization.

In the following, we consider a different topology i.e., German network (17 nodes, 26 links) [114], which is known by its short links contrary to NSFNET. Transponder model is also varied considering at first stage 200 Gbps transponders, and then excluding them from simulations. This allows identifying the potential impact of transponder model and network topology on simulation results. Moreover, we vary the gold percentage in order to show how this affects network overall cost.

Since this part considers only optical layer cost, MILP/ILP formulations can be used with acceptable optimality gaps. Instead of the genetic algorithm, we use the ILP formulation proposed in [114] for resource provisioning in Phase I (optimality gap $<$ 10%). This ILP formulation minimizes optical layer cost given a traffic matrix routed on a known physical topology, taking into account both wavelength continuity constraint and heterogeneous transponder reaches (i.e., regenerator placement).

Network overall cost in both topologies is shown in Table 4.4. Again, optical restoration cost in MLR networks is so expensive that the network cost significantly exceeds IP-P restoration scenario. Actually, the main reason for this effect is that initial traffic demands are cut into several sequential demands due to traffic grooming interest (IP interfaces are not considered), resulting in significant additional cost when lightpaths are later restored with high datarate transponders. Similar results have earlier been obtained with multilayer dimensioning when only optical layer cost is shown (Fig. 4.6).

Now, we exclude 200 Gbps transponders from simulations (Table 4.5). As expected, NSFNET network results are almost identical as 200 Gbps transponders were little used (shown in Fig. 4.7). For German network, optical restoration gets absolutely costless for both multilayer restoration scenarios. This happens when all transponders concerned by optical restoration can send best effort traffic on backup paths with no regeneration, meaning that transponder elasticity is not useful anymore.

Figures 4.10 and 4.11 show optical layer cost as a function of gold traffic percentage variation for NSFNET and German networks respectively. The Gold curve represents

Table 4.4 — Optical layer cost in NSFNET and German networks

Restoration scenarios	NSFNET network			German network		
	IP restoration	Optical restoration	Total cost	IP restoration	Optical restoration	Total cost
IP-P	180	0	180	146	0	146
M-MLR/HDF	136	88	224	122	48	170
M-ELS ($\alpha = 0$)	136	26	162	122	6	128

Table 4.5 — Optical layer cost for different scenarios in both NSFNET and German networks without 200 Gbps transponder

Restoration scenarios	NSFNET network			German network		
	IP restoration	Optical restoration	Total cost	IP restoration	Optical restoration	Total cost
IP-P	182	0	182	172	0	172
M-MLR/HDF	138	92	230	152	0	152
M-ELS ($\alpha = 0$)	138	22	160	152	0	152

optical layer cost portion related to gold traffic protection. It can also be regarded as the total cost if best effort traffic drop is permitted. The gap between Gold and multilayer restoration curves (M-MLR and M-ELS) is then the extra charge of optical restoration. For both topologies (Fig. 4.10 and Fig. 4.11) these curves have the same behavior.

Actually, as optical layer has less traffic amount to restore when gold percentage increases, elastic transponders can operate at lower datarates and then cover longer distances. In contrast, high datarate transponders that have been selected in Phase I to support gold traffic increase, can be an issue for M-MLR scenario when it has to optically restore best effort traffic on longer paths. However, since some traffic demands can be completely restored in phase II due to lower best effort traffic volume, optical restoration cost (extra charge) in M-MLR scenario fluctuates and does not strictly respect the decreasing order. In other words, having less best effort traffic amount to restore with M-MLR transponders presents no interest, if after increasing gold traffic percentage (i. e. decreasing best effort) no traffic demand can be completely served in Phase II.

Contrary to IP restoration (Gold curve), the optical restoration cost (extra charge) in M-ELS scenario is strictly decreasing and it gets costless from 50% of gold traffic. This means that offloading all the best effort traffic to the optical layer, is not the best approach. Instead, a part of the best effort traffic can be advantageously golden in order to optimize the network overall cost.

Based on the overall results, we conclude that optical restoration in elastic optical networks is always useful for any network topology, provided that elastic transponders allow reach adaptation.

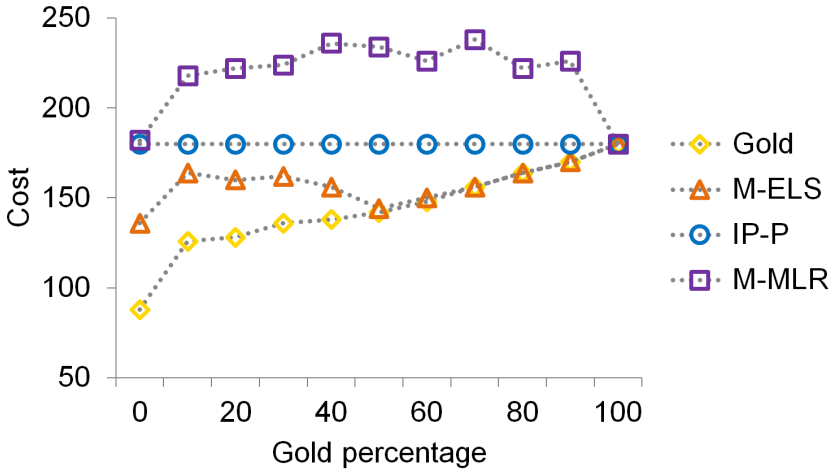

Figure 4.10 — Impact of gold percentage variation on restoration scenario optical layer cost in NSFNET network.

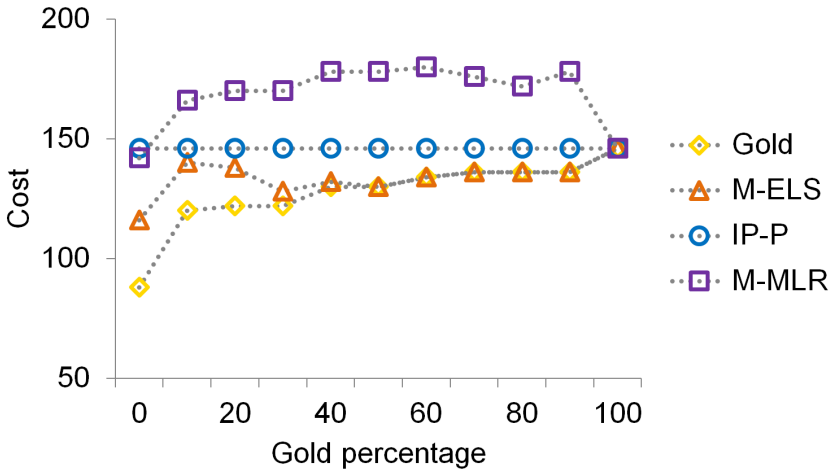

Figure 4.11 — Impact of gold percentage variation on restoration scenario optical layer cost in German network.

4.5 Conclusion

In this Chapter, we have proposed and thoroughly described a multilayer dimensioning tool for offline resource provisioning and traffic restoration in both mixed line rates and elastic optical networks. Specifically, a genetic algorithm for large instances and a mathematical formulation for validation purposes have been proposed and discussed.

We have identified and evaluated a new datarate elasticity-based multilayer architecture for traffic restoration that takes benefit from best effort traffic low priority in a multilayer dimensioning context under single failure assumptions.

Interestingly, simulations revealed that our architecture can significantly reduce net-

work overall cost by saving on both IP and optical layer equipment. This is obtained by offloading a part of backup best effort traffic to optical layer for later restoration avoiding therefore some IP interfaces that would be needed for higher traffic volume. Subsequently, performing optical restoration with elastic transponders for the offloaded traffic, allows saving on some WDM regenerators which are required for long backup paths in mixed line rates optical networks as transponder model impact is quite counteracted. Even in case where best effort traffic drop is allowed, datarate elasticity is still relevant and permits to significantly minimize the non-recovered traffic part. Actually, datarate-elasticity-based optical restoration is a cost-effective approach that ensures best effort traffic recovery irrespectively of network topology and high datarate transponders.

We have also shown that elasticity gain is still significant for considerable elasticity extra cost in the full network migration worst case in which all fixed rate transponders are replaced by elastic ones. In addition, gold percentage variation has no significant impact on optical restoration cost in mixed line rates networks. In contrast, in multilayer elastic scenario, IP and optical restoration costs are, respectively, proportional and reversely proportional to gold traffic increase. This means that instead of offloading all best effort traffic to optical layer, performing a joint optimization should lead to significant cost reductions.

Therefore, operator network planner can forecast for the uncertain traffic growth (using high datarates) while being protected against the unforeseen network failures (using low datarates) thanks to elasticity concept.

However, we have considered some general hypothesis upon which results might be dependant. We did not consider traffic evolution, which is expected to compete the optical restoration in the use of available resources. We have assumed that gold percentage is the same for all traffic demands. Indeed, considering variable percentage per demand is more realistic, but will introduce further complexity in the tools.

Furthermore, the cost ratio between IP interfaces and transponders can vary depending on cost erosion and product evolution. This might have impact on the results but the interest for elasticity is expected to remain the same. Likewise, performing traffic demand splitting and grooming freely in the network, requires some advanced capabilities at the network level which might be difficult to carry out in today's core networks.

It is noteworthy that the use case we have proposed in this chapter is only for link failure cases. This is because optical restoration cannot be applied under node failure assumptions since the same equipment is used for working and backup traffic.

CHAPTER 5

Optical Power Aware Network Dimensioning and Link Design in Flex-grid Optical Networks

5.1 Introduction

The current work is dedicated to the evaluation of optical layer flexibility in its diverse forms. In Chapter 3, we have evaluated the spectrum flexibility provided by flex-grid ROADMs and spectrum management. Chapter 4 focuses on the flexibility in tuning datarate and reach of optical transponders (datarate elasticity). This Chapter studies another type of flexibility in per-channel optical power management.

As explained in Chapter 2, flex-grid consists in adapting the optical channel spacing to its real spectrum requirements in such a way that spectral efficiency is maximized. However, the deployment of new ROADMs with flex-grid WSSs, and more powerful optical amplifiers, in addition to the operational cost, makes flex-grid technology expensive for network operators in spite of its capacity increase promises.

Keeping legacy optical amplifiers is an interesting case to study in this respect, and should be taken into account in migration policies, when moving from the conventional fixed grid to the flex-grid technology. Indeed, considering the same spectral bandwidth (e.g., C band), the total required optical power per fiber span depends on the number of optical channels the fiber span is carrying. For this reason, physical links in flex-grid optical networks need more optical power than before on account of the increase of the number of channels, and the total required power may exceed the maximum power of legacy amplifiers if they are not replaced by more powerful ones.

Therefore, using the freed spectrum in flex-grid links may be impossible, due to the lack of optical power. Indeed, it would imply in this case that the optimum powers of the already established channels get reduced as soon as the freed spectrum is used. This is unacceptable since channel performance would be degraded and possibly the associated services would be interrupted. In other words, the freed spectrum may not be usable.

Besides, during the offline system design, every physical link between two adjacent ROADMs is designed to support the same maximum capacity a wavelength division multiplexing system can transport while maximizing the optical reach. Therefore, the offline design does not depend on the actual requirement of traffic demands as it prepares resource provisioning for the worst case (i.e., full capacity, and maximum transmission reach). This consequently leads to power resource overdimensioning with considerable power margins on some links, due to the non-uniform distribution of traffic demands and their required reaches.

To the best of our knowledge, we are the first to address the optical power limitation issue in flex-grid optical networks [8, 115].

In the following, we evaluate how optical power margins can be used to support the increase of the number of channels in flex-grid optical networks. We also propose real uncompensated link design method using dual-stage EDFA model over non-identical fiber spans. Uncompensated links assume that the chromatic dispersion which is a linear effect in optical fibers, is compensated for at the receiver side and not at intermediate dual-stage amplifiers. This specific type of link design is optimized for 100 Gbps transmissions (and beyond) which make use of coherent detection [25].

5.2 Link Design

A physical link is a set of different successive fiber spans and amplifiers installed between two ROADMs (Fig. 5.1). The link design consists in specifying the channel launch optical power and the set of amplifiers that optimize signal performance at the receiver side, in such a way that amplifier limits are not exceeded.

Under specific assumptions, signal performance is estimated by SNR, considering both amplification and non-linear noises. We use the LOGON strategy which performs a local optimization of the SNR, assuming that the spans are independent from each other [116]. The optimum power spectral density is given in Equation (5.1), where h, ν, F_n, and $\rho_{NLI,n}$ stand for the Planck's constant, the electromagnetic wave frequency, the noise figure of the amplifier at the output of the n^{th} span, and its non-linear effect contribution, respectively [116].

This strategy leads to global optimal solutions in case where all spans are identical (same span loss a_n), and associated with the same non-power-limited amplifiers. We

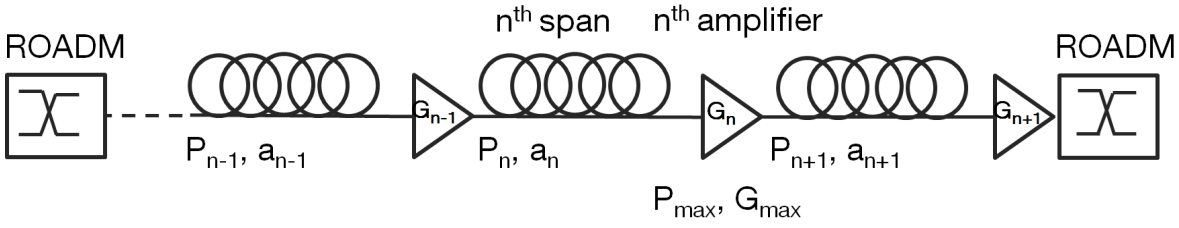

Figure 5.1 — Example of a physical link, between two ROADMs, with $n+1$ fiber spans and amplifiers.

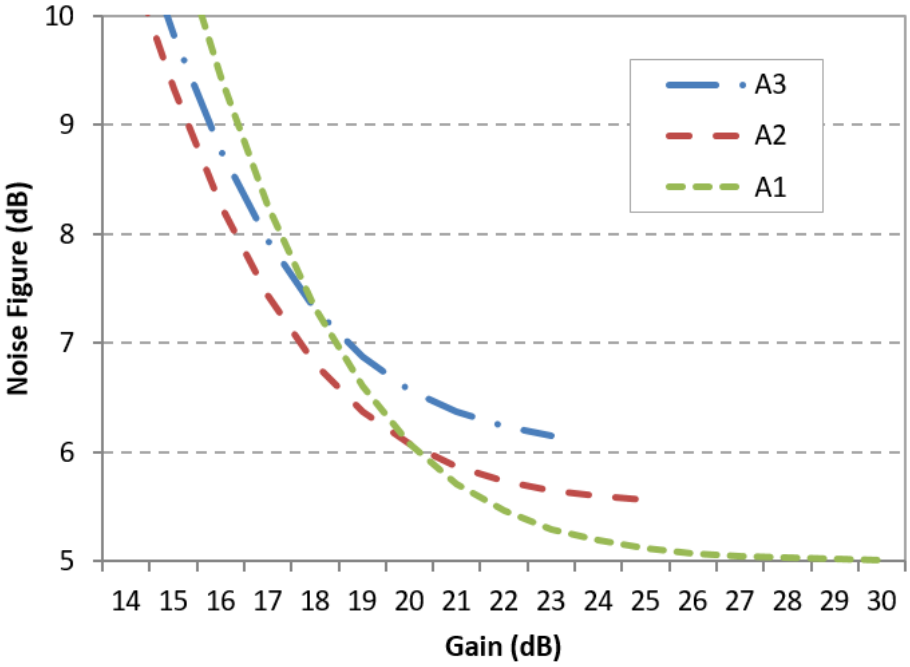

Figure 5.2 — Gain variation vs noise figure for the dual-stage amplifier model of Table 5.1.

point out that for two successive spans, the optimum launch powers of both spans depend on the gain G_n of the amplifier to be deployed between them. Therefore, they cannot be set independently, especially if the spans are not identical. It is shown in Equation (5.2) where the gain of the n^{th} amplifier is computed as a function of the launch power of the $n+1^{th}$ span.

We consider different types of variable gain dual-stage amplifiers without mid-stage access (no DCM module) with parameters (F_1, F_2, G_{max}, P_{max}, D) (Table 5.1). F_1 and F_2 are the noise figures for the first and the second stage respectively, G_{max} is the amplifier maximum gain, P_{max} is the amplifier maximum power, and D denotes the power ratio for both stages to take into account the difference between preamplifier and booster performance. The resulting noise figure, which varies according to gain adaptation [117], can be written as in Equation (5.3).

Figure 5.2 shows noise figure variation as a function of required gain for the dual-stage amplifier model of Table 5.1 using Equation (5.3).

The non-linear relationship between system variables can be noticed. On the one hand, the optimum power used in a given span is calculated in terms of the noise figure of the amplifier to be located next to it. On the other hand, this amplifier should deliver the optimum power required in the next span. This last constraint is satisfied through amplifier gain adaptation, which impacts the noise figure and, therefore, the already calculated optimum power for the previous span. Solving the non-linear equation resulting from the compilation of Equations (5.1), (5.2) and (5.3), we obtain the optimum required gain (G_n^{op}) in Equation (5.4). This last equation is the key element of our design method, as it ensures that optimum powers are used for all channels in every span while respecting the power propagation model in the physical

link (Equation (5.2)).

$$P_n = \left(\frac{h\,\nu\,F_n}{2\,\rho_{NLI,n}} \right)^{\frac{1}{3}} \tag{5.1}$$

$$G_n = a_n \frac{P_{n+1}}{P_n} \tag{5.2}$$

$$F_n = F_1 + \frac{F_2\,D\,G_{max}}{G_n^2} \tag{5.3}$$

$$G_n^{op} = \sqrt{\frac{4\,F_2\,D\,G_{max}}{3\,F_1}} sinh \left(\frac{1}{3}\, asinh \left(\frac{\rho_{NLI,n}\,a_n^3\,P_{n+1}^3 \sqrt{\frac{27\,F_1}{F_2^3\,D^3\,G_{max}^3}}}{h\,\nu} \right) \right) \tag{5.4}$$

The link design is performed from the last span to the first one. We choose the amplifier type that can satisfy both required gain and optimum power while achieving smallest noise figure (see Fig. 5.2). If no amplifier can satisfy these requirements, the one with the closest maximum power (P_{max}) is chosen. The difference to the required power is subsequently recovered by re-tuning the gain(s) of the following (downstream) amplifier(s) as explained in Algorithm 3. Apart from the robust mathematical aspect of the design method, it has been validated through intensive comparisons with real link design data stemming from an existing link design tool of Orange.

Note that this design method is based on the LOGON strategy, and it performs a local optimization at the amplifier level for each two successive spans. A global optimization for the whole link is difficult to carry out due to the non-linear aspect between system variables, being complicated with the increase of the number of spans. Furthermore, in the results presented in this work, ROADM nodes are assumed ideal with no contribution to the amplified spontaneous noise. Recent studies consider ROADM contribution to the SNR and optimize the optimum power at the ROADM level as well [118]. This approach could be integrated into our design method, even if the optimization would come to the downside of the LOGON main idea, which considers that a local optimization leads to near global optimum.

Type	**Characteristics**				
	P_{max} (dBm)	G_{max} (dB)	F_1 (dB)	F_2 (dB)	D (dB)
A_1	17	30	5	6.5	3
A_2	19	25	5.5	7	5
A_3	20	23	6	7.5	7

Table 5.1 — Dual-stage EDFA amplifier model

5.3 Network Optimization

As mentioned above, the optimum optical power may exceed the limitations of existing amplifiers, when moving from the conventional fixed grid to the flexible one. Indeed,

Algorithm 3 Link Design Algorithm

Require: Link, span characteristics (length, attenuation), and $SetOfAmpli$

$CurrentAmpliPosition \leftarrow LastPosition$
$RequiredPowerNextSpan \leftarrow ROADMPower$
while $CurrentAmpliPosition \neq FirstPosition - 1$ **do**
  for $Ampli$ in $SetOfAmplis$ **do**
    $CandidateAmpli \leftarrow \emptyset$
    calculate G_n^{op} using Equation (5.4)
    if $(G_n^{op} \leq G_{max})$ and $(RequiredPowerNextSpan \leq P_{max})$ **then**
      push $Ampli$ onto $CandidateAmpli$
    end if
  end for
  if $CandidateAmplis \neq \emptyset$ **then**
    among $CandidateAmplis$ add to $Solutions$ the amplifier with the smallest F_n calculated with Equation (5.3)
  else
    add to $Solutions$ the amplifier with P_{max} closest to and strictly less than $RequiredPowerNextSpan$
    recover the difference by increasing the gain(s) of the next amplifier(s) stored in $Solutions$
  end if
  $CurrentAmpliPosition \leftarrow PreviousPosition$
  set $RequiredPowerNextSpan$ to the optimum power calculated with Equation (5.1)
end while
$RequiredPowerNextSpan$ is the design power that should be injected in the first span
return $Solutions$

when the initial fixed grid design is accomplished, most of the amplifiers have an extra power reserve, since the received power in the design is not necessarily equal to the maximum power of the amplifier. However, this power reserve varies from one span to another and can be insufficient to support flex-grid additional channels over some links. This additional constraint is a strong limitation if the saved spectrum cannot be used over these links, bringing into question flex-grid expected gains.

A straightforward solution consists in replacing all the deployed amplifiers with more powerful ones, and performing a new design for the maximum number of channels that can be transported by flex-grid based links. However, this procedure is expensive and can lead to power resource overdimensioning.

Another possible and more pragmatic way consists in changing the design paradigm. Indeed, maximizing the SNR at the receiver side is not always effective, since it wastes power margins for the channels that do not have stringent requirements in terms of optical reach. Therefore, tailoring the SNR to the actual needs reducing per-channel power seems interesting to save on optical power, and consequently increase link capacity [102].

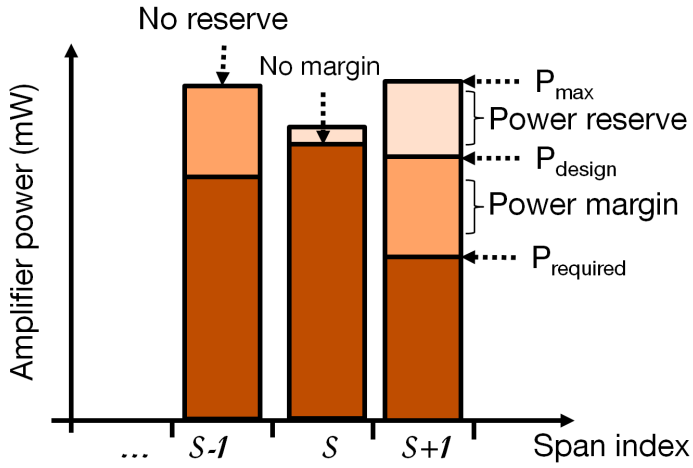

Figure 5.3 — Example of amplifier power margin and power reserve for three different spans. In this link no channel can be added using P_{design} since the smallest power reserve over the link is null.

In the rest of this chapter, we mean by power reserve the difference between the amplifier maximum power and the optimum design power that considers the worst case (i.e., full capacity, and maximum transmission reach). Meanwhile, the power margin herein refers to the difference between optimum design power and current power after power adaptation using the new design paradigm (Fig. 5.3).

Figure 5.3 depicts a link of three fiber spans. The amplifier corresponding to the span $S-1$ will be used at its maximum power when all optical channels are established simultaneously. Therefore, it has a null reserve preventing the other spans from establishing additional channels (more than the limit of the design).

This issue can be overcome reducing individual channel powers to their minimum values ($P_{required}$ in Fig. 5.3). Consequently, Power margin in the span $S-1$, power reserve in span S, and both in the span $S+1$ can be used to establish additional channels, with no impact on existing channel performance.

5.3.1 Power Adaptation and Migration Scenarios

Flex-grid technology introduces a degree of flexibility at the spectrum level, allocating different optical channels with different spectrum widths. Another degree of flexibility can also be introduced at the power level by the means of power adaptation. It consists in adapting the initial launch power to its minimum value given a minimum acceptable SNR at the receiver (Fig. 5.4). This SNR_{min} target depends on both modulation format, and decision decoding method. Once it is known, the initial launch power ($P_{required}$ in Fig. 5.4) can be simply determined as in Equation (5.5), where P_{design} and SNR_{design} are the optimum launch power calculated with Equation (5.1) and corresponding SNR, respectively.

$$P_{required} = \frac{P_{design} \times SNR_{min}}{SNR_{design}} \tag{5.5}$$

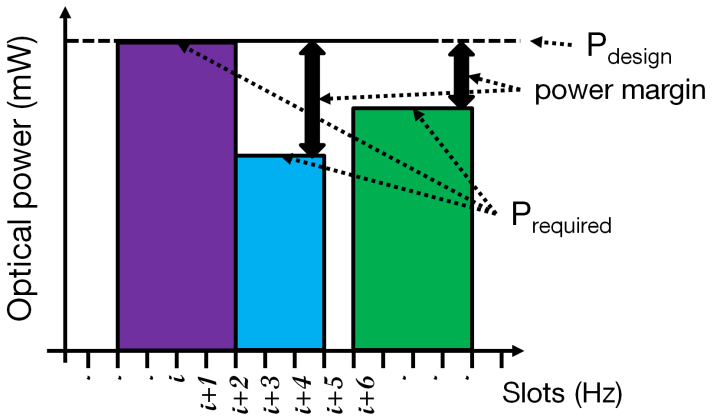

Figure 5.4 — Example of power margin for one fiber span with three optical channels. Horizontal flexibility (flex-grid), and vertical flexibility (power adaptation) are illustrated.

This approximate equation of the initial launch power results from the fact that the SNR target, calculated for one path of successive links, is the inverse of the sum of the inverse SNR of each link along the path [116]. However, it does not take into account non-linear penalty variation induced by power adaptation. Actually, it underestimates signal performance as the per-channel power is rather reduced with respect to the initial power design (P_{design}). This guarantees that the new SNR related to $P_{required}$ is greater or equal to SNR_{min} [119].

In order to evaluate the potential power adaptation impact on both cost and capacity of the network, we identify and study the following network migration scenarios:

- Fixed grid (FG): the initial design is performed for eighty channels over a 50 GHz grid. This scenario is representative of nowadays core optical networks, and it is used in this work as a benchmarking reference for the other scenarios. Blocking in this scenario can only be due to the lack of spectrum resources.

- Flex-grid with legacy design and non-power-limited amplifiers ($FX80$): this "whatif" scenario considers the legacy design i.e., optimal per-channel power calculated with the FG design, but it allows that the amplifiers exceed their maximum power limits P_{max}. This scenario does not reflect any realistic case and it is only used for benchmarking purposes.

- Flex-grid with legacy design ($FX80D$): the existing amplifiers are maintained in use with respect to the FG initial design for eighty channels (no extra amplifier cost). In $FX80D$, the power aware dimensioning takes benefit from the extra power reserve of the amplifiers to establish more than eighty channels. The span with the smallest power reserve will however limit the other spans along the physical link. This scenario reflects what happens if flex-grid technology is deployed with the legacy amplifiers.

- Flex-grid with legacy design and power adaptation ($FX80DP$): it is an extension of $FX80D$ scenario with the possibility of adapting individual channel powers to the real requirements according to the minimum SNR acceptable value. Both

$FX80D$ and $FX80DP$ can be blocked due to the lack of spectrum, to the spectrum fragmentation and to the lack of optical power.

- Flex-grid with new design ($FX106$): the links are designed to support the maximum number of channels in flex-grid optical networks (i.e., 106, considering the same 4 THz band as for FG and 37.5 GHz spacing). Network dimensioning is that of a greenfield deployment with new well-adapted to flex-grid amplifiers thus leading to an extra cost. Since the offline link design is performed to support the maximum number of channels, the only origins of blocking are the lack of spectrum and the spectrum fragmentation.

These network scenarios are compared using the planning tool described in Chapter 3, the 32 Gbaud 16QAM and QPSK transponder/superchannel types and the cost model presented in Table 3.4 of Chapter 3. The cost of one EDFA amplifier is assumed equal to 10% of the cost of one 100 Gbps transponder. This cost ratio is what we observe in the WDM systems being deployed nowadays, but it may vary depending on the manufacturers [111].

5.4 Results

Simulations are performed on a 32-node and 42-link European backbone network (Table 3.6 of Chapter 3) using single mode fiber (chromatic dispersion = $17\,ps.nm^{-1}.km^{-1}$, fiber attenuation = $0.22\,dB/km$, non-linearity coefficient = $1\,W^{-1}.km^{-1}$). Links are designed using the three amplifier types of Table 5.1 and assuming non-identical span lengths, randomly drawn according to a Gaussian distribution $\mathcal{N}(\mu = 100\,km, \sigma = 27\,km)$. SNR filtering penalties induced by transit across one ROADM are 0.05 dB and 0.64 dB for 50 GHz and 37.5 GHz channel spacing, respectively [83]. The minimum acceptable SNR at the receiver side, using 0.1 nm noise reference bandwidth, including operational margins, is fixed to 13.5 dB for QPSK and 22 dB for 16QAM for a bit error rate equal to 10^{-3}.

The span loss distribution of the topology is representative of some of Orange's networks. Most of the spans in the topology are not constraining and their corresponding amplifiers have some power margin to support more than eighty channels. However, some links have span configurations with large losses, which prevent from obtaining the optimal power tuning even when used at their maximal gain and/or power. It would have been possible on these spans to use other amplifiers more powerful or with larger gain, but these are more expensive, and we chose to keep the same amplifier portfolio for the whole network for cost reason.

Similarly, we assumed that the amplifier sites were fixed and that additional amplification site could not be envisaged on these constraining spans. As a result, the constraining spans of these links have often no power reserve, and this impacts the whole link: even if its other spans have some power reserve, the link cannot support more power (already explained in Fig. 5.3). It is important to note that some topologies do not exhibit such large span loss, and in this case the power limitation is not an issue.

Dimensioning process is triggered for seven successive forecasted periods of time, assuming a 35% traffic growth rate. This is the maximum number of periods that all scenarios can support without blocking. This ensures a fair comparison between network scenarios as they would have to deal with the same traffic volume. Twenty initial traffic matrices, normalized to $6\,Tbps$, have been randomly drawn according to a realistic logical topology. Demands are optimally served choosing the set of transponders (with regenerator placement) that first minimizes cost and then minimizes spectrum occupancy [83].

Figure 5.5 depicts the current power level for $FX80$, $FX80D$, and $FX80DP$ scenarios in each used span, the P_{max} and the P_{design} of corresponding amplifier (the one located at the input of the span) in the last planning period. Fiber spans are ordered in a decreasing way according to the total traffic demand volume they are carrying in $FX80DP$. Optical power usage varies from one span to another due to the variable design and the non-uniform distribution of traffic in the whole network. In spite of the non-null power reserve in each amplifier (emerging orange part in Fig. 5.5), it can be noticed that about fifteen spans exceed the maximum power limit in the non-realistic scenario $FX80$. This means that a part of the saved spectrum in the other flex-grid scenario: $FX80D$ cannot be used due to the lack of power, as it is constrained by the characteristics of legacy amplifiers and the optimum launch powers. The significant emerging green part in Fig. 5.5 represents the optical power amount that is saved - and still not used - thanks to power adaptation approach in $FX80DP$. We can notice that the amplifier power reserve is relatively small in comparison with power adaptation savings.

It is commonly agreed that flex-grid cost savings are produced in the long term [9–11]. This is confirmed by our results which indicate that network cost is identical for all scenarios until the fifth planning period, except for $FX106$ which has an extra optical cost due to the replacement of legacy amplifiers with more powerful ones. This extra cost does not take into account the operational expenses of amplifier deployment and the subsequent interruption of the fiber link. Figure 5.6 shows network cost evolution in the last three periods in which some scenarios start using longer paths looking for either spectrum or power, thus giving rise to an additional cost due to signal regeneration. In all periods, $FX80DP$ outperforms $FX106$ and saves up to 10% of cost with respect to conventional fixed grid (FG). This is obtained thanks to flex-grid saved spectrum, and power adaptation, which avoid some longer paths and consequently potential regenerators. In contrast, flex-grid has almost no cost savings when power adaptation is not allowed with the traditional design ($FX80D$), meaning that the amplifier power reserve is not enough to exploit all flex-grid saved spectrum.

Figure 5.7 shows the saved spectrum percentage for flex-grid scenarios in comparison with conventional fixed grid. As expected, all flex-grid scenarios provide the same spectrum savings with the shortest path routing corresponding to the first four planning periods. During this dimensioning phase, results show a steady spectrum saving decrease over time, since less spectrum effective transponders are more likely to be used with the exponential growth of traffic when optimizing network overall cost. The last three periods see a similar dramatic growth in the spectrum savings for both $FX80DP$ and $FX106$ as the reference (FG) is disadvantaged by longer path lengths. $FX80D$

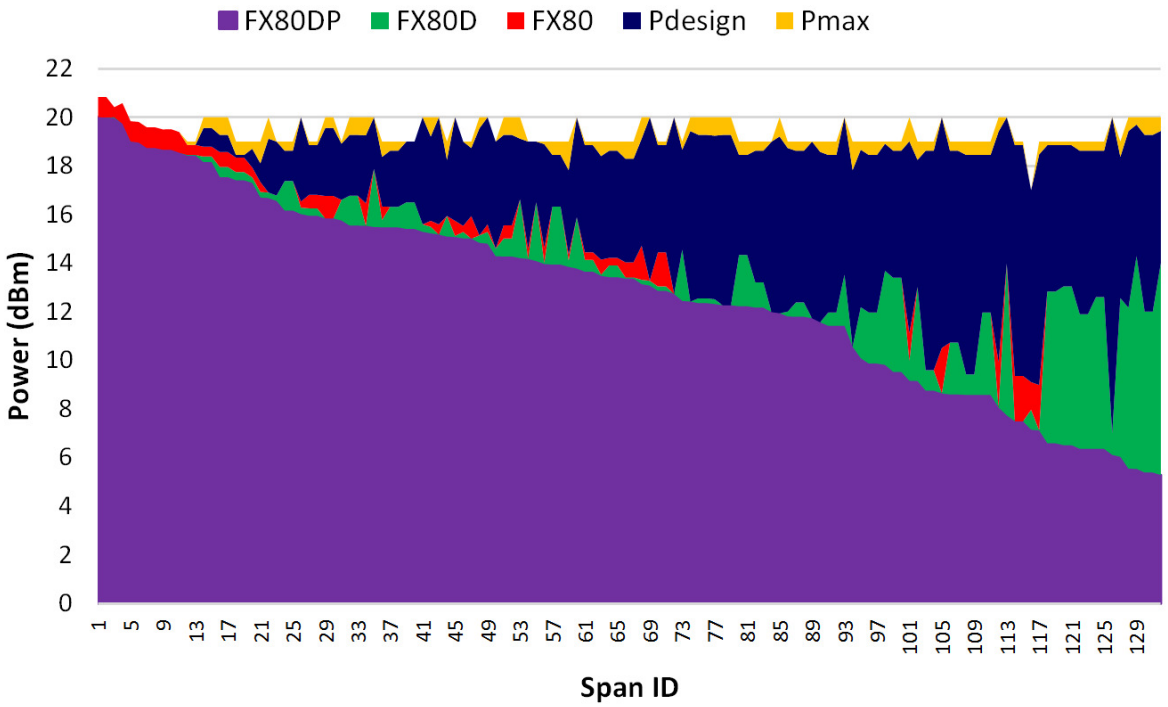

Figure 5.5 — Optical power level in each fiber span for different flex-grid scenarios constrained by legacy amplifiers. P_{max} and P_{design} correspond to the EDFA amplifier located at the input of the fiber span.

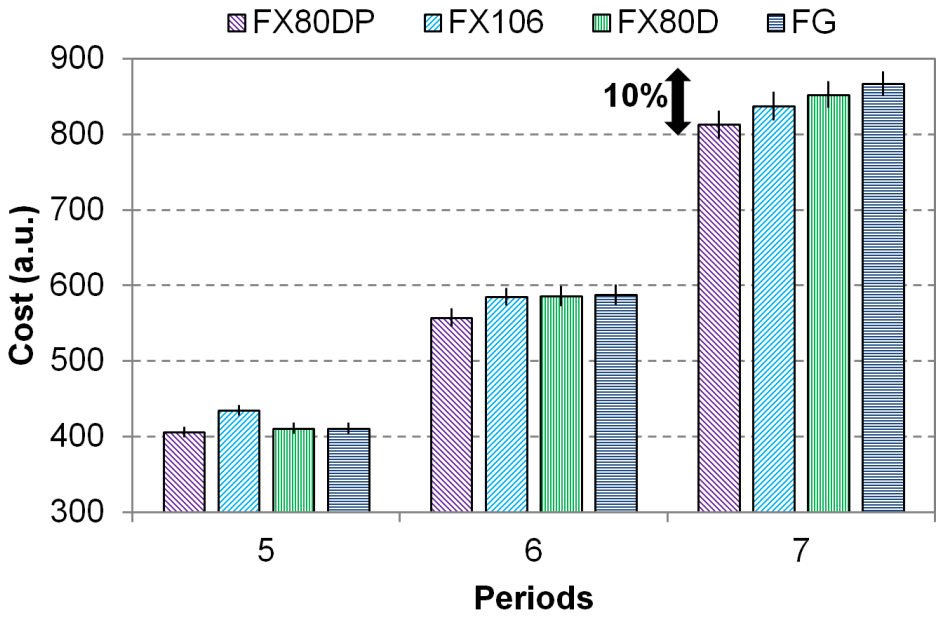

Figure 5.6 — Cost evolution over time for the different scenarios in the last three periods when the shortest paths are left due to the lack of either power or spectrum. Results are obtained with a 90% confidence interval.

scenario being limited by the amplifier reserves, fails to save as much spectrum as $FX80DP$ and $FX106$ do. We then compute the amount of saved spectrum for which

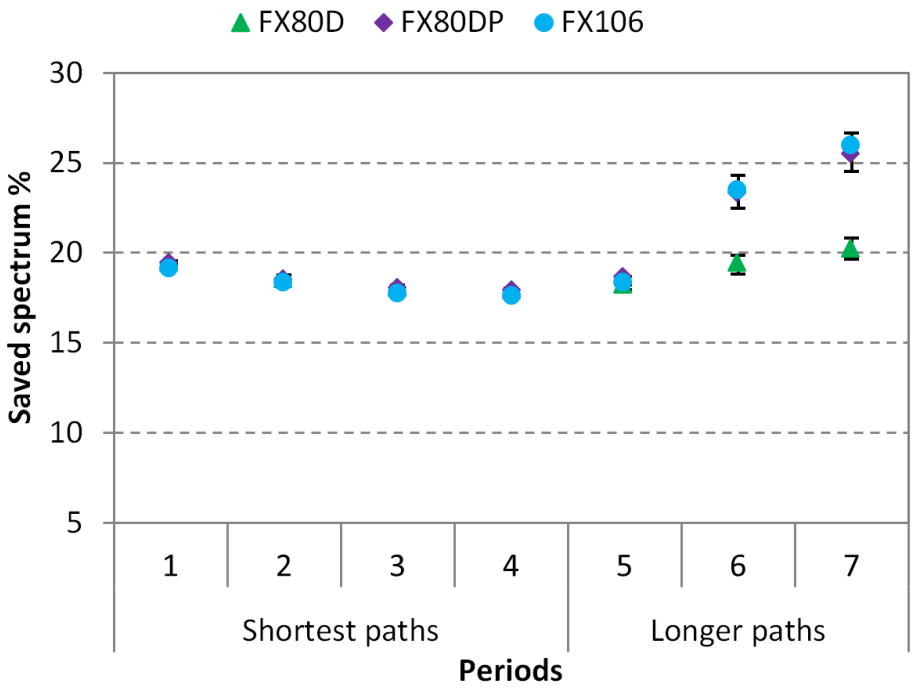

Figure 5.7 — Flex-grid saved spectrum evolution with respect to conventional fixed grid network (FG) using a 90% confidence interval. In the first four periods, the shortest paths are always selected. After that, the routing process selects longer paths looking for either power or spectrum depending on migration scenario.

enough amplification power exists. Indeed, not all saved spectrum shown in Fig. 5.7 can be used to accommodate future traffic demands, as it relies on the available optical power at the moment these demands arrive. in case of $FX80D$ scenario, it is relatively easy to know whether a given part of the saved spectrum is usable or not. Actually, this scenario makes always use of the optimum launch power unlike $FX80DP$ whose power adaptation depends on the characteristics of the future traffic demands. To overcome this, we consider the worst case to which $FX80DP$ can be exposed. The worst case is produced using the optimum launch power assuming that power adaptation cannot be performed for future traffic demands. In this way, we can have a lower bound for the usable saved spectrum in $FX80DP$ as well. In contrast, such a limitation does not arise for $FX106$ scenario since the deployment of new amplifiers guarantees enough power for all optical channels.

Figure 5.8 shows the exact usable saved spectrum for $FX80D$ and its lower bound for $FX80DP$. Contrary to $FX80D$, we observe a small impact on $FX80DP$ saved spectrum despite the pessimistic assumptions. In other words, at any given moment in network life cycle, the already saved optical power through per-channel power adaptation process is quite enough to reap near-full benefits from flex-grid saved spectrum for future traffic demands. This is understandable given the significant non-used saved power amount already shown in Fig. 5.5 (the green emerging part). As expected, $FX106$ saved spectrum remains the same as it is in Fig. 5.7, since there is enough amplification power for all optical channels.

In a nutshell, in $FX80D$ where only amplifier power reserve is taken advantage of, a

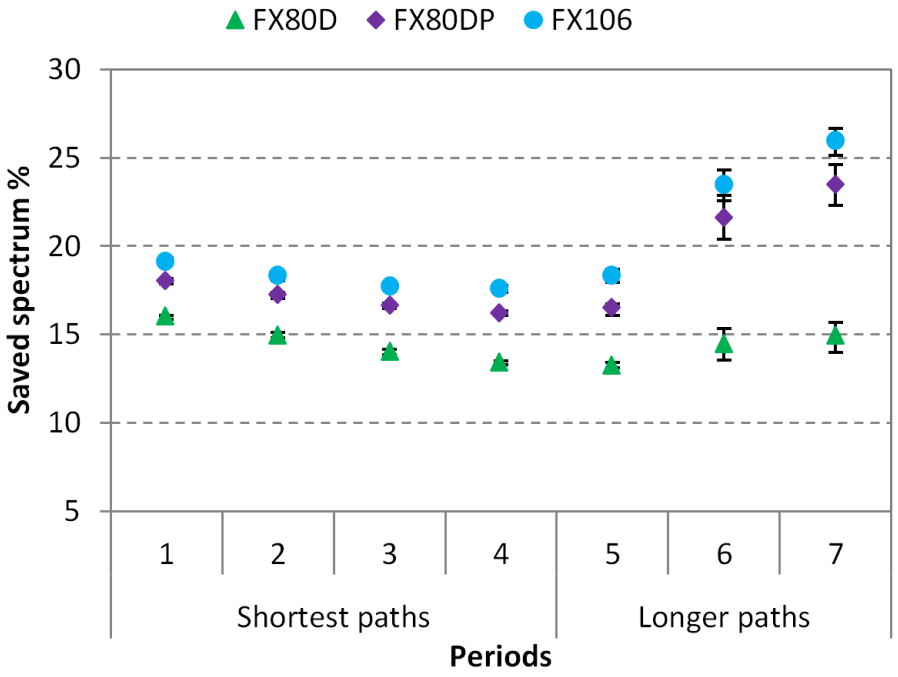

Figure 5.8 — Percentage of flex-grid saved spectrum that is usable with respect to conventional FG scenario. $FX106$ is the same as in Fig. 5.7 since the initial design is performed for all optical channels.

significant part of saved spectrum is unusable due to the lack of optical power. This impact constantly increases over time causing more than 40% loss of flex-grid saved spectrum in the last planning period. In contrast, the power adaptation approach in flex-grid optical networks ($FX80DP$) provides almost the same performance as the flex-grid specific design ($FX106$), while maintaining in use legacy amplifiers.

5.5 Conclusions

In this Chapter, we have tackled the optical power limitation issue induced by the increase of the number of optical channels in flex-grid optical networks. This increase is due to the new narrower channel spacing with respect to the conventional fixed grid width.

We have proposed and thoroughly described a link design method based on the LOGON strategy [116] for different dual-stage EDFA amplifier types over non-identical span lengths. Results of the design have been given as input to an optical power aware multi-period planning tool with the aim of evaluating different flex-grid migration scenarios.

Simulations have indicated that flex-grid optical network savings in terms of cost and capacity can substantially decrease if legacy amplifiers are used with the traditional power design.

More importantly, we have shown that adapting optical launch powers to the actual per-channel requirements in terms of SNR is an effective approach to maintain in use the legacy amplifiers and reap full benefits from flex-grid saved spectrum.

However, results strongly depends on network topology and span distribution. Topologies without constraining spans, will probably have enough power margin to support flex-grid additional channels with no impact on flex-grid benefits. We expect that the addressed problem will not arise for British Telecom network [114], and that it will be serious for NSFNET topology (Shown in Figure 4.4 of Chapter 4).

These results should be of a great interest for network operators, as optical power limitation issue affects both OPEX and CAPEX. The problem statement, the power adaptation approach, and the link design method are proper to this work. Indeed, related works are often focused on flex-grid WSS additional cost and dimensioning complexity. Flex-grid impact on legacy amplifiers has never been studied before.

However, our proposal necessitates an optical power-aware control plane with suitable routing algorithms. This requires some modifications of the existing standards. Taking GMPLS as an example, despite recent efforts of Internet Engineering Task Force (IETF) to enrich it with physical layer awareness [120], neither the parameters that we need for the optical power control process nor the process itself are defined. Therefore, several extensions for Open Shortest Path First (OSPF)-Traffic Engineering (TE) and Resource ReSerVation Protocol (RSVP)-TE protocols should be standardized [115].

Note that, our proposal can also be used with the extra amplifier bandwidth, which allows increasing the number of channels as well. In such a case, the arising problem is due to the under-design and it is not specific to flex-grid technology.

Conclusions and Perspectives

THIS work investigates the performance of optical layer flexibility within core optical networks. Specifically, three types of flexibility have been studied and thoroughly discussed: a) optical channel variable spacing (i.e., flex-grid), b) transponder datarate elasticity, and c) per-channel optical power adaptation.

The contribution of this thesis can be divided into two categories. The first concerns the modeling of flexible optical networks. Different mathematical tools have been proposed and developed. These tools are mainly used to evaluate optical layer flexibility.

The second category identifies profitable and advantageous use cases and networking scenarios that bring forward the interest of flex-grid and/or elastic optical networks. This category also deals with the main disadvantages and the potential troubles of flexibility and provides solutions to them.

Both categories complement each other, and together offer an evaluation and a deep analysis on the way the expected benefits can be attained with minimal impacts.

Along this thesis, flexible optical network dimensioning has been studied by the means of a variety of optimization techniques, including ILP/MILP formulations, simple heuristics such as greedy algorithms, baseline methods, meta-heuristics like genetic algorithms, and analytical models specifically Markov chains.

Tool choice depends on the studied problem, the relevant parameters, and the dimensioning context. For instance, in Chapter 3 we use a k-shortest path routing within an optical layer aware dimensioning context, considering some operational constraints. The reason is that it is representative of today's core networks, and we aimed at evaluating spectrum fragmentation within real circumstances.

The contributions and the results of each chapter are summarized as follows:

- Chapter 1 defines the research context and the background of this work, and it introduces today's network architecture. This chapter also introduces research problematic, and briefly explains optical layer flexibility.
- Chapter 2 presents the state of the art of flexible optical networks, and it deeply explains and discusses optical layer flexibility. This chapter also situates this work, and highlights the weaknesses and the open questions in the literature.

- Spectrum fragmentation issue in flex-grid optical networks is thoroughly investigated and evaluated in Chapter 3. The problem is tackled as follows:

  At first sight, we proposed to dissociate spectrum fragmentation that is due to spectrum continuity constraint from the one that is due to spectrum contiguity constraint. We then focused on the later as it is coming with flex-grid technology seeing that the former type has been enough studied in conventional fixed grid networks.

  Subsequently, we identified two different types of spectrum losses caused by spectrum fragmentation (i.e., the absolute spectrum loss and the relative spectrum loss), and proposed a new spectrum fragmentation metric (i.e., ABP) in this matter.

  ABP metric is afterwards compared with some existing ones in two different manners. A global comparison with regard to metric value meaning and its relevance, and an accurate comparison using an analytical Markov chain. The performance of each fragmentation metric was assessed in terms of spectrum blocking that is due to spectrum fragmentation and the efficiency in spectrum use. Numerical results show that ABP metric performed well compared to others.

  Note that some other fragmentation metrics have been introduced in the literature after the proposition of ABP. For a complete state of the art, these metrics have been cited in Section 2.3.2.1 of Chapter 2.

  We then used ABP metric to evaluate spectrum fragmentation in the incremental traffic context, taking into account some operational constraints of operator core networks. We have defined and evaluated a new 50 GHz frequency slot based flex-grid scenario compliant with the already deployed fixed grid networks.

  Intensive simulations showed that spectrum fragmentation is a real effect of flex-grid but it does not compromise its advantages. Two different engineering traffic strategies have been proposed and evaluated to face spectrum fragmentation instead of spectrum defragmentation techniques. Other existing strategies have been recommended based on the overall results.

  It is noteworthy that some works conducted in parallel with our work have achieved similar results. Researchers are henceforth more focused on spectrum fragmentation issue in dynamic scenarios. In networks with moderate dynamicity, spectrum fragmentation seems avoidable [95, 121].

- In Chapter 4, we proposed and evaluated a novel multilayer architecture for traffic restoration in elastic optical networks. This architecture guarantees a 1+1 protection for high priority traffic (gold), and performs an optical restoration for low priority traffic (best effort) using elastic transponders. It aims at alleviating WDM regenerator additional cost from which the conventional optical restoration has been suffering.

  This architecture was evaluated in both multilayer and optical layer aware dimensioning contexts, with different assumptions for the parameters (i.e., network topology, transponder model, gold traffic percentage, and elasticity additional cost).

A multilayer dimensioning tool for elastic optical network has been proposed. It consists of a genetic algorithm and a MILP formulation for the offline dimensioning, and combined heuristic/ILP for best effort online restoration.

Using this tool, we compared the proposed architecture with conventional IP restoration (protection), and multilayer restoration in MLR networks. It was shown that this architecture significantly reduces network overall cost. Specifically, datarate elasticity permits to plan for the uncertain traffic growth (with high datarates) while being protected against the unforeseen link failures (with low datarates and optical restoration).

It was also shown that optical restoration in MLR networks is interesting only in a multilayer dimensioning context. Contrarily, it saves on both IP layer and optical layer equipment if performed with elastic transponders.

- Chapter 5 tackles the optical power limitation issue that arises when legacy power-limited amplifiers are used with flex-grid technology. The problem statement is proper to this work.

  We proposed a new flex-grid link design method based on the recently proposed LOGON strategy [116]. Different to-flex-grid migration scenarios have been identified and evaluated using the optical power aware multi-period planning tool (presented in Chapter 3) that makes use of the link design method above.

  Specifically, we proposed a per-channel power adaptation approach that takes benefits from link margins, tailoring the launched channel power to the minimum requirements depending on traffic matrix. It was demonstrated that this approach performs as well as the greenfield scenario while maintaining in use the in-place legacy EDFA amplifiers. Without this approach, it was shown that using legacy amplifiers strongly affects flex-grid benefits.

  Despite the attention paid to flex-grid in the literature, related works have often been focused on the additional cost of flex-grid ROADMs. Legacy amplifier impact has never been studied before. We believe that this work will open the way for further studies regarding this matter. For example, current research on control plane required capabilities for real implementation, is already ongoing [115].

This thesis presented algorithmic tools and analysis within the framework of global studies at Orange in order to evaluate the potential benefits of optical layer flexibility. The provided results helped to better understand spectrum fragmentation issue in operator network context, and shed light on the way its impact can be minimized. Thanks to this work, optical restoration can take place in next generations of operator networks, seeing that its additional cost can be significantly reduced with datarate elasticity. It has also proposed a solution to manage the channel power in order to avoid the need for a greenfield deployment of optical amplifiers. Like any research work, these results can be further improved taking into account one of the following research directions:

Inputs: considering another transponder model, instead of the one we considered in Chapter 3 and Chapter 5, can lead to different results regarding spectrum losses. For

instance, with 3-slot and 4-slot transponders, only blocks of one and two frequency slots can be lost due to spectrum fragmentation. In addition, transponder cost model could be different for superchannels that are based on photonic integration components. In the literature, some argue that the availability of cost effective high speed channels is the main reason to deploy flex-grid technology [122].

Similarly, elastic transponder model used in Chapter 4 was based on format adaptation. We expect that FEC adaptation would give further improvements to the use case efficiency. It gets inefficient if datarate elasticity does not allow reach adaptation.

Besides, the legacy amplifier issue we identified in Chapter 5, has been simulated on a single physical topology. In networks with short links, we expect that flex-grid additional channels can be supported with no need to adapt per-channel optical power.

Tools: the spectrum fragmentation metric (i.e., ABP) proposed in Chapter 3 assumes that all transponders have the same chance to be selected (equiprobability). A weighting method can be used in order to have more meaningful values for relative fragmentation.

We evaluated datarate elasticity in a single use case. The proposed architecture in Chapter 4 would perform better combining flex-grid and elasticity. The MILP formulation proposed in Section 4.3.1.1 assumes the same spectrum occupancy for all transponders. It can be slightly adapted to flex-grid networks, by optimizing the number of frequency slots in the whole network. Likely, its associated genetic algorithm does not permit multi-path routing. The chromosome encoding method may be rethought and adapted to such requirements.

Assumptions:

- Instead of generalizing some results on transport networks, one has to differentiate between metro and core networks. The traffic growth rate is greater in metro than in core networks and it is more dynamic in the former. Therefore, most of the conclusions concern incremental traffic scenarios and not networks with high dynamicity.

- In this work, we stated that horizontal fragmentation and vertical fragmentation are often mixed up, and that they should be studied separately. Indeed, even if horizontal fragmentation existed before, it is still the underlying reason of vertical fragmentation. For instance, vertical fragmentation does not exist in opaque flex-grid optical networks if the first-fit provisioning policy is used. Therefore, we expect that it would be worthwhile to study the interaction between both types of fragmentation.

- The multilayer architecture proposed in Chapter 4 does not consider node failure cases due to optical restoration restrictions. Moreover, its additional cost can be further reduced by migrating (i.e., towards elasticity feature) only the transponders that are concerned by optical restoration.

- The power adaptation approach proposed in Chapter 5 can also be used in the case of the under design.
- This work studied optical layer flexibility from the point of view of cost and capacity. It could be also evaluated considering energy consumption and/or network QoS requirements.
- If deployed, flex-grid will certainly delay fiber capacity crunch but it has its limits. Space Division Multiplexing (SDM) is the next technology according to some researchers [27, 43]. This will however introduce a new dimension of fragmentation (i.e., spatial fragmentation) [87], making network dimensioning more challenging with the new constraints of spectrum and core allocation [123].

Finally, the works outlined in this PhD dissertation have been developed within the SASER-SIEGFRIED European Project, and have been published in ten international peer-reviewed journals and conferences (two papers are still under review). We think that the proposed algorithmic and software tools will be of interest for the scientific community, and believe that the obtained results will help network operators in their planning decision to deploy the future networks.

Contributions and Distinctions

International Journals

1. M. Kanj, E. Le Rouzic, J. Meuric, B. Cousin, and **D. Amar** "Optical Power Control in GMPLS Control Plane" Journal of Optical Communications and Networking (JOCN), Under review.

2. **D. Amar**, E. Le Rouzic, N. Brochier, and C. Lepers, "A Class-of-Service Based Multilayer Architecture for Traffic Restoration in Elastic Optical Networks," Journal of Optical Communications and Networking (JOCN), 2016.

3. **D. Amar**, N. Brochier, E. Le Rouzic, J.-L. Auge, C. Lepers, B. Cousin, and M. Kanj, "Link Design and Legacy Amplifier Limitation in Flex-grid Optical Networks," IEEE Photonics Journal, 2016.

4. **D. Amar**, E. Le Rouzic, N. Brochier, J.-L. Auge, C. Lepers, and N. Perrot, "Spectrum fragmentation issue in flexible optical networks: Analysis and good practices," Journal of Photonic Network communications (PNET), Springer, 2015.

International Conferences

5. M. Kanj, E. Le Rouzic, **D. Amar**, J-L. Auge, B. Cousin, and N. Brochier, "Optical Power Control to Efficiently Handle Flex-Grid Spectrum Gain over Existing Fixed-Grid Networks Infrastructures," International Conference on Computing, Networking and Communications (ICNC), Hawaii, USA, February, 2016.

6. **D. Amar**, M. Kanj, J-L. Auge, N. Brochier, E. Le Rouzic, C. Lepers, and B. Cousin, "On the Legacy Amplifier Limitation in Flexgrid Optical Networks," Photonics in Switching (PS), Florence, Italy, September, 2015 **(High Scored)**.

7. **D. Amar**, E. Le Rouzic, N. Brochier, and C. Lepers, "Multilayer Restoration in Elastic Optical Networks," Optical Network Design and Modeling (ONDM), Pisa, Italy, May, 2015.

8. **D. Amar**, E. Le Rouzic, N. Brochier, E. Bonetto, and C. Lepers, "Traffic forecast impact on spectrum fragmentation in gridless optical networks," European Conference on Optical Communications **(ECOC)**, Cannes, France, September, 2014.

9. **D. Amar**, E. Le Rouzic, N. Brochier, J.-L. Auge, N. Perrot, C. Lepers, and S. Fazel, "How problematic is spectrum fragmentation in operator's gridless network?," Optical Network Design and Modeling (ONDM), Stockholm, Sweden, May, 2014, **(Best Paper Award)**.

10. **D. Amar**, N. Brochier, E. Le Rouzic, and C. Lepers, "Multilayer dimensioning of flexible optical networks," Experimental UpdateLess Evolutive Routing (EULER summer school), Barcelona, Spain, July, 2013.

Other events

- PhD work selected for presentation during young researchers' day to compete for SAMOVAR price to be held on May, 30th, 2016.
- PhD work popularization on EDEn (Expérience Doctorale en Entreprise) final day at Orange, Issy-Les-Moulineaux, September, 2015.
- Fragmentation du spectre dans les réseaux optiques flexibles, PhD day at Orange, Issy-Les-Moulineaux, September, 2014.
- PhD work selected for private presentation in front of Nicolas Demassieux (senior vice president of Orange Labs Research) and Cedric Villani (2010 Fields Medal) on PhD day at Orange, Issy-Les-Moulineaux, September, 2014.

Bibliography

[1] I. Chlamtac, A. Ganz, and G. Karmi. Lightpath communications: an approach to high bandwidth optical wan's. *Communications, IEEE Transactions on*, 40 (7):1171–1182, Jul 1992. 1, 13

[2] M. Jinno, H. Takara, B. Kozicki, Y. Tsukishima, T. Yoshimatsu, T. Kobayashi, Y. Miyamoto, K. Yonenaga, A. Takada, O. Ishida, and S. Matsuoka. Demonstration of novel spectrum-efficient elastic optical path network with per-channel variable capacity of 40 gb/s to over 400 gb/s. In *Optical Communication, 2008. ECOC 2008. 34th European Conference on*, pages 1–2, Sept 2008. 1, 12, 17, 20, 24

[3] H. Takara, T. Goh, K. Shibahara, K. Yonenaga, S. Kawai, and M. Jinno. Experimental demonstration of 400 gb/s multi-flow, multi-rate, multi-reach optical transmitter for efficient elastic spectral routing. In *Optical Communication (ECOC), 2011 37th European Conference and Exhibition on*, pages 1–3, Sept 2011. 28

[4] V. Vgenopoulou, A. Amari, M. Song, E. Pincemin, I. Roudas, and Y. Jaouen. Volterra-based nonlinear compensation in 400 gb/s wdm multiband coherent optical ofdm systems. In *Asia Communications and Photonics Conference 2014*, page AF1E.4. Optical Society of America, 2014. 1

[5] A.N. Patel, P.N. Ji, J.P. Jue, and T. Wang. Traffic grooming in flexible optical wdm (fwdm) networks. In *OptoeElectronics and Communications Conference (OECC), 2011 16th*, pages 405–406, July 2011. 1, 14

[6] Z. Shuqiang, M. Tornatore, S. Gangxiang, and B. Mukherjee. Evolution of traffic grooming from sdh/sonet to flexible grid. In *Optical Communication (ECOC 2013), 39th European Conference and Exhibition on*, pages 1–3, Sept 2013. 1, 14

[7] S.L. Woodward and M.D. Feuer. Benefits and requirements of flexible-grid roadms and networks [invited]. *Optical Communications and Networking, IEEE/OSA Journal of*, 5(10):A19–A27, Oct 2013. 2, 21, 22

[8] D. Amar, M. Kanj, J.-L. Auge, N. Brochier, E. Le Rouzic, C. Lepers, and B. Cousin. On the legacy amplifier limitation in flexgrid optical networks. In *International Conference on Photonics in Switching*, pages 1–3, Sept 2015. 2, 20, 84

[9] P. Papanikolaou, K. Christodoulopoulos, and E. Varvarigos. Multilayer flex-grid network planning. In *Optical Network Design and Modeling (ONDM), International Conference on*, pages 151–156, May 2015. 2, 91

[10] L. Velasco, A. Castro, M. Ruiz, and G. Junyent. Solving routing and spectrum allocation related optimization problems: From off-line to in-operation flexgrid network planning. *Lightwave Technology, Journal of*, 32(16):2780–2795, Aug 2014.

[11] E. Palkopoulou, M. Angelou, D. Klonidis, K. Christodoulopoulos, A. Klekamp, F. Buchali, E. Varvarigos, and I. Tomkos. Quantifying spectrum, cost, and energy efficiency in fixed-grid and flex-grid networks [invited]. *Optical Communications and Networking, IEEE/OSA Journal of*, 4(11):B42–B51, Nov 2012. 2, 91

[12] R. Wang and B. Mukherjee. Provisioning in elastic optical networks with non-disruptive defragmentation. *Lightwave Technology, Journal of*, 31(15):2491–2500, Aug 2013. 2, 28, 31, 35

[13] P. Wright, M.C. Parker, and A. Lord. Simulation results of shannon entropy based flexgrid routing and spectrum assignment on a real network topology. In *Optical Communication (ECOC 2013), 39th European Conference and Exhibition on*, pages 1–3, Sept 2013. 14, 28, 29, 38

[14] A.N. Patel, P.N. Ji, J.P. Jue, and Ting Wang. Defragmentation of transparent flexible optical wdm (fwdm) networks. In *Optical Fiber Communication Conference and Exposition (OFC/NFOEC), 2011 and the National Fiber Optic Engineers Conference*, pages 1–3, March 2011. 28, 30

[15] M. Zhang, W. Shi, L. Gong, W. Lu, and Z. Zhu. Bandwidth defragmentation in dynamic elastic optical networks with minimum traffic disruptions. In *Communications (ICC), 2013 IEEE International Conference on*, pages 3894–3898, June 2013. 2, 31

[16] L. G. Kazovsky, W.-T. Shaw, D. Gutierrez, N. Cheng, and S.-W. Wong. Next-generation optical access networks. *J. Lightwave Technol.*, 25(11):3428–3442, Nov 2007. 5

[17] Metro network traffic growth: An architecture impact study. *Strategic White Paper*, 2013. 5, 9

[18] H. Zimmerman. Osi reference model — the iso model of architecture for open systems interconnection. *IEEE Transactions on Communications*, pages 425–432, Apr 1980. 6

[19] T. B. Robert. Requirements for internet hosts-communication layers. *IEEE Transactions on Communications*, RFC 1122:425–432, Oct 1989. 6

[20] *Interfaces for the optical transport network, ITU-T G.709.* . 6

[21] E. Mannie. Generalized multi-protocol label switching (gmpls) architecture. RFC 3945, Oct 2004. 6

[22] Software-defined networking: The new norm for networks. *White Paper*, Apr 2012. 7

[23] A. Triki. *Etude des techniques de transport de données par commutation de rafales optiques sans résolution spectrale de la contention*. PhD thesis, OPT - Dépt. Optique (Institut Mines-Télécom-Télécom Bretagne-UEB), May 2014. Th. doct. : Sciences et Technologies de l'Information et de la Communication, Institut Mines-Télécom-Télécom Bretagne-UEB, may 2014. 7

[24] Cisco visual networking index: Forecast and methodology, 2013-2018. *White Paper*, Jun 2014. 9

[25] E. Ip, A. P. Tau Lau, D. J. F. Barros, and J. M. Kahn. Coherent detection in optical fiber systems. *Opt. Express*, 16(2):753–791, Jan 2008. 10, 17, 84

[26] A. D. Ellis, J. Zhao, and D. Cotter. Approaching the non-linear shannon limit. *Lightwave Technology, Journal of*, 28(4):423–433, Feb 2010. 10, 17

[27] D. J. Richardson, J. M. Fini, and L. E. Nelson. Space-division multiplexing in optical fibres. In *Nature Photonics*, volume 7, pages 354–362, 2013. 11, 101

[28] T. Morioka, M. Jinno, H. Takara, and H. Kubota. Innovative future optical transport network technologies. In *NTT Technical Review*, volume 9, 2011. 11

[29] *Spectral grids for WDM applications: CWDM wavelength grid, ITU-T G.694.2.* . 10

[30] *Spectral grids for WDM applications: DWDM frequency grid, ITU-T G.694.1.* . 12, 19

[31] Balancing performance, flexibility, and scalability in optical networks. *White Paper*, Feb 2012. 12

[32] I. Tomkos, E. Palkopoulou, and M. Angelou. A survey of recent developments on flexible/elastic optical networking. In *Transparent Optical Networks (ICTON), 2012 14th International Conference on*, pages 1–6, July 2012. 12

[33] A. Bianco, E. Bonetto, and A. Arsalan. Energy awareness in the design of optical core networks. In *Optical Fiber Communication Conference/National Fiber Optic Engineers Conference 2013*, page NW3E.2. Optical Society of America, 2013. 13, 22

[34] A. Ahmad, A. Bianco, E. Bonetto, D. Cuda, G. Castillo, and F. Neri. Power-aware logical topology design heuristics in wavelength-routing networks. In *Optical Network Design and Modeling (ONDM), 2011 15th International Conference on*, pages 1–6, Feb 2011. 13, 22

[35] J. Carlson, A. Jaffe, and A. Wiles. The millennium prize problems. *American Mathematical Society*, 2006. 13

[36] S. Shirazipourazad, Z. Chenyang, Z. Derakhshandeh, and A. Sen. On routing and spectrum allocation in spectrum-sliced optical networks. In *INFOCOM, 2013 Proceedings IEEE*, pages 385–389, April 2013. 13, 23

[37] Y. Wang, X. Cao, and Y. Pan. A study of the routing and spectrum allocation in spectrum-sliced elastic optical path networks. In *INFOCOM, 2011 Proceedings IEEE*, pages 1503–1511, April 2011. 14, 23, 49

[38] A. Pages, J. Perello, and S. Spadaro. Lightpath fragmentation for efficient spectrum utilization in dynamic elastic optical networks. In *Optical Network Design and Modeling (ONDM), 2012 16th International Conference on*, pages 1–6, April 2012. 14, 17, 18, 27, 35

[39] Y. Yin, M. Zhang, Z. Zhu, and S.J.B. Y. Fragmentation-aware routing, modulation and spectrum assignment algorithms in elastic optical networks. In *Optical Fiber Communication Conference and Exposition and the National Fiber Optic Engineers Conference (OFC/NFOEC), 2013*, pages 1–3, March 2013. 28, 29, 35

[40] R. Wang and B. Mukherjee. Spectrum management in heterogeneous bandwidth optical networks. *Optical Switching and Networking*, 11, Part A(0):83 – 91, 2014. 28, 29

[41] A. Pages, J. Perello, S. Spadaro, and J. Comellas. Optimal route, spectrum, and modulation level assignment in split-spectrum-enabled dynamic elastic optical networks. *Optical Communications and Networking, IEEE/OSA Journal of*, 6 (2):114–126, Feb 2014. 14, 26, 27, 35

[42] J.-K. Rhee, F. Garcia, A. Ellis, B. Hallock, T. Kennedy, T. Lackey, R.G. Lindquist, J.P. Kondis, B.A. Scott, J.M. Harris, D. Wolf, and M. Dugan. Variable passband optical add-drop multiplexer using wavelength selective switch. In *Optical Communication, 2001. ECOC '01. 27th European Conference on*, volume 4, pages 550–551 vol.4, 2001. 17, 20

[43] I. Tomkos, S. Azodolmolky, J. Sole-Pareta, D. Careglio, and E. Palkopoulou. A tutorial on the flexible optical networking paradigm: State of the art, trends, and research challenges. *Proceedings of the IEEE*, 102(9):1317–1337, Sept 2014. 18, 22, 101

[44] M. Jinno, B. Kozicki, H. Takara, A. Watanabe, Y. Sone, T. Tanaka, and A. Hirano. Distance-adaptive spectrum resource allocation in spectrum-sliced elastic optical path network [topics in optical communications]. *Communications Magazine, IEEE*, 48(8):138–145, August 2010. 18, 24

[45] X. Wang, Q. Zhang, I. Kim, P. Palacharla, and M. Sekiya. Blocking performance in dynamic flexible grid optical networks – what is the ideal spectrum granularity? In *Optical Communication (ECOC), 2011 37th European Conference and Exhibition on*, pages 1–3, Sept 2011. 18

[46] L. Velasco, M. Ruiz, A. Castro, O. Pedrola, M. Klinkowski, D. Careglio, and J. Comellas. On the performance of flexgrid-based optical networks. In *Transparent Optical Networks (ICTON), 2012 14th International Conference on*, pages 1–4, July 2012. 18, 22

[47] P.S. Khodashenas, J.M. Rivas-Moscoso, D. Klonidis, D.M. Marom, and I. Tomkos. Evaluating the performance of ultra-fine spectrum granularity flexible optical networks. In *Transparent Optical Networks (ICTON), 2015 17th International Conference on*, pages 1–4, July 2015. 18

[48] G. Shen and Q. Yang. From coarse grid to mini-grid to gridless: How much can gridless help contentionless? In *Optical Fiber Communication Conference and Exposition (OFC/NFOEC), 2011 and the National Fiber Optic Engineers Conference*, pages 1–3, March 2011. 18

[49] O. Pedrola, A. Castro, L. Velasco, M. Ruiz, J. P. Fernández-Palacios, and D. Careglio. Capex study for a multilayer ip/mpls-over-flexgrid optical network. *J. Opt. Commun. Netw.*, 4(8):639–650, Aug 2012. 18

[50] Y. Li, L. Gao, G. Shen, and L. Peng. Impact of roadm colorless, directionless, and contentionless (cdc) features on optical network performance. *J. Opt. Commun. Netw.*, 4(11):B58–B67, Nov 2012. 20

[51] Introduction to edfa technology. *White Paper*, Jun 2009. 20

[52] A. Morea, O. Rival, N. Brochier, and E. Le Rouzic. Datarate adaptation for night-time energy savings in core networks. *Lightwave Technology, Journal of*, 31(5):779–785, March 2013. 21, 22, 32

[53] O. Gerstel, M. Jinno, A. Lord, and S.J.B. Yoo. Elastic optical networking: a new dawn for the optical layer? *Communications Magazine, IEEE*, 50(2):s12–s20, February 2012. 21

[54] R. Goscien, K. Walkowiak, and M. Klinkowski. On the regenerators usage in cloud-ready elastic optical networks with distance-adaptive modulation formats. In *Optical Communication (ECOC), 2014 European Conference on*, pages 1–3, Sept 2014. 22

[55] M. Liu, M. Tornatore, and B. Mukherjee. Survivable traffic grooming in elastic optical networks—shared protection. *Lightwave Technology, Journal of*, 31(6): 903–909, March 2013. 22, 32

[56] M. Jinno, Y. Sone, H. Takara, A. Hirano, K. Yonenaga, and S. Kawai. Ip traffic offloading to elastic optical layer using multi-flow optical transponder. In *Optical Communication (ECOC), 2011 37th European Conference and Exhibition on*, pages 1–3, Sept 2011. 22

[57] D. Amar, E. Le Rouzic, N. Brochier, and C. Lepers. Multilayer restoration in elastic optical networks. In *Optical Network Design and Modeling (ONDM), 2015 International Conference on*, pages 239–244, May 2015. 22

[58] X. Zhou, L.E. Nelson, and P. Magill. Rate-adaptable optics for next generation long-haul transport networks. *Communications Magazine, IEEE*, 51(3):41–49, March 2013. 22

[59] M. Klinkowski, M. Ruiz, L. Velasco, D. Careglio, V. Lopez, and J. Comellas. Elastic spectrum allocation for time-varying traffic in flexgrid optical networks. *Selected Areas in Communications, IEEE Journal on*, 31(1):26–38, January 2013. 22, 24

[60] R. Aparicio-Pardo, P. Pavon-Marino, N. Skorin-Kapov, B. Garcia-Manrubia, and J. Garcia-Haro. Algorithms for virtual topology reconfiguration under multi-hour traffic using lagrangian relaxation and tabu search approaches. In *Transparent Optical Networks (ICTON), 2010 12th International Conference on*, pages 1–4, June 2010. 23

[61] S. Talebi, E. Bampis, G. Lucarelli, I. Katib, and G. N. Rouskas. The spectrum assigment (sa) problem in optical networks: A multiprocessor scheduling perspective. In *Optical Network Design and Modeling, 2014 International Conference on*, pages 55–60, May 2014. 23, 25

[62] M. Klinkowski, K. Walkowiak, and M. Jaworski. Off-line algorithms for routing, modulation level, and spectrum assignment in elastic optical networks. In *Transparent Optical Networks (ICTON), 2011 13th International Conference on*, pages 1–6, June 2011. 23

[63] L. Velasco, M. Klinkowski, M. Ruiz, and J. Comellas. Modeling the routing and spectrum allocation problem for flexgrid optical networks. *Photonic Network Communications*, 24(3):177–186, 2012. 24, 26

[64] K. Christodoulopoulos, I. Tomkos, and E.A. Varvarigos. Routing and spectrum allocation in ofdm-based optical networks with elastic bandwidth allocation. In *Global Telecommunications Conference (GLOBECOM 2010), 2010 IEEE*, pages 1–6, Dec 2010. 24

[65] A.N. Patel, P.N. Ji, J.P. Jue, and T. Wang. A naturally-inspired algorithm for routing, wavelength assignment, and spectrum allocation in flexible grid wdm networks. In *Globecom Workshops (GC Wkshps), 2012 IEEE*, pages 340–345, Dec 2012. 24

[66] S. Shirazipourazad, Z. Derakhshandeh, and A. Sen. Analysis of on-line routing and spectrum allocation in spectrum-sliced optical networks. In *Communications (ICC), 2013 IEEE International Conference on*, pages 3899–3903, June 2013. 24

[67] T. Takagi, H. Hasegawa, K. Sato, Y. Sone, B. Kozicki, A. Hirano, and M. Jinno. Dynamic routing and frequency slot assignment for elastic optical path networks that adopt distance adaptive modulation. In *Optical Fiber Communication Conference and Exposition (OFC/NFOEC), 2011 and the National Fiber Optic Engineers Conference*, pages 1–3, March 2011. 24, 31

[68] I. Olszewski. Routing and spectrum assignment in spectrum flexible transparent optical networks. In Ryszard S. Choras, editor, *Image Processing and Communications Challenges 5*, volume 233 of *Advances in Intelligent Systems and Computing*, pages 407–417. Springer International Publishing, 2014. 24

[69] C. Rottondi, M. Tornatore, A. Pattavina, and G. Gavioli. Routing, modulation level, and spectrum assignment in optical metro ring networks using elastic transceivers. *Optical Communications and Networking, IEEE/OSA Journal of*, 5(4):305–315, April 2013. 25

[70] X. Wan, N. Hua, and X. Zheng. Dynamic routing and spectrum assignment in spectrum-flexible transparent optical networks. *Optical Communications and Networking, IEEE/OSA Journal of*, 4(8):603–613, Aug 2012. 25

[71] A. Rosa, C. Cavdar, S. Carvalho, J. Costa, and L. Wosinska. Spectrum allocation policy modeling for elastic optical networks. In *High Capacity Optical Networks and Enabling Technologies (HONET), 2012 9th International Conference on*, pages 242–246, Dec 2012. 25, 28, 37, 40

[72] Y. Yu, J. Zhang, Y. Zhao, X. Cao, X. Lin, and W. Gu. The first single-link exact model for performance analysis of flexible grid wdm networks. In *Optical Fiber Communication Conference and Exposition and the National Fiber Optic Engineers Conference (OFC/NFOEC), 2013*, pages 1–3, March 2013. 25, 41

[73] M. Klinkowski. On the effect of regenerator placement on spectrum usage in translucent elastic optical networks. In *Transparent Optical Networks (ICTON), 2012 14th International Conference on*, pages 1–6, July 2012. 26

[74] S. Acharya, B. Gupta, P. Risbood, and A. Srivastava. Mobipack: optimal hitless sonet defragmentation in near-optimal cost. In *INFOCOM 2004. Twenty-third AnnualJoint Conference of the IEEE Computer and Communications Societies*, volume 3, pages 1819–1829 vol.3, March 2004. 26

[75] C.-M. Chao and S.-H. Wang. A joint code/time assignment strategy with minimal fragmentations for cdma systems. In *Wireless Communications and Networking Conference, 2006. WCNC 2006. IEEE*, volume 3, pages 1620–1625, April 2006. 26

[76] M. S. Johnstone and P. R. Wilson. *The memory fragmentation problem: solved?* October 1998. 26, 28, 38

[77] J. L. Gross and J. Yellen. Handbook of graph theory. CRC Press, 2003. 26

[78] F. Cugini, F. Paolucci, G. Meloni, G. Berrettini, M. Secondini, F. Fresi, N. Sambo, L. Poti, and P. Castoldi. Push-pull defragmentation without traffic disruption in flexible grid optical networks. *Lightwave Technology, Journal of*, 31(1):125–133, Jan 2013. 28, 30

[79] Y. Sone, A. Hirano, A. Kadohata, M. Jinno, and O. Ishida. Routing and spectrum assignment algorithm maximizes spectrum utilization in optical networks. In *Optical Communication (ECOC), 2011 37th European Conference and Exhibition on*, pages 1–3, Sept 2011. 28, 35

[80] X. Wang, Q. Zhang, I. Kim, P. Palacharla, and M. Sekiya. Utilization entropy for assessing resource fragmentation in optical networks. In *Optical Fiber Communication Conference and Exposition (OFC/NFOEC), 2012 and the National Fiber Optic Engineers Conference*, pages 1–3, March 2012. 28

[81] J. Zhang and Y. Zhao. Routing and spectrum assignment problem in three-c-aware dynamic flexible optical networks. In *Communications and Photonics Conference and Exhibition, 2011. ACP. Asia*, pages 1–7, Nov 2011. 28, 29

[82] D. Amar, E. Le Rouzic, N. Brochier, J.-L. Auge, C. Lepers, N. Perrot, and S. Fazel. How problematic is spectrum fragmentation in operator's gridless network? In *Optical Network Design and Modeling, International Conference on*, pages 67–72, May 2014. 28, 57

[83] D. Amar, E. Le Rouzic, N. Brochier, J.-L. Auge, C. Lepers, and N. Perrot. Spectrum fragmentation issue in flexible optical networks: analysis and good practices. *Photonic Network Communications*, 29(3):230–243, 2015. 28, 57, 90, 91

[84] Z. s. Shen, H. Hasegawa, and K.-I. Sato. A novel flexible grid/semi-flexible grid optical path network design algorithm that reserves exclusive frequency slots for high bitrate signals. In *Optical Network Design and Modeling, 2014 International Conference on*, pages 287–292, May 2014. 29

[85] K. Christodoulopoulos, I. Tomkos, and E. Varvarigos. Dynamic bandwidth allocation in flexible ofdm-based networks. In *Optical Fiber Communication Conference and Exposition (OFC/NFOEC), 2011 and the National Fiber Optic Engineers Conference*, pages 1–3, March 2011. 29

[86] S. Sugihara, Y. Hirota, S. Fujii, H. Tode, and T. Watanabe. Routing and spectrum allocation method for immediate reservation and advance reservation requests in elastic optical networks. In *Photonics in Switching (PS), 2015 International Conference on*, pages 178–180, Sept 2015. 29

[87] L. Liu, Z. Zhu, and S.J.B. Yoo. 3d elastic optical networks in temporal, spectral, and spatial domains with fragmentation-aware rssma algorithms. In *Optical Communication (ECOC), 2014 European Conference on*, pages 1–3, 2014. 29, 101

[88] T. Takagi, H. Hasegawa, K. Sato, Y. Sone, A. Hirano, and M. Jinno. Disruption minimized spectrum defragmentation in elastic optical path networks that adopt distance adaptive modulation. In *Optical Communication (ECOC), 2011 37th European Conference and Exhibition on*, pages 1–3, Sept 2011. 30

[89] R. Proietti, R. Yu, K. Wen, Y. Yin, and S.J.B. Yoo. Quasi-hitless defragmentation technique in elastic optical networks by a coherent rx lo with fast tx wavelength tracking. In *Photonics in Switching (PS), 2012 International Conference on*, pages 1–3, Sept 2012. 30

[90] M. Zhang, Y. Yin, R. Proietti, Z. Zhu, and S.J.B. Yoo. Spectrum defragmentation algorithms for elastic optical networks using hitless spectrum retuning techniques. In *Optical Fiber Communication Conference and Exposition and the National Fiber Optic Engineers Conference (OFC/NFOEC), 2013*, pages 1–3, March 2013. 30, 31

[91] W. Ju, S. Huang, Z. Xu, J. Zhang, and W. Gu. Dynamic adaptive spectrum defragmentation scheme in elastic optical path networks. In *Opto-Electronics and Communications Conference (OECC), 2012 17th*, pages 20–21, July 2012. 30

[92] P. Soumplis, K. Christodoulopoulos, and E. Varvarigos. Dynamic connection establishment and network re-optimization in flexible optical networks. In *Optical Network Design and Modeling, 2014 International Conference on*, pages 61–66, May 2014. 31

[93] L. Liu, Y. Yin, M. Xia, M. Shirazipour, Z. Zhu, R. Proietti, Q. Xu, S. Dahlfort, and S.J.B. Yoo. Software-defined fragmentation-aware elastic optical networks enabled by openflow. In *Optical Communication (ECOC 2013), 39th European Conference and Exhibition on*, pages 1–3, Sept 2013. 31

[94] L. Gifre, F. Paolucci, A. Aguado, R. Casellas, A. Castro, F. Cugini, P. Castoldi, L. Velasco, and V. López. Experimental assessment of in-operation spectrum defragmentation. *Photonic Netw. Commun.*, 27(3):128–140, June 2014. 31

[95] A. Lord. Core networks in the flexgrid era. In *Optical Communication (ECOC), 2014 European Conference on*, pages 1–3, Sept 2014. 31, 98

[96] C. Metz. Ip protection and restoration. *Internet Computing, IEEE*, 4(2):97–102, 2000. 31

[97] D. Colle, S. De Maesschalck, C. Develder, P. Van Heuven, A. Groebbens, J. Cheyns, U. Lievens, M. Pickavet, P. Lagasse, and P. Demeester. Data-centric optical networks and their survivability. *Selected Areas in Communications, IEEE Journal on*, 20(1):6–20, Jan 2002. 31

[98] O. Gerstel, C. Filsfils, and W. Wakim. Ip-optical interaction during traffic restoration. In *Optical Fiber Communication Conference and Exposition and the National Fiber Optic Engineers Conference (OFC/NFOEC), 2013*, pages 1–3, March 2013. 32

[99] M. Gunkel, A. Autenrieth, M. Neugirg, and J. Elbers. Advanced multilayer resilience scheme with optical restoration for ip-over-dwdm core networks. In *Ultra Modern Telecommunications and Control Systems and Workshops (ICUMT), 2012 4th International Congress on*, pages 657–662, Oct 2012. 32, 65, 73

[100] A. Morea, G. Charlet, and D. Verchere. Elasticity for dynamic recovery in otn networks. In *Asia Communications and Photonics Conference 2014*, page AW4E.2. Optical Society of America, 2014. 32

[101] O. Gerstel, V. Lopez, and D. Siracusa. Multi-layer orchestration for application-centric networking. In *Photonics in Switching (PS), 2015 International Conference on*, pages 318–320, Sept 2015. 32

[102] A. Bononi, P. Serena, and A. Morea. Regeneration savings in coherent optical networks with a new load-dependent reach maximization. In *Optical Communication (ECOC), European Conference on*, pages 1–3, Sept 2014. 32, 33, 87

[103] A. Mitra, A. Lord, S. Kar, and P. Wright. Effect of link margins and frequency granularity on the performance and modulation format sweet spot of multiple flexgrid optical networks. In *Optical Fiber Communications Conference and Exhibition (OFC), 2014*, pages 1–3, March 2014. 32, 33

[104] D.J. Ives, P. Bayvel, and S.J. Savory. Assessment of options for utilizing snr margin to increase network data throughput. In *Optical Fiber Communications Conference and Exhibition (OFC)*, pages 1–3, March 2015. 32, 33

[105] J.-L. Auge. Can we use flexible transponders to reduce margins? In *Optical Fiber Communication Conference and Exposition and the National Fiber Optic Engineers Conference (OFC/NFOEC)*, pages 1–3, March 2013. 33

[106] A. Nag, M. Tornatore, and B. Mukherjee. Power management in mixed line rate optical networks. In *Integrated Photonics Research, Silicon and Nanophotonics and Photonics in Switching*, page PTuB4. Optical Society of America, 2010. 33

[107] G. Bosco, V. Curri, A. Carena, P. Poggiolini, and F. Forghieri. On the performance of nyquist-wdm terabit superchannels based on pm-bpsk, pm-qpsk, pm-8qam or pm-16qam subcarriers. *Lightwave Technology, Journal of*, 29(1):53–61, Jan 2011. 35

[108] A. Eira, J. Pedro, and J. Pires. On the impact of optimized guard-band assignment for superchannels in flexible-grid optical networks. In *Optical Fiber Communication Conference and Exposition and the National Fiber Optic Engineers Conference (OFC/NFOEC), 2013*, pages 1–3, March 2013. 47

[109] P. Poggiolini. The gn model of non-linear propagation in uncompensated coherent optical systems. *Lightwave Technology, Journal of*, 30(24):3857–3879, Dec 2012. 47

[110] R. Aparicio-Pardo, P. Pavon-Marino, and B. Mukherjee. Robust upgrade in optical networks under traffic uncertainty. In *Optical Network Design and Modeling (ONDM), 2012 16th International Conference on*, pages 1–6, April 2012. 57

[111] F. Rambach, B. Konrad, L. Dembeck, U. Gebhard, M. Gunkel, M. Quagliotti, L. Serra, and V. Lopez. A multilayer cost model for metro/core networks. *Optical*

Communications and Networking, IEEE/OSA Journal of, 5(3):210–225, March 2013. 62, 90

[112] G. Swallow, A. Atlas, and P. Pan. Fast reroute extensions to rsvp-te for lsp tunnels. RFC 4090, 2005. 63

[113] M. Pióro and D. Medhi. *Routing, Flow, and Capacity Design in Communication and Computer Networks*. Morgan Kaufmann Publishers Inc., San Francisco, CA, USA, 2004. 69

[114] A. Nag and M. Tornatore. Optical network design with mixed line rates. *Optical Switching and Networking*, 6(4):227–234, 2009. 78, 95

[115] M. Kanj, E. Le Rouzic, D. Amar, J.-L. Auge, B. Cousin, and N. Brochier. Optical power control to efficiently handle flex-grid spectrum gain over existing fixed-grid networks infrastructures. In *International Conference on Computing, Networking and Communications (ICNC)*, 2016 (accepted). 84, 95, 99

[116] P. Poggiolini, G. Bosco, A. Carena, R. Cigliutti, V. Curri, F. Forghieri, R. Pastorelli, and S. Piciaccia. The logon strategy for low-complexity control plane implementation in new-generation flexible networks. In *Optical Fiber Communication Conference and Exposition and the National Fiber Optic Engineers Conference (OFC/NFOEC)*, pages 1–3, March 2013. 84, 89, 94, 99

[117] M. Lelic, A. Bauco, N. Menon, K. Wundke, and T. Zahnley. Smart edfa with embedded control. In *Lasers and Electro-Optics Society. The 14th Annual Meeting of the IEEE*, volume 2, pages 419–420, 2001. 85

[118] A. Mitra, D. Ives, A. Lord, P. Wright, and S. Kar. Non-linear impairment modeling for flexgrid network and its application in offline network equipment upgrade strategy. In *Optical Network Design and Modeling (ONDM), International Conference on*, pages 57–62, May 2015. 86

[119] F. Vacondio, O. Rival, C. Simonneau, E. Grellier, A. Bononi, L. Lorcy, J.-C. Antona, and S. Bigo. On nonlinear distortions of highly dispersive optical coherent systems. *Opt. Express*, 20(2):1022–1032, Jan 2012. 89

[120] G. Martinelli, X. Zhang, G. Galimberti, A. Zanardi, D. Siracusa, F. Pederzolli, Y. Lee, and F. Zhang. Information model for wavelength switched optical networks (wsons) with impairments validation. IETF Internet-Draft, Oct 2015. 95

[121] C. Betoule, G. Thouenon, E. Pincemin, M. Song, D. Klonidis, and I. Tomkos. Impact of optical flexibility and sub-band switching on multi-layer transport network architectures. In *Transparent Optical Networks (ICTON), 2014 16th International Conference on*, pages 1–8, 2014. 98

[122] J.P. Fernandez-Palacios, V. Lopez, B. Cruz, and O. Gonzalez de Dios. Elastic optical networking: An operators perspective. In *Optical Communication (ECOC), 2014 European Conference on*, pages 1–3, Sept 2014. 100

[123] A. Muhammad, G. Zervas, D. Simeonidou, and R. Forchheimer. Routing, spectrum and core allocation in flexgrid sdm networks with multi-core fibers. In *Optical Network Design and Modeling, 2014 International Conference on*, pages 192–197, May 2014. 101